

Neutron and Gamma Fluxes and dpa Rates for HFIR Vessel Beltline Region (Present and Upgrade Designs) Supplement 2

August 2010

Prepared by
E. D. Blakeman
R. D. Cheverton

DOCUMENT AVAILABILITY

Reports produced after January 1, 1996, are generally available free via the U.S. Department of Energy (DOE) Information Bridge.

Web site <http://www.osti.gov/bridge>

Reports produced before January 1, 1996, may be purchased by members of the public from the following source.

National Technical Information Service
5285 Port Royal Road
Springfield, VA 22161
Telephone 703-605-6000 (1-800-553-6847)
TDD 703-487-4639
Fax 703-605-6900
E-mail info@ntis.gov
Web site <http://www.ntis.gov/support/ordernowabout.htm>

Reports are available to DOE employees, DOE contractors, Energy Technology Data Exchange (ETDE) representatives, and International Nuclear Information System (INIS) representatives from the following source.

Office of Scientific and Technical Information
P.O. Box 62
Oak Ridge, TN 37831
Telephone 865-576-8401
Fax 865-576-5728
E-mail reports@osti.gov
Web site <http://www.osti.gov/contact.html>

This report was prepared as an account of work sponsored by an agency of the United States Government. Neither the United States Government nor any agency thereof, nor any of their employees, makes any warranty, express or implied, or assumes any legal liability or responsibility for the accuracy, completeness, or usefulness of any information, apparatus, product, or process disclosed, or represents that its use would not infringe privately owned rights. Reference herein to any specific commercial product, process, or service by trade name, trademark, manufacturer, or otherwise, does not necessarily constitute or imply its endorsement, recommendation, or favoring by the United States Government or any agency thereof. The views and opinions of authors expressed herein do not necessarily state or reflect those of the United States Government or any agency thereof.

Nuclear Science and Technology Division

**NEUTRON AND GAMMA FLUXES AND dpa RATES FOR
HFIR VESSEL BELTLINE REGION
(PRESENT AND UPGRADE DESIGNS)
SUPPLEMENT 2**

E. D. Blakeman
R. D. Cheverton

Date Published: August 2010

Prepared by
OAK RIDGE NATIONAL LABORATORY
Oak Ridge, Tennessee 37831-6283
managed by
UT-Battelle, LLC
for the
U.S. DEPARTMENT OF ENERGY
under contract DE-AC05-00OR22725

CONTENTS

	Page
LIST OF FIGURES	v
LIST OF TABLES	vii
ACRONYMS AND ABBREVIATIONS.....	ix
ACKNOWLEDGMENTS.....	xi
ABSTRACT	xiii
1. INTRODUCTION.....	1
2. BRIEF DISCUSSION OF ANALYTIC AND GEOMETRIC MODELS USED TO CALCULATE dpa RATES	3
2.1 ANALYTIC MODEL.....	3
2.1.1 Time Periods.....	3
2.1.2 Software.....	3
2.1.3 “Upgrades” and “Sets” of Calculated dpa Rates.....	3
2.1.4 An Anomaly in the Analytic Model for Calculating dpa Rates for the Vessel Structural Integrity Analysis.....	4
2.1.5 Possible Future Models.....	5
2.2 GEOMETRIC MODEL.....	7
2.2.1 General Comments	7
2.2.2 Specific Comments Regarding Input to the Structural Integrity Analysis.....	23
3. CALCULATED (UPGRADE 2) NEUTRON AND GAMMA FLUXES AND dpa RATES FOR THE SURVEILLANCE AND DOSIMETRY CAPSULE LOCATIONS AND THE 31 REGIONS USED IN THE VESSEL STRUCTURAL INTEGRITY ANALYSIS.....	25
3.1 CALCULATED dpa RATES (UPGRADE 2) FOR ALL SURVEILLANCE AND DOSIMETRY CAPSULE LOCATIONS.....	25
3.2 CALCULATED dpa RATES (UPGRADE 2) FOR THE HFIR VESSEL 31 REGIONS USED IN THE VESSEL STRUCTURAL INTEGRITY ANALYSIS (SECT. 5 OF [5])	27
3.3 CALCULATED NEUTRON AND GAMMA FLUXES AND dpa RATES PERTAINING TO THE DOSIMETRY OBTAINED FROM HFIR FUEL CYCLES 400 AND 401	28
3.3.1 Dosimeters and Their Locations	28
3.3.2 Calculated Multigroup Neutron and Gamma Fluxes	37
3.3.3 Calculated dpa Rates.....	37
3.4 CALCULATED NEUTRON AND GAMMA dpa RATES PERTAINING TO HFIR DOSIMETRY OBTAINED IN 1993	37
4. DATA/CODE ARCHIVE AND QUALITY ASSURANCE	49
5. SUMMARY	51

CONTENTS (continued)

	Page
6. REFERENCES.....	53
APPENDIX A: dpa RATES USED FOR HFIR VESSEL STRUCTURAL INTEGRITY EVALUATIONS SINCE THE ENLARGEMENT OF THE HB-2 AND HB-4 BEAM TUBES	A-1
APPENDIX B: MESH-INTERVAL-BASED INTERPOLATION PROCESS FOR CALCULATION OF dpa RATES	B-1
APPENDIX C: REVISED dpa RATE CALCULATIONS PERFORMED USING THE OAK RIDGE NATIONAL LABORATORY CPILE COMPUTER AND INCORPORATING INTERPOLATION AND CURVE-FITTING ENHANCEMENTS	C-1
APPENDIX D: MONTE CARLO METHOD ANALYSIS	D-1
APPENDIX E: COMPUTER MODEL DESCRIPTIONS AND ARCHIVE.....	E-1

LIST OF FIGURES

		Page
Fig. 1.	Cross section of HFIR core, beam tubes, and pressure vessel at horizontal midplane of core for $t > 22.7$ EFY (100 MW). Surveillance capsule locations (Keys) are shown.	8
Fig. 2.	Geometry/material model for HB-1 and HB-4 (original design; HB-4 shown; HB-1 is mirror image) with specimen mount (Key 4) included.....	9
Fig. 3.	Geometry/material model for HB-2 (original design). The regions are as shown in Fig. 2. ..	10
Fig. 4.	Geometry/material model for HB-2 (modified design) with specimen mount included. The regions are as shown in Fig. 2.	11
Fig. 5.	Geometry/material model for HB-3. The specimen mount is shaded to improve visibility. The regions are as shown in Fig. 2.	12
Fig. 6.	Geometry/material model for HB-4 (new design) with specimen mount included. The regions are as shown in Fig.2.....	13
Fig. 7.	Geometry/material model for HFIR reactor core.....	14
Fig. 8.	Coordinate systems for HFIR beam tubes HB-1, -2, -3, -4. For HB-2, the beam tube origin is the center of the core. For HB-1, -3, -4, the origin is the normal intersection of a horizontal line from the center of the reactor core with the beam tube centerline.....	15
Fig. 9.	Schematic horizontal midplane cross section ($Z = 0$) diagram showing location of the nozzle “corner,” “annulus,” and “weld” for the HFIR beam tube HB-2. Horizontal (X,Y)–axis coordinates are shown for the three locations. The Z-axis coordinate projects outward toward the reader (similar for HB-3 and HB-4).....	16
Fig. 10.	Schematic of the offset locations at nozzle corner and weld at 12:00 positions caused by representation with a 2D model.	23
Fig. 11.	Locations (x,y,z coordinates) for HB-2 tubular dosimeters 2D1C, 2D2C, 2D1W, 2D2W, and 2D3W. (+X-axis is perpendicular to image away from reader.).....	30
Fig. 12.	Locations of dosimeters in (x,y,z) coordinate dimensions at HB-3. +X-axis is along longitudinal axis of beam tube (normal to page) away from the reactor core.	31
Fig. 13.	Iso-plots of neutron (left) and gamma (right) dpa rates for HB-2 (modified, enlarged design) showing approximate axial and radial locations of dosimeters.....	32
Fig. 14.	Iso-plots of neutron (left) and gamma (right) dpa rates for HB-3 showing approximate locations of dosimeters (Key 3) in the reactor horizontal midplane ($Z = 0$).	33
Fig. 15.	Iso-plots of neutron (left) and gamma (right) dpa rates for HB-4 (modified, enlarged design).....	34
Fig. 16.	Iso-plots of neutron (top) and gamma (bottom) dpa rates for the HFIR reactor model showing approximate location of Key 7 positions at the vessel wall.	35
Fig. 17.	Iso-plots of neutron (left) and gamma (right) dpa rates for HB-2 (original design) showing approximate location of the Key 2 radial dosimeter.	46

LIST OF FIGURES (continued)

	Page
Fig. 18. Iso-plots of neutron (left) and gamma (right) dpa rates for HB-4 (original design). The plot is through the horizontal midplane, but the approximate locations of Key 4, Positions P2 and P10 are shown in the inset diagram on the right-hand figure. Key 4 position coordinates (X,Y,Z) are shown. Also, the approximate location for Key 7, Position P5 is shown. Calculations for Key 7, however, were performed using a model expanded in the Y dimension to 60.96 cm.	47
Fig. B.1. Linear interpolation scheme for estimation of dpa rate at specified location from discrete mesh calculations	B-2
Fig. C.1. Convention for specifying angles for capsule locations in a beam tube.....	C-2
Fig. C.2. Key 3 (HB-3) neutron dpa rate vs angle showing uninterpolated and interpolated data and interpolated data with straight-line and sine-curve fits.....	C-4
Fig. C.3. Key 3 (HB-3) gamma dpa rate vs angle showing uninterpolated and interpolated data, and interpolated data with straight-line and sine-curve fits.....	C-5
Fig. C.4. Key 3 (HB-3) neutron and gamma dpa rates for Key positions plotted vs angle showing uninterpolated, interpolated, and sine-curve-fit (where used) data.	C-6
Fig. C.5. Key 4 (HB-4 original design) neutron dpa rate vs angle showing uninterpolated and interpolated data and interpolated data with straight-line and sine-curve fits	C-7
Fig. C.6. Key 4 (HB-4 original design) gamma dpa rate vs angle showing uninterpolated and interpolated data and interpolated data with straight-line and sine-curve fits.	C-8
Fig. C.7. Key 4 (HB-4 original design) neutron and gamma dpa rates for Key positions plotted vs angle showing uninterpolated, interpolated, and sine-curve-fit (where used) data.....	C-9
Fig. C.8. Key 4 (HB-4 modified design) neutron dpa rate vs angle showing uninterpolated and interpolated data and interpolated data with straight-line and sine-curve fits.	C-10
Fig. C.9. Key 4 (HB-4 modified design) gamma dpa rate vs angle showing uninterpolated and interpolated data and interpolated data with straight-line and sine-curve fits	C-11
Fig. C.10. Key 4 (HB-4 modified design) neutron and gamma dpa rates for Key positions plotted vs angle showing uninterpolated, interpolated, and sine-curve-fit (where used) data.....	C-12
Fig. C.11. Key 6 (HB-1 [4] original extended design) neutron and gamma dpa rates for Key positions showing uninterpolated and interpolated data.....	C-13
Fig. C.12. Key 7 (HB-4 original extended design) neutron and gamma dpa rates for Key positions showing uninterpolated and interpolated data.....	C-14
Fig. C.13. Key 7 (HB-4 modified extended design) neutron and gamma dpa rates for Key positions showing uninterpolated and interpolated data.....	C-15
Fig. C.14. Schematic showing locations of corner, annulus, and weld for a beam tube with a discrete-ordinates mesh overlaying the geometry	C-22
Fig. E.1. Directory structure for High Flux Isotope Reactor displacements-per-atom-per-second (dpa) model files.....	E-1

LIST OF TABLES

	Page
Table 1. Summary of code sequence for beam-tube calculations	3
Table 2. VELM neutron group boundaries and original and revised Fe dpa cross-section values	6
Table 3. VELM gamma group boundaries and dpa cross-section values	6
Table 4. Interval boundaries for 3D TORT model for HB-1 and HB-4 (original design)	17
Table 5. Interval boundaries for 2D DORT model for HB-2 (original design)	18
Table 6. Interval boundaries for 2D DORT model for HB-2 (modified design)	19
Table 7. Interval boundaries for 3D TORT model for HB-3	20
Table 8. Interval boundaries for 3D TORT model for HB-4 (modified design).....	21
Table 9. Interval boundaries for 2D DORT model for HFIR vessel.....	22
Table 10. Key 1 and 4 Set 4 dpa rates (HB-4 original design, $t < 22.7$ EFPY (100 MW))	25
Table 11. Key 2, 2C, and 2W dpa rates (HB-2).....	25
Table 12. Key 3 dpa rates (HB-3).....	26
Table 13. Key 4 dpa rates (HB-4, modified design, $t > 22.7$ EFPY (100 MW))	26
Table 14. Key 6 dpa rates (HB-1)	26
Table 15. Key 7 dpa rates (HB-4, original design, $t < 22.7$ EFPY (100 MW))	27
Table 16. dpa rates at HB-2 nozzle corner and weld dosimeters [$t > 22.7$ EFPY (100 MW)]	27
Table 17. Neutron and gamma calculated dpa rates for the 31 vessel regions considered in the vessel structural integrity study	28
Table 18. Dosimetry-dedicated capsules used for HFIR fuel cycles 400 and 401.....	29
Table 19. Actual vs DORT model locations of HB-2 nozzle and weld tubular dosimeters	36
Table 20. Actual vs DORT model locations of HB-2 capsules	36
Table 21. Actual vs DORT model locations of vessel capsule	36
Table 22. Neutron fluxes for HB-2 nozzle corner and weld tubular dosimeters	38
Table 23. Gamma fluxes for HB-2 nozzle corner and weld tubular dosimeters.....	39
Table 24. Neutron and gamma fluxes for HB-2 Key 2C	40
Table 25. Neutron fluxes for HB-2 Key 2W Positions 1, 2, and 3	41
Table 26. Gamma fluxes for HB-2 Key 2W Positions 1, 2, and 3.....	42
Table 27. Neutron fluxes (EOC) for HB-3 Key 3 Positions 3, 8, and 10	43
Table 28. Gamma fluxes (EOC) for HB-3 Key 3 Positions 3, 8, and 10.....	44
Table 29. Neutron and gamma fluxes for reactor vessel wall.....	45
Table 30. Calculated dpa rates for dosimeters used during HFIR fuel cycles 400 and 401	46
Table 31. Actual vs DORT/TORT model dosimeter locations for HB-2 and HB-4 (original designs)....	48

LIST OF TABLES (continued)

	Page
Table 32. Summary of calculated dpa rates for indicated HB-2 and HB-4 beam-tube locations for $t < 22.7$ EFPY (original designs).....	48
Table A.1. Summary of conditions for dpa-rate sets.....	A-2
Table C.1. Calculated neutron and gamma dpa rates for Key 3 (HB-3) surveillance capsule positions.....	C-16
Table C.2. Calculated neutron and gamma dpa rates for Key 4 surveillance capsule positions (original HB-4 and Key 4 designs, $t < 22.7$ EFPY).....	C-16
Table C.3. Calculated neutron and gamma dpa rates for Key 4 surveillance capsule positions (modified HB-4 and Key 4 designs, $t > 22.7$ EFPY).....	C-16
Table C.4. Calculated neutron and gamma dpa rates for Key 6 (HB-1 [4], original extended design) surveillance capsule positions	C-17
Table C.5. Calculated neutron and gamma dpa rates for Key 7 (HB-4, original extended design) surveillance capsule positions	C-17
Table C.6. Calculated neutron and gamma dpa rates for Key 7 (HB-4, modified extended design) surveillance capsule positions	C-17
Table C.7. Summary of calculated (unnormalized) neutron and gamma dpa rates for HFIR surveillance capsule Keys for times before and after 22.7 EFPY (3 rd upgrade).....	C-18
Table C.8. Locations of corner, annulus, and weld regions in beam-tube coordinates and numerical models	C-21
Table C.9. Calculated neutron and gamma dpa rates for the 31 vessel regions considered in the vessel structural integrity study: previous reported values (2 nd upgrade) and updated values using the CPILE computer system and interpolation, and including Keys in models (3 rd upgrade).....	C-23
Table E.1. Summary of files for beam-tube dpa rate analysis	E-2
Table E.2. Software file cross index	E-4
Table E.3. Updated file-naming convention	E-5

ACRONYMS AND ABBREVIATIONS

2D	two dimensional
3D	three dimensional
BOC	beginning of cycle
CADIS	Consistent Adjoint Driven Importance Sampling
dpa	displacements-per-atom
dpa rate	displacements-per-atom-per-second
EFPY	effective full-power years
EOC	end of cycle
HFIR	High Flux Isotope Reactor
K	Key
M/C	measured-to-calculated
NSTD	Nuclear Science and Technology Division
ORNL	Oak Ridge National Laboratory
P	position within a Key
p	position within a capsule

ACKNOWLEDGMENTS

The authors are thankful to I. Remec who provided displacements-per-atom-per-second cross sections and other valuable technical contributions. Appreciation is also extended to H. A. Kmieciak, Jr., for helpful comments, suggestions, and support. The authors are also grateful to D. J. Weaver, H. E. Turpin, and V. A. Williams for preparation and formatting of the final report.

ABSTRACT

This report documents (1) the calculated dpa rates (displacements-per-atom-per-second) that were used in the most recent High Flux Isotope Reactor vessel structural integrity analysis, (2) calculated dpa rates for all surveillance-capsule and dosimetry-dedicated-capsule locations based on a “second” upgrade of the analytic models, (3) calculated dpa rates for all surveillance-capsule and dosimetry-dedicated-capsule locations and for the 31 vessel regions used in the vessel structural integrity analysis based on a “third” upgrade of the analytic models, and (4) calculated neutron and gamma fluxes that were used to help derive “measured” dpa rates associated with the dosimetry experiments conducted during fuel cycles 400 and 401. Also, arguments are made for using Monte Carlo methods of analysis in addition to the discrete-ordinates method presently being used.

1. INTRODUCTION

The life of the High Flux Isotope Reactor (HFIR) pressure vessel is limited by neutron- and gamma-radiation-induced embrittlement. Thus, surveillance specimens of HFIR vessel materials are irradiated close to the vessel wall and periodically removed for testing, and these data and calculated values of dpa rate (displacements-per-atom-per-second) are used in a vessel structural integrity analysis to determine vessel-related safe operating conditions and the vessel's permissible lifetime. The overall accuracy of the analysis is improved by obtaining dosimetry data from the surveillance capsules and dosimetry-dedicated capsules and then using these data to improve the accuracy of the calculated dpa rates. These normalized dpa rates and the surveillance data are used to construct and update the HFIR vessel materials radiation embrittlement trend curve; and this curve and the normalized dpa rates are then used in the vessel integrity analysis.

In 1998 a decision was made to enlarge the HB-2 and HB-4 beam tubes, which would increase the dpa rates at the corresponding beam-tube nozzles (location of maximum embrittlement rate). The first analysis of the increased dpa rates [1]^{*} was based on preliminary data and shortly thereafter was upgraded by including the surveillance-capsule mounts (Keys) in the models. These improved models were included in a supplement [2] to [1], and this upgrade, for the sake of clarity, is referred to as the first upgrade (see Appendix A). More recently, an improved set of neutron dpa cross sections was used to upgrade the models in [2], and this upgrade, referred to as the second upgrade, is documented in this report.

After the enlarged HB-2 beam tube was installed, additional dosimetry data from dosimetry-dedicated capsules were obtained [3], and another set of surveillance specimens was tested [4]. In the manner indicated above, these data and the calculated dpa rates based on [1] for reactor operating times less than 22.7 effective full-power years (EFPY)[†] (original designs of HB-2 and HB-4 beam tubes) and on the second upgrade for $t > 22.7$ EFPY, were used in the most recent HFIR vessel structural integrity analysis (Sect. 5 of [5]).

Following this latest vessel structural integrity analysis, three events took place that led to a third upgrade of the calculated dpa rates: (1) it was decided that to cope with problems inherent in numerical analysis, interpolation and curve fitting should be used for "smoothing" the calculated dpa-rate distributions (Appendices B and C); (2) it was discovered that some neutron-scattering terms were missing from the cross section data for the HB-4 analytic model ($t > 22.7$ EFPY); and (3) it was necessary to shift the HFIR analyses to an alternative computer (CPILE) that was properly quality assured for HFIR studies. Thus, the third upgrade includes interpolation and curve fitting of calculated dpa rates, the inclusion of the necessary scattering terms for HB-4 ($t > 22.7$ EFPY), and the use of the CPILE computer for calculation of dpa rates. A corresponding set of dpa rates is included in Appendix C and was used in Appendix B of [5] and also in [6].

The three basic objectives of this report are to (1) provide a record of the unnormalized calculated dpa rates used in the HFIR vessel structural integrity analysis described in Sect. 5 of [5], which made use of the "preliminary" and second upgrade sets of calculated dpa rates; (2) develop the third updated set of dpa rates mentioned above, which were used in Appendix B of [5] and in [6] and are for future use; and (3) provide a record of multigroup neutron and gamma fluxes and dpa cross sections that were used to derive dpa rates from the measured activities of the dosimeters included for HFIR fuel cycles 400 and 401 (following the installation of the enlarged HB-2 beam tube).

^{*} References are for the "main body" of the report only. Appendices have separate reference sections.

[†] Effective full-power years, based on full power = 100 MW.

An additional possible improvement is the use of Monte Carlo methodology as an alternative to the discrete-ordinates approach. Included in this report (Appendix D) is a discussion of the pros and cons of the Monte Carlo vs the discrete-ordinates approach. Also briefly discussed is the use of the Monte Carlo methodology augmented with a discrete-ordinates-based, Oak Ridge National Laboratory (ORNL)–developed acceleration methodology, which is applied to the calculation of dpa rates at one of the Key locations.

2. BRIEF DISCUSSION OF ANALYTIC AND GEOMETRIC MODELS USED TO CALCULATE dpa RATES

2.1 ANALYTIC MODEL

2.1.1 Time Periods

There are two time periods of particular interest with regard to the analytic model: (1) the initial period, during which the original-design HB-2 and HB-4 beam tubes were installed, and (2) the ongoing second period, during which enlarged HB-2 and HB-4 beam tubes and new HB-2 and HB-4 Keys (surveillance/dosimetry capsule mounts) have been installed. The first period ended at 22.7 EFPY.

2.1.2 Software

The software used for the neutron- and gamma-flux and dpa-rate calculations used codes from the ORNL DOORS [7] code system, which are based on the discrete-ordinates methodology. The sequence of codes required to perform either two- or three-dimensional (2D or 3D) analyses are summarized in Table 1 (see also [1], Table 1). A discussion of the sequenced steps in Table 1 is presented in [1]. The DOORS code system has been quality assured [8] for safety-related HFIR calculations on the CPILE computer. The codes AXMIX and DTD, which are not a part of the DOORS system, have been separately quality assured [9, 10] for safety-related HFIR calculations on the CPILE computer.

Table 1. Summary of code sequence for beam-tube calculations

Step	Process	Code ^a	
0	Macro-cross-section library preparation	AXMIX	
1	Core eigenvalue (k_{eff}) calculation	DORT	
2	Fixed-source extended-core calculation	DORT	
3	Flux ordering and normalization	VISA	
		2D models	3D models
4	Boundary source calculation for beam-tube model	DTD	TORSED
5	Calculation of beam-tube fluxes and dpa rates	DORT	TORT

^aCodes, with the exception of AXMIX and DTD, are from the DOORS code system.

2.1.3 “Upgrades” and “Sets” of Calculated dpa Rates

The dpa rate is defined as follows:

$$d = \int_E \phi(E)\sigma(E)dE ,$$

where

$\phi(E)$ = neutron or gamma energy-dependent flux per unit energy,

$\sigma(E)$ = neutron or gamma energy-dependent microscopic dpa cross section for a specified material,

d = dpa rate.

For all the analyses discussed herein, $\sigma(E)$ is for iron, the primary constituent of the vessel wall, nozzles, and welds.

Since the time that enlargement of the HB-2 and HB-4 beam tubes was considered two “upgrades” have been made in the calculated dpa rates used in the HFIR vessel structural integrity analysis; and before the dpa rates are used in the integrity analysis they are normalized (corrected) making use of dosimetry data (only unnormalized values of dpa rates are presented in this report). Two sets of normalization factors and three sets of unnormalized calculated dpa rates have resulted in five “sets” of dpa rates being used in the vessel integrity evaluation since 1999. The “original” and two “upgrades” in the unnormalized dpa rates and the five “sets” of dpa rates used in the vessel analysis are defined in Appendix A, Table A.1, and the more important features are discussed in the following paragraphs:

Two sets of neutron dpa cross sections have been used. The updated set is based on an improved spectral averaging process described as follows: * The dpa cross sections in the broad-group structure (VELM [11]) were obtained by collapsing the American Society for Testing and Materials dpa cross sections for iron from the 640 energy groups (SAND II group structure) [12]. The fine-group data were obtained from the LSL-M2 cross-section library and collapsed with the FLXPRO code from the LSL-M2 code package [13]. The fine-group weighting spectrum consisted of the Watt fission spectrum matched to the 1/E spectrum at 0.5 MeV and to the Maxwellian spectrum with the effective temperature of 50°C at 1.4×10^{-7} MeV.

The revised and original iron dpa cross sections (σ_n) are shown in Table 2 for the VELM energy bin structure. The average difference between the two sets, excluding the thermal energy group (61), is 1.5%. In general the dpa rates calculated with the revised cross sections are slightly higher than those calculated with the original ones. The revised thermal group dpa cross section is ~60% higher than the earlier value. However, the contribution from the thermal neutrons is typically only a few percent of the total dpa rate value. Therefore, the result of the increased thermal dpa cross section is a small increase in the total calculated neutron dpa rate. Iron gamma dpa cross sections (σ_γ) are unchanged from previous analyses [14] and are shown in Table 3.

The most recent set of normalized dpa rates, referred to as the “fifth set” (see Appendix A), has been calculated using (1) the improved set of dpa cross sections; (2) interpolation and curve fitting of the calculated dpa rates for each key and both time periods; (3) the inclusion of the missing scattering terms (see Section 2.1.4) for the enlarged HB-4 model ($t > 22.7$ EFPY); and (4) the use of a computer (CPILE), not used previously, that is quality assured for HFIR safety studies using the DOORS software. This set was used for [6] and Appendix B of [5] and is discussed further in Appendix C.

2.1.4 An Anomaly in the Analytic Model for Calculating dpa Rates for the Vessel Structural Integrity Analysis

Sometime after the vessel structural integrity analysis [5] was completed, it was discovered that neutron-scattering terms were missing from the cross-section library for the analytic model used to calculate the dpa rates for the enlarged HB-4 beam tube and new Key 4 ($t > 22.7$ EFPY). Since then the omission has been corrected, and new dpa rates (“second upgrade”) have been calculated (included in Appendix C). As indicated by a comparison of neutron dpa rates for the HB-4 nozzle corner (Regions 15, 16, 17) for $t > 22.7$ EFPY (Table C.9), the correction of the omission resulted in a 31% increase in the neutron dpa rate. However, the corresponding increase in the conditional probability of vessel failure at 50 EFPY has been assessed and is negligible.

* Revised dpa cross-section spectral averaging performed by I. Remec, ORNL.

2.1.5 Possible Future Models

Future modeling will include Monte Carlo techniques discussed in Appendix D and applied to the calculation of dpa rates at one location (Key 5) in Appendix C.

Table 2. VELM neutron group boundaries and original and revised Fe dpa cross-section values

Energy group	Upper energy (eV)	Fe σ_n (original) (cm ²)	Fe σ_γ (revised) (cm ²)	Energy group	Upper energy (eV)	Fe dpa (original) (cm ²)	Fe dpa (revised) (cm ²)
1	1.4918e+7	2.744e-21	2.672e-21	31	1.2277e+5	1.075e-22	1.109e-22
2	1.2214e+7	2.446e-21	2.410e-21	32	8.6517e+4	1.100e-22	1.038e-22
3	1.0000e+7	2.213e-21	2.190e-21	33	5.6562e+4	7.913e-23	7.927e-23
4	8.1873e+6	2.037e-21	2.023e-21	34	5.2475e+4	6.693e-23	6.720e-23
5	6.7032e+6	1.874e-21	1.861e-21	35	3.4307e+4	2.042e-22	2.112e-22
6	5.4881e+6	1.718e-21	1.709e-21	36	2.8501e+4	4.334e-22	4.334e-22
7	4.4933e+6	1.539e-21	1.533e-21	37	2.7000e+4	6.080e-23	6.076e-23
8	3.6788e+6	1.371e-21	1.370e-21	38	2.6058e+4	2.889e-23	2.816e-23
9	3.0119e+6	1.272e-21	1.273e-21	39	2.4788e+4	3.810e-24	3.806e-24
10	2.4660e+6	1.161e-21	1.159e-21	40	2.3579e+4	7.355e-24	7.596e-24
11	2.3457e+6	1.042e-21	1.041e-21	41	1.5034e+4	1.194e-23	1.218e-23
12	2.2313e+6	1.047e-21	1.048e-21	42	9.1188e+3	2.400e-23	2.293e-23
13	2.0190e+6	8.667e-22	8.624e-22	43	5.5308e+3	6.707e-24	6.686e-24
14	1.6530e+6	8.127e-22	8.103e-22	44	3.7074e+3	4.857e-24	4.839e-24
15	1.3534e+6	5.900e-22	5.878e-22	45	3.0354e+3	4.156e-24	4.148e-24
16	1.1080e+6	4.302e-22	4.292e-22	46	2.6126e+3	3.666e-24	3.660e-24
17	9.0718e+5	4.658e-22	4.662e-22	47	2.2487e+3	3.245e-24	3.242e-24
18	7.4274e+5	3.612e-22	3.614e-22	48	2.0347e+3	2.426e-24	2.365e-24
19	6.0810e+5	2.747e-22	2.746e-22	49	1.2341e+3	3.410e-24	3.005e-24
20	5.2340e+5	3.605e-22	3.605e-22	50	7.4852e+2	2.234e-25	2.037e-25
21	4.9787e+5	3.946e-22	4.005e-22	51	4.5400e+2	9.134e-26	9.229e-26
22	3.8774e+5	2.480e-22	2.429e-22	52	2.7536e+2	1.173e-25	1.185e-25
23	3.0197e+5	1.638e-22	1.644e-22	53	1.6702e+2	1.506e-25	1.522e-25
24	2.9849e+5	1.921e-22	1.921e-22	54	1.0130e+2	2.038e-25	2.086e-25
25	2.9721e+5	1.921e-22	1.921e-22	55	4.7851e+1	2.966e-25	3.036e-25
26	2.9452e+5	2.077e-22	2.083e-22	56	2.2603e+1	4.315e-25	4.417e-25
27	2.7324e+5	1.754e-22	1.766e-22	57	1.0677e+1	6.278e-25	6.427e-25
28	2.2371e+5	2.196e-22	2.218e-22	58	5.0435e+0	9.135e-25	9.352e-25
29	1.8316e+5	1.399e-22	1.386e-22	59	2.3824e+0	1.326e-24	1.357e-24
30	1.4996e+5	1.781e-22	1.744e-22	60	1.1253e+0	2.031e-24	2.118e-24
				61	4.1399e-1	5.296e-24	8.481e-24

Table 3. VELM gamma group boundaries and dpa cross-section values

Energy group	Upper energy (eV)	Fe σ_γ (cm ²)	Energy group	Upper energy (eV)	Fe σ_γ (cm ²)
1	1.4000e+7	7.600e-24	16	5.1000e+5	0
2	1.0000e+7	6.249e-24	17	4.0000e+5	0
3	8.0000e+6	4.677e-24	18	3.0000e+5	0
4	7.5000e+6	4.111e-24	19	1.5000e+5	0
5	7.0000e+6	3.314e-24	20	1.0000e+5	0
6	6.0000e+6	2.388e-24	21	7.0000e+4	0
7	5.0000e+6	1.585e-24	22	4.5000e+4	0
8	4.0000e+6	9.269e-25	23	2.0000e+4	0
9	3.0000e+6	5.278e-25			
10	2.5000e+6	3.133e-25			
11	2.0000e+6	1.456e-25			
12	1.5000e+6	4.030e-26			
13	1.0000e+6	4.333e-27			
14	7.0000e+5	0			
15	6.0000e+5	0			

2.2 GEOMETRIC MODEL

2.2.1 General Comments

A cross section of the HFIR core, beam tubes, and vessel at the horizontal midplane* of the core is shown in Fig. 1 for the upgraded design (enlarged HB-2 and HB-4 beam tubes), and a similar cross section for the original design is shown in Fig. 2 of [1]. The corresponding horizontal midplane cross sections for the beam-tube calculation models are shown in Figs. 2 – 6. (Note that the materials in the models shown in Figs. 2 – 6 are assigned consistent designations, which are identified only in the legend in Fig. 2). The HB-2 models are 2D (X,R),[†] and the others are 3D (X,Y,Z). Also, a 2D model (Z,R) [Height, Radius] of the HFIR core, reflector, vessel, and shielding (Fig. 7) was used to calculate boundary fluxes for the beam-tube models and for calculating dpa rates at the vessel wall away from the beam tubes. Interval boundaries, which have not been reported previously, are included in Tables 4 – 9.

The (X,Y) coordinate system for each beam tube is depicted schematically in Fig. 8. The coordinate-system origin for each beam tube is located at the intersection of a core radial vector with the longitudinal axis of the beam tube at a point where a right angle is formed. The longitudinal axis of the beam tube is designated as the X axis. The Z axis is normal to the horizontal midplane with the positive direction toward the top of the core. With this orientation, and when looking through one of the beam tubes HB-2, -3, or -4 toward the vessel wall (in the positive X direction), the positive Y axis is on the left and positive Z is upward. (HB-1 shares a coordinate system with HB-4. As a result, when looking toward the vessel wall along the HB-1 longitudinal axis, the positive Y axis is to the right.) Also included in Fig. 8 are labels for the “sunny” and “shady”[‡] sides of HB-3.

A partial schematic view of a typical beam-tube nozzle is shown in Fig. 9, which includes the relative locations of the nozzle “corner,” “weld,” and “annulus.” The actual corner, before the sharp edge is removed to reduce stress concentration, is the line intersection of the nozzle bore surface and the inner surface of the vessel. In the vessel structural integrity analysis, the nozzle “corner” is a finite

* The term “horizontal midplane” in this context is defined as a horizontal plane through the vertical center of the reactor core and is perpendicular to the positive vertical (Z) axis, which is aligned with the longitudinal axis of the reactor core. The horizontal midplane is also parallel to the longitudinal axis of each of the beam tubes and bisects each beam tube along that axis.

[†] Normally for a 2D model, the radius dimension is cited first and the axial dimension second, that is (R,Z). However, for the beam tube models, the axial dimension is the longitudinal axis of the beam tube, which we refer to as the X dimension, and the radial dimension, R, is the combined Y and Z dimensions. Thus, it is consistent to use the (X,R) coordinate terminology to be consistent with the 3D, that is (X,Y,Z), beam tube terminology. In addition, for the 2D models representing a cross section in the horizontal midplane, we have chosen to replace R with -Y (because Z = 0). The “-” label in front of Y is used because the plotting program outputs the Y values on the right side as positive when in fact they are negative using our convention.

[‡] This concept was described in [1], but for convenience and clarity is also described here. The “sunny” side is the side of the beam tube at the nozzle where a line from the reactor core center to the nozzle corner on that side does not intersect the beam tube. Conversely, on the “shady” side, a similar line must pass through, and hence be “shaded” by, the beam tube as though a beam of light were originating from the core and the tube were opaque. Unfortunately, the analogy is somewhat misleading because the beam tube, which contains a vacuum and does not have sufficiently thick walls to be highly absorbing, is not as effective at attenuating (i.e., “shading”) radiation as an equivalent thickness of water. Consequently, neutron- and gamma-flux (and dpa-rate) values at a location near the nozzle on the inside of the vessel wall on the “shady” side tend to be higher than the values at an equivalent location (equal distance from the core center in the horizontal midplane) on the “sunny” side.

region, as are the “annulus” (the region between the nozzle “corner” region and the “weld” region), and the “weld,” which attaches the nozzle to the vessel wall, as indicated in Fig. 1 (also see Appendix C in [15]).

The calculated values of dpa rate used as input to the vessel structural integrity analysis are the maximum values on the inner surface of each region. The maximum value used for the nozzle corner is at the location of the intersection of the nozzle bore and the vessel inner surface because there is little attenuation of the dpa rate along the nozzle-bore surface. (The value on the “blunted” corner is somewhat less.) Attenuation of the dpa rate through the vessel wall is accounted for in the vessel structural integrity analysis [15, 5].

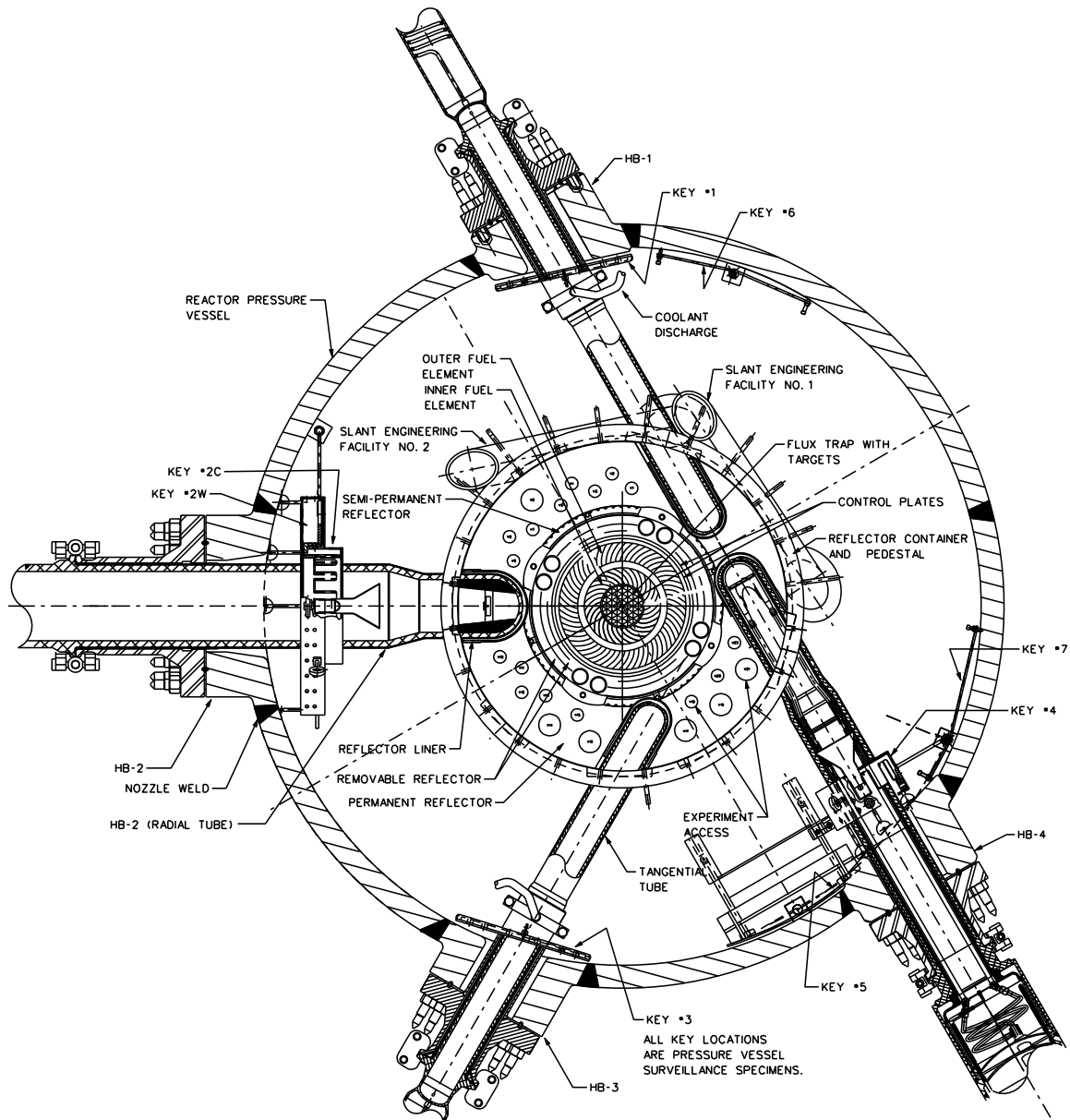


Fig. 1. Cross section of HFIR core, beam tubes, and pressure vessel at horizontal midplane of core for $t > 22.7$ EFPY (100 MW). Surveillance capsule locations (Keys) are shown.

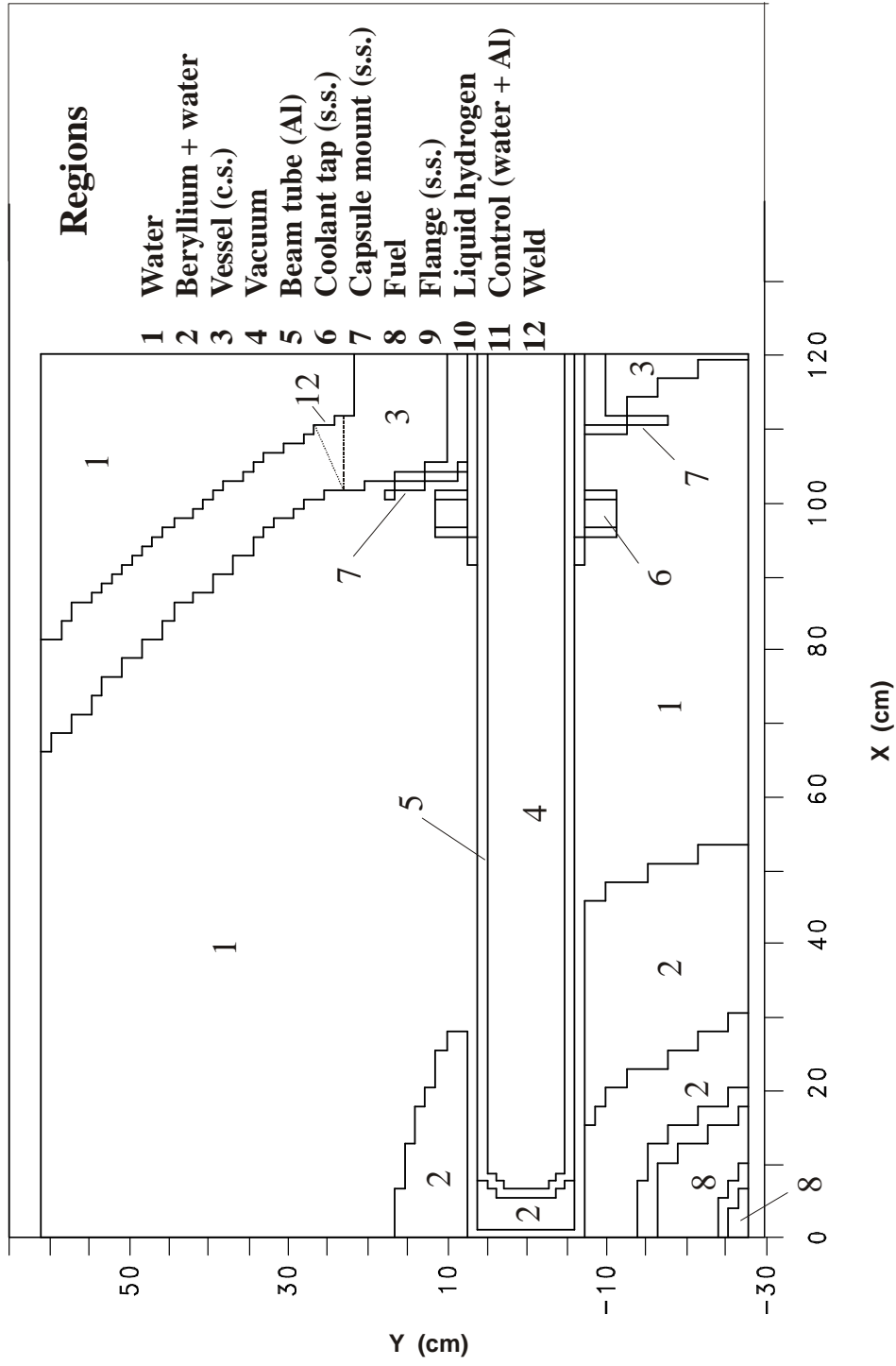


Fig. 2. Geometry/material model for HB-1 and HB-4 (original design; HB-4 shown; HB-1 is mirror image) with specimen mount (Key 4) included.

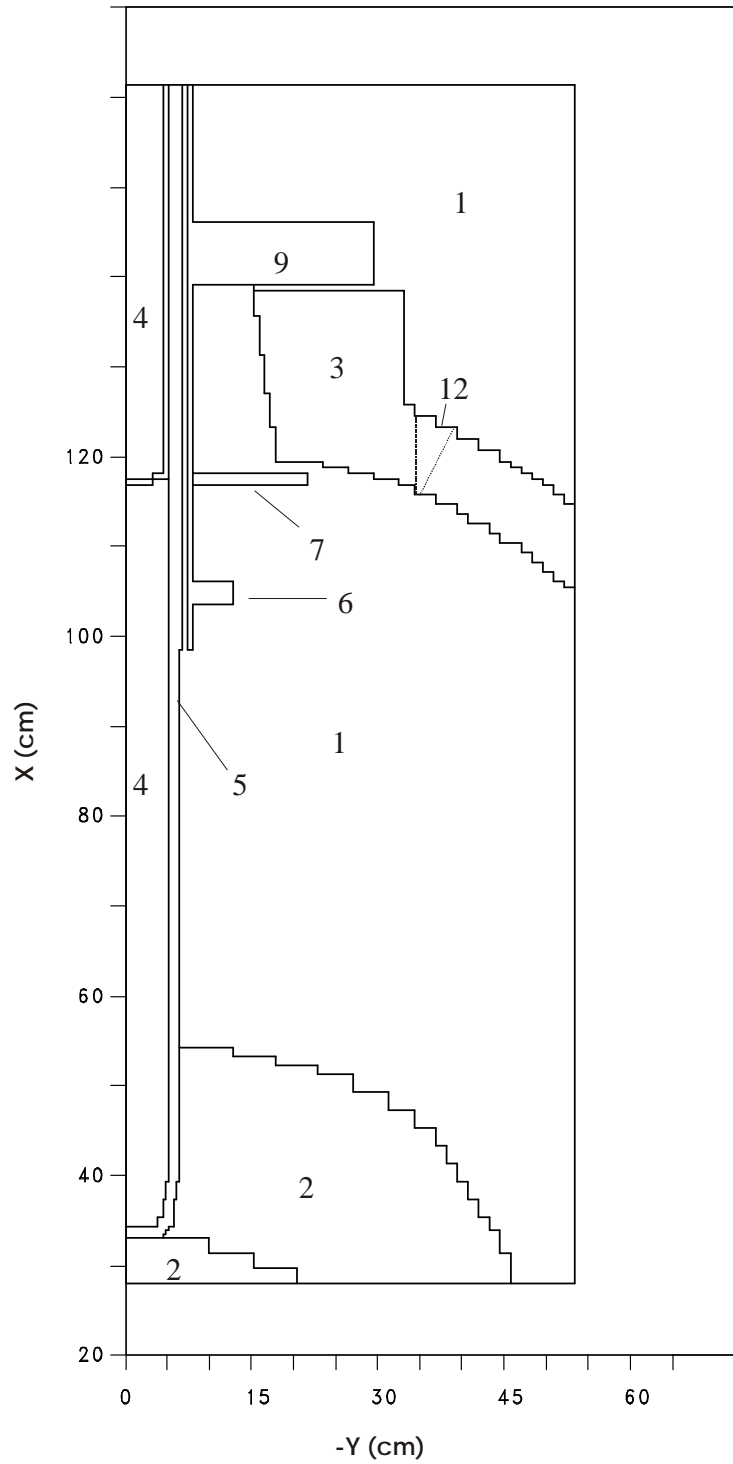


Fig. 3. Geometry/material model for HB-2 (original design). The regions are as shown in Fig. 2.

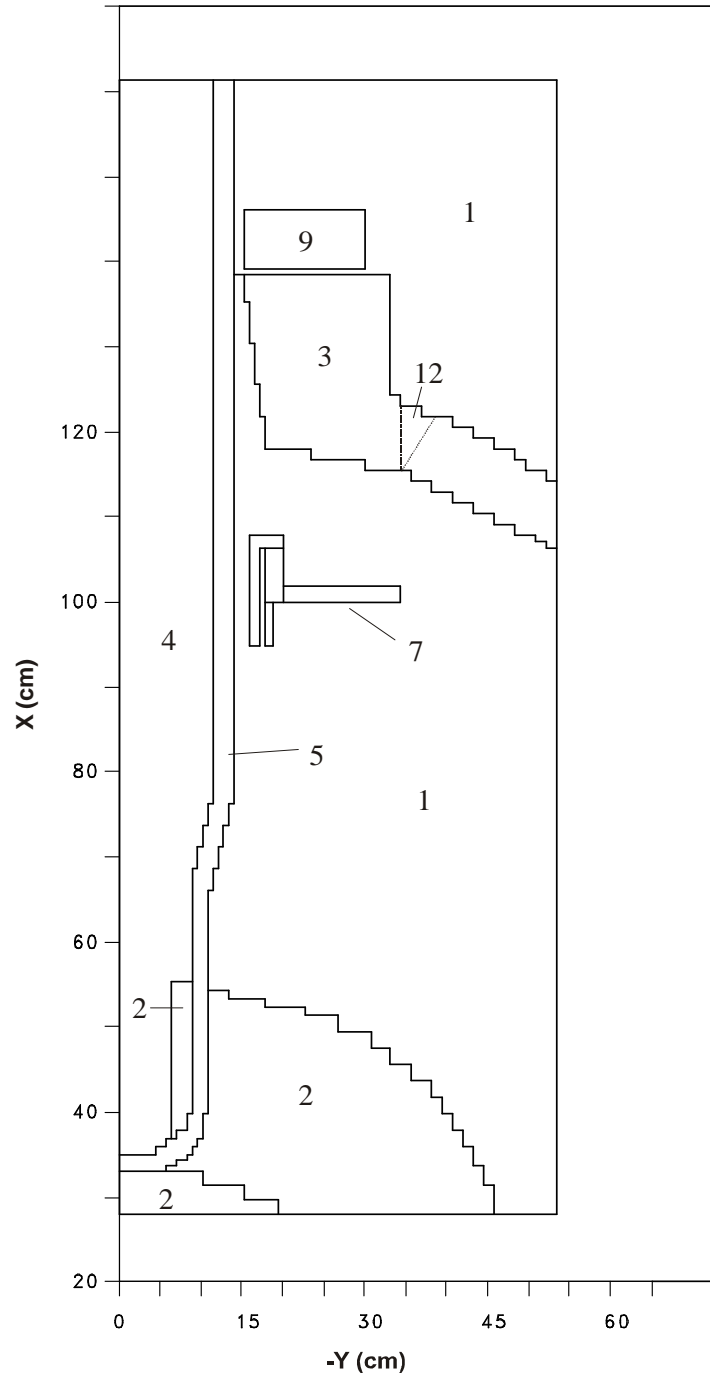


Fig. 4. Geometry/material model for HB-2 (modified design) with specimen mount included. The regions are as shown in Fig. 2.

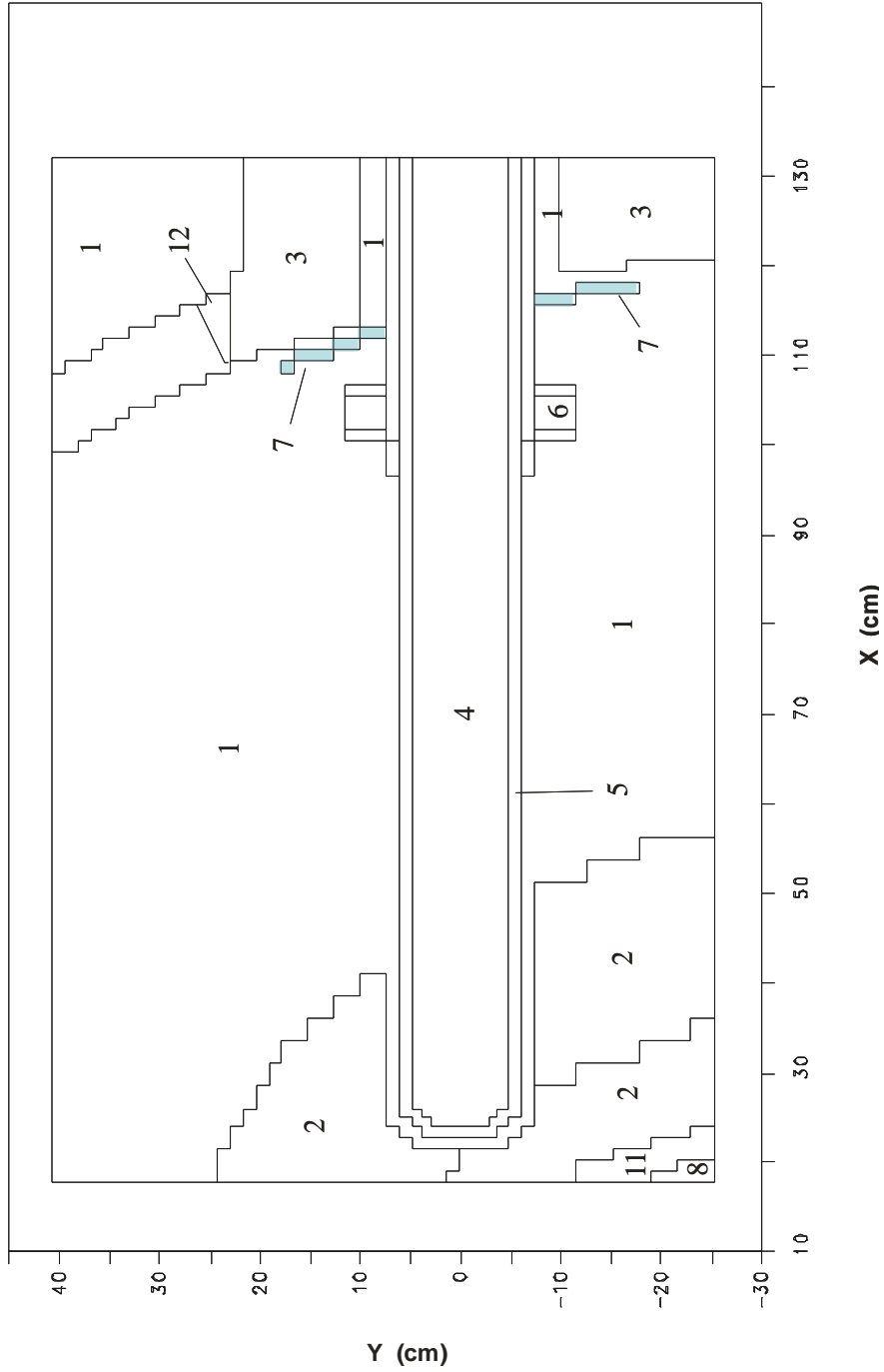


Fig. 5. Geometry/material model for HB-3. The specimen mount is shaded to improve visibility. The regions are as shown in Fig. 2.

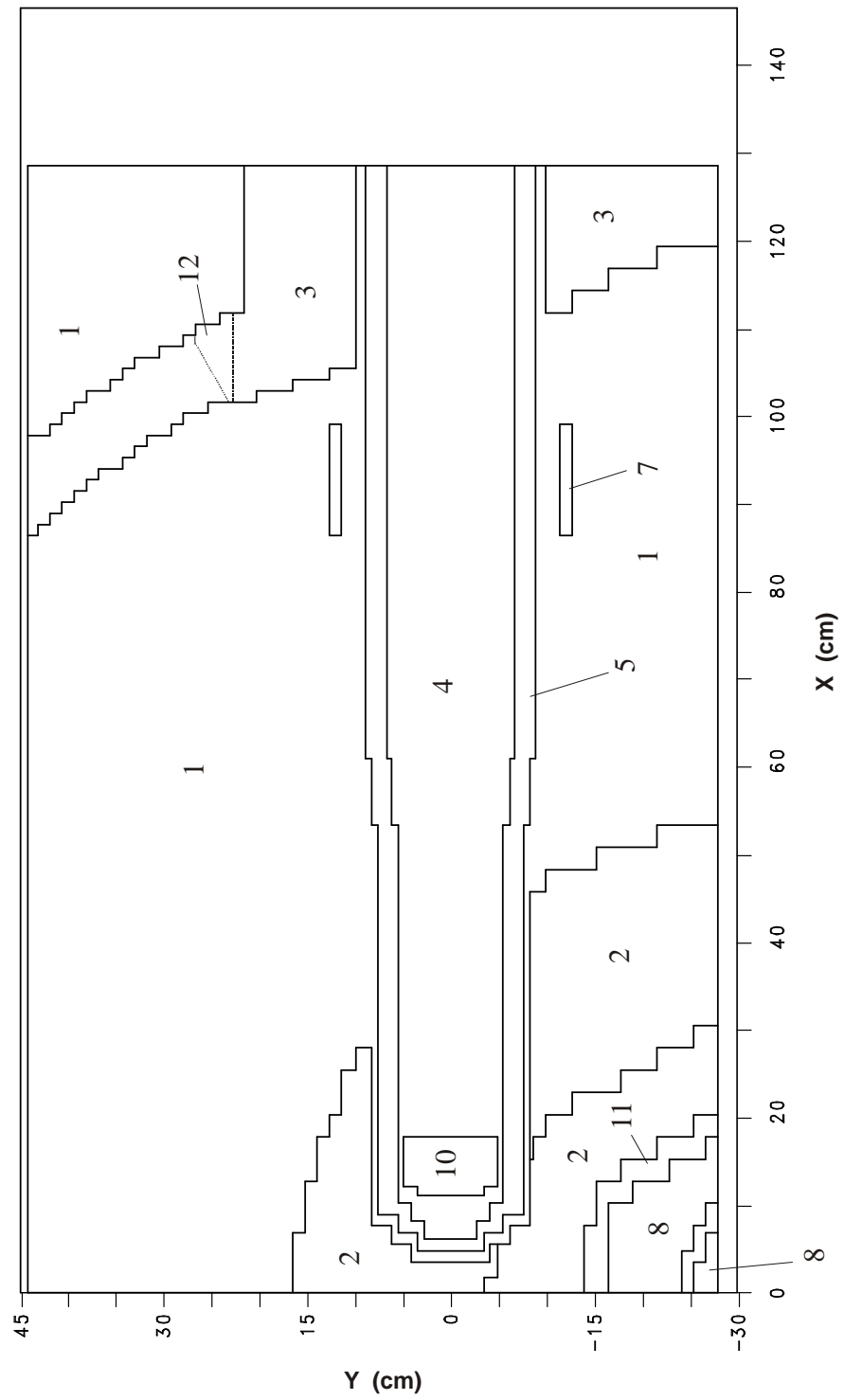


Fig. 6. Geometry/material model for HB-4 (new design) with specimen mount included. The regions are as shown in Fig.2.

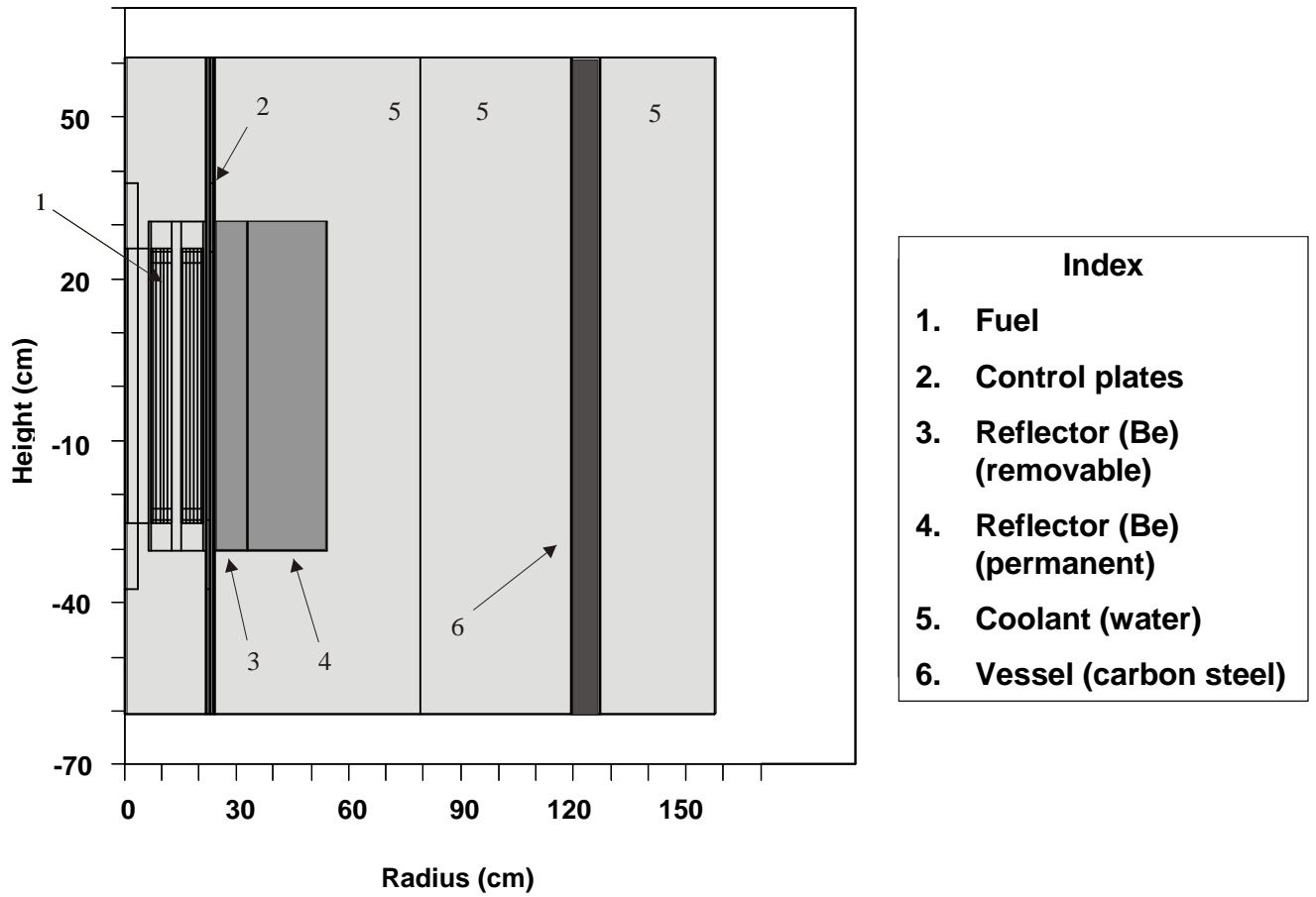


Fig. 7. Geometry/material model for HFIR reactor core.

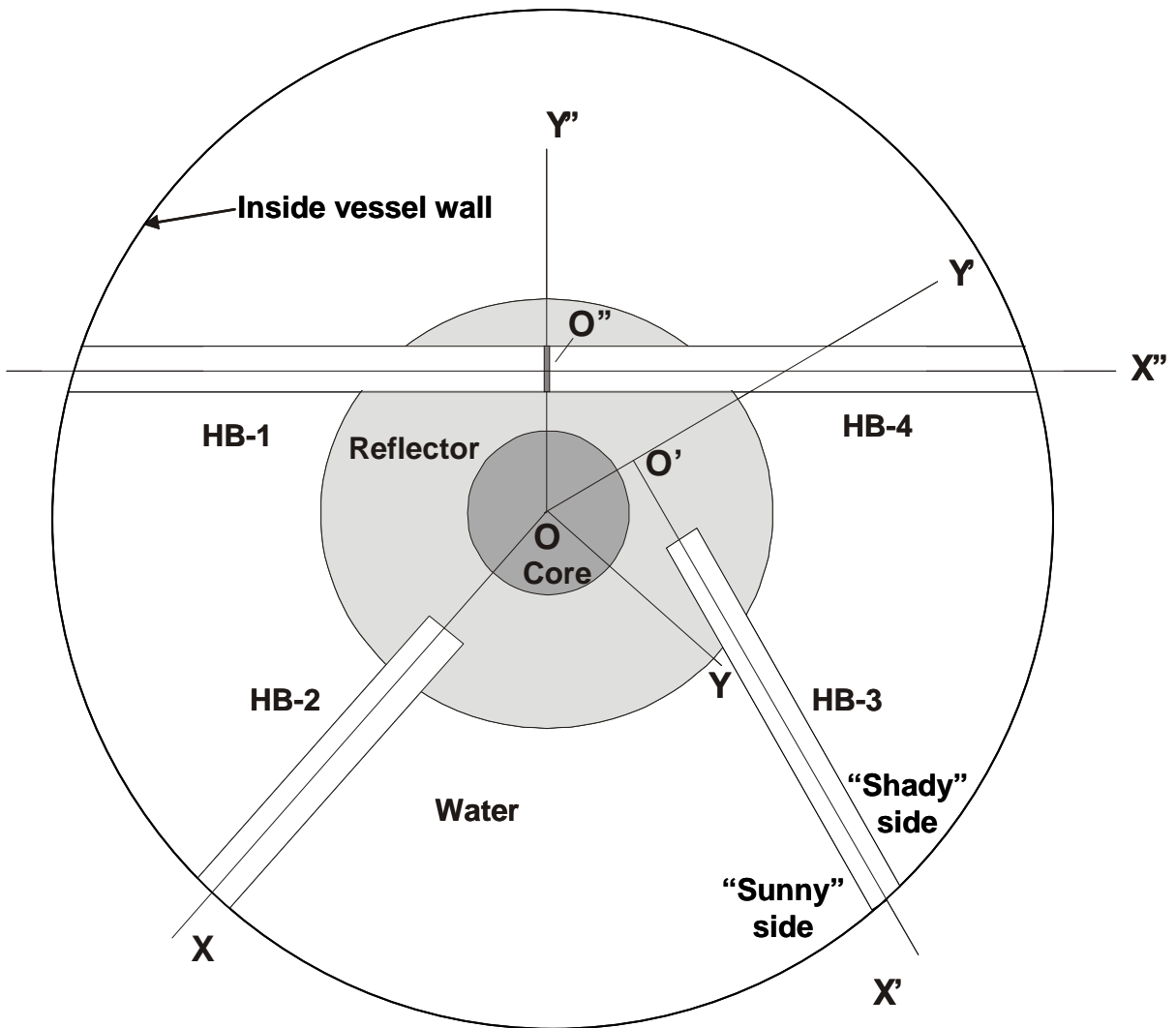


Fig. 8. Coordinate systems for HFIR beam tubes HB-1, -2, -3, -4. For HB-2, the beam tube origin is the center of the core. For HB-1, -3, -4, the origin is the normal intersection of a horizontal line from the center of the reactor core with the beam tube centerline.

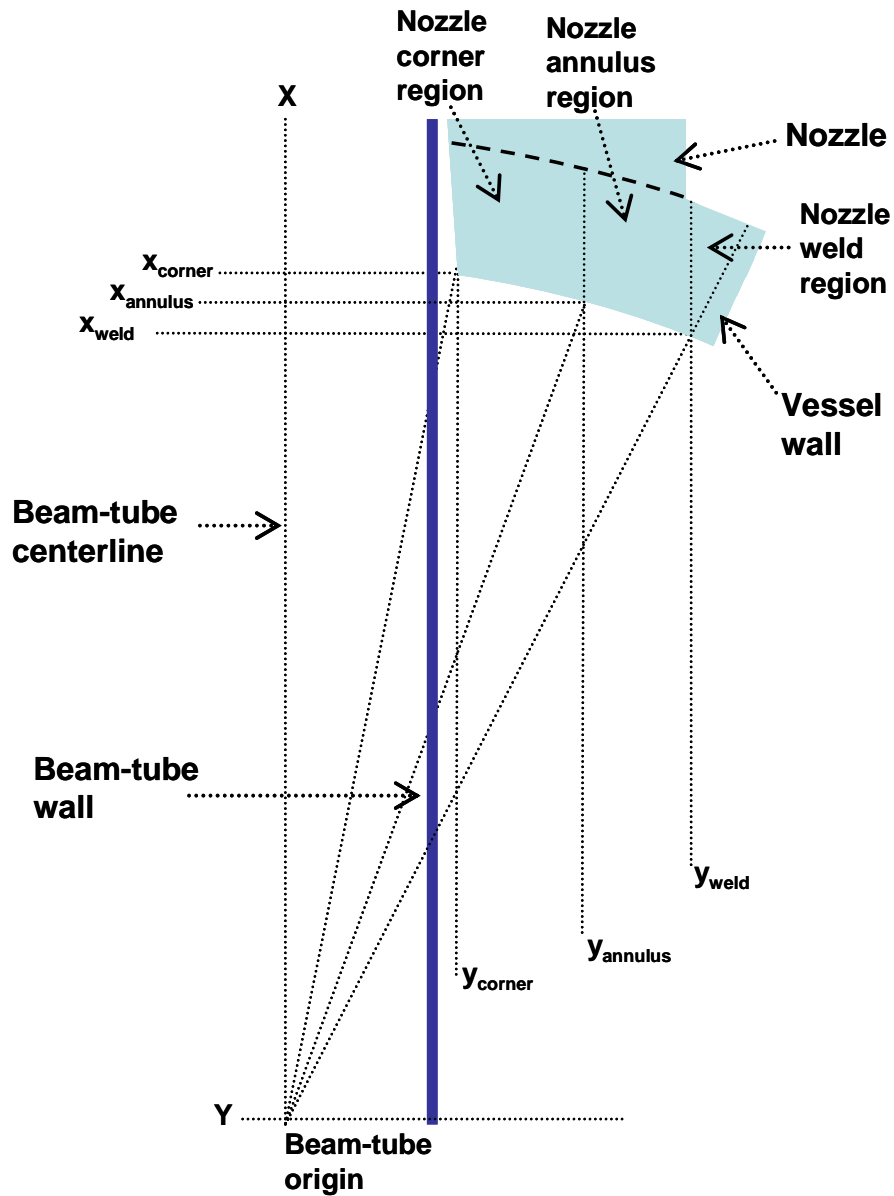


Fig. 9. Schematic horizontal midplane cross section ($Z = 0$) diagram showing location of the nozzle “corner,” “annulus,” and “weld” for the HFIR beam tube HB-2. Horizontal (X, Y)–axis coordinates are shown for the three locations. The Z -axis coordinate projects outward toward the reader (similar for HB-3 and HB-4).

Table 4. Interval boundaries for 3D TORT model for HB-1 and HB-4 (original design)

No.	x ^a	y	z	No.	x	y	No.	x	y
1	0.00	-27.94	0.00	26	50.80	3.76	51	100.33	35.56
2	1.02	-26.67	1.43	27	53.34	4.84	52	101.60	36.83
3	2.46	-25.40	2.85	28	55.88	6.11	53	102.87	38.10
4	3.89	-24.13	3.76	29	58.42	7.38	54	104.14	39.37
5	5.33	-22.86	4.84	30	60.96	8.65	55	105.41	40.64
6	6.60	-21.59	6.11	31	63.50	9.92	56	106.68	41.91
7	7.68	-20.32	7.38	32	66.04	11.43	57	107.95	43.18
8	8.59	-19.05	8.65	33	68.58	12.7	58	109.22	44.20
9	10.02	-17.78	9.92	34	71.12	13.97	59	110.49	45.72 ^b
10	11.44	-16.51	11.43	35	73.66	15.24	60	111.76	46.99
11	12.70	-15.24	13.97	36	76.20	16.51	61	114.30	48.26
12	15.24	-13.97	16.51	37	78.74	17.78	62	116.84	49.53
13	17.78	-12.70	19.05	38	81.28	19.05	63	119.38	50.80
14	20.32	-11.43	21.59	39	83.82	20.32	64	121.92	52.07
15	22.86	-9.92	24.13	40	86.36	21.59	64	124.46	53.04
16	25.40	-8.65	25.40	41	87.63	22.86	66	127.00	54.61
17	27.94	-7.38		42	88.90	24.13	67	128.52	55.88
18	30.48	-6.11		43	90.17	25.40	68		57.15
19	33.02	-4.84		44	91.44	26.67	69		58.42
20	35.56	-3.76		45	92.71	27.94	70		59.69
21	38.10	-2.85		46	93.98	29.21	71		60.96
22	40.64	-1.43		47	95.25	30.48			
23	43.18	0.00		48	96.52	31.75			
24	45.72	1.43		49	97.79	33.02			
25	48.26	2.85		50	99.06	34.29			

^a Boundaries in centimeters.^b Y-dimension values beyond boundary number 58 are for the extended model only.

Table 5. Interval boundaries for 2D DORT model for HB-2 (original design)

No.	x ^a	r	No.	x	r	No.	x	r	No.	x	r
1	27.94	0.00	26	53.23	9.84	51	103.51	26.40	76	128.43	50.80
2	29.63	0.48	27	54.23	10.80	52	104.14	27.00	77	129.86	52.07
3	31.33	0.95	28	56.44	11.75	53	104.78	27.61	78	131.29	53.34
4	33.02	1.43	29	58.65	12.70	54	105.41	28.21	79	132.72	
5	33.44	1.91	30	60.86	13.34	55	106.05	28.81	80	134.14	
6	33.87	2.22	31	63.07	13.97	56	107.12	29.41	81	135.57	
7	34.29	2.54	32	65.28	14.61	57	108.20	30.01	82	137.00	
8	35.29	2.86	33	67.49	15.24	58	109.28	30.61	83	138.43	
9	36.28	3.18	34	69.70	15.88	59	110.36	31.22	84	139.07	
10	37.28	3.49	35	71.91	16.51	60	111.44	31.82	85	140.46	
11	38.28	3.81	36	74.12	17.15	61	112.52	32.42	86	141.86	
12	39.27	4.13	37	76.33	17.78	62	113.60	33.02	87	143.26	
13	40.27	4.45	38	78.54	18.42	63	114.68	34.29	88	144.65	
14	41.27	4.76	39	80.75	19.05	64	115.76	35.56	89	146.05	
15	42.27	5.08	40	82.96	19.69	65	116.84	36.83	90	147.00	
16	43.26	5.40	41	85.17	20.32	66	117.48	38.10	91	149.38	
17	44.26	5.72	42	87.38	20.96	67	118.11	39.37	92	151.76	
18	45.26	6.03	43	89.59	21.59	68	118.74	40.64	93	154.15	
19	46.25	6.35	44	91.80	22.19	69	119.38	41.91	94	156.53	
20	47.25	6.71	45	94.01	22.79	70	120.65	43.18	95	158.91	
21	48.25	7.00	46	96.22	23.39	71	121.92	44.45	96	161.29	
22	49.24	7.30	47	98.43	24.00	72	123.19	45.72			
23	50.24	7.62	48	99.70	24.60	73	124.46	46.99			
24	51.24	7.94	49	100.97	25.20	74	125.73	48.26			
25	52.24	8.89	50	102.24	25.80	75	127.00	49.53			

^a Boundaries in centimeters.

Table 6. Interval boundaries for 2D DORT model for HB-2 (modified design)

No.	x ^a	r	No.	x	R	No.	x	r	No.	x
1	27.94	0.00	26	53.26	15.88	51	100.82	33.02	76	133.59
2	29.63	0.64	27	54.23	16.51	52	101.77	34.29	77	135.21
3	31.33	1.27	28	54.74	17.15	53	103.27	35.56	78	136.82
4	33.02	1.91	29	55.25	17.78	54	104.77	36.83	79	138.43
5	33.66	2.54	30	55.88	18.73	55	106.27	38.10	80	139.07
6	34.29	3.18	31	57.15	19.39	56	107.04	39.37	81	140.46
7	34.93	3.81	32	59.69	20.05	57	107.80	40.64	82	141.86
8	35.89	4.45	33	62.23	20.72	58	109.06	41.91	83	143.26
9	36.86	5.08	34	64.77	21.38	59	110.33	43.18	84	144.65
10	37.82	5.72	35	66.04	22.04	60	111.59	44.45	85	146.05
11	38.79	6.35	36	68.58	22.70	61	112.86	45.72	86	147.00
12	39.75	6.99	37	71.12	23.36	62	114.12	46.99	87	149.38
13	40.72	7.62	38	73.66	24.02	63	115.38	48.26	88	151.76
14	41.68	8.26	39	76.20	24.68	64	116.65	49.53	89	154.15
15	42.65	8.89	40	77.47	25.34	65	117.91	50.80	90	156.53
16	43.61	9.53	41	79.94	26.01	66	119.18	52.07	91	158.91
17	44.58	10.16	42	82.42	26.67	67	120.45	53.34	92	161.29
18	45.54	10.80	43	84.89	27.33	68	121.72			
19	46.51	11.43	44	87.36	27.99	69	122.99			
20	47.47	12.07	45	89.83	28.65	70	124.26			
21	48.44	12.70	46	92.31	29.31	71	125.53			
22	49.40	13.34	47	94.78	29.97	72	127.14			
23	50.37	13.97	48	96.37	30.73	73	128.76			
24	51.33	14.61	49	97.96	31.50	74	130.37			
25	52.30	15.24	50	99.86	32.26	75	131.98			

^a Boundaries in centimeters.

Table 7. Interval boundaries for 3D TORT model for HB-3

No.	x ^a	y	z	No.	x	y	No.	x	y
1	17.78	-25.40	0	26	71.29	6.11	51	115.57	38.10
2	18.97	-24.13	1.43	27	73.81	7.38	52	116.84	39.37
3	21.15	-22.86	2.85	28	76.34	8.65	53	118.11	40.64
4	21.34	-21.59	3.76	29	78.86	9.92	54	119.38	
5	22.61	-20.32	4.84	30	81.38	11.43	55	120.65	
6	23.88	-19.05	6.11	31	83.90	12.70	56	121.92	
7	24.96	-17.78	7.38	32	86.43	13.97	57	124.46	
8	25.87	-16.51	8.65	33	88.95	15.24	58	127.00	
9	28.39	-15.24	9.92	34	91.47	16.51	59	129.54	
10	30.92	-13.97	11.43	35	94.00	17.78	60	132.08	
11	33.44	-12.70	13.97	36	96.52	19.05			
12	35.96	-11.43	16.51	37	97.79	20.32			
13	38.49	-9.92	19.05	38	99.06	21.59			
14	41.01	-8.65	21.59	39	100.33	22.86			
15	43.53	-7.38	24.13	40	101.60	24.13			
16	46.06	-6.11	26.67	41	102.87	25.40			
17	48.58	-4.84		42	104.14	26.67			
18	51.10	-3.76		43	105.41	27.94			
19	53.63	-2.85		44	106.68	29.21			
20	56.15	-1.43		45	107.95	30.48			
21	58.67	0		46	109.22	31.75			
22	61.20	1.43		47	110.49	33.02			
23	63.72	2.85		48	111.76	34.29			
24	66.24	3.76		49	113.03	35.56			
25	68.76	4.84		50	114.30	36.83			

^a Boundaries in centimeters.

Table 8. Interval boundaries for 3D TORT model for HB-4 (modified design)

No.	x ^a	y	z	No.	x	y	z	No.	x	y
1	0.00	-27.94	0.00	26	38.10	-4.13	25.40	51	92.71	17.78
2	1.75	-26.67	1.43	27	40.64	-3.49		52	93.98	19.05
3	3.51	-25.40	2.50	28	43.18	-2.74		53	95.25	20.32
4	4.78	-24.13	2.74	29	45.72	-1.50		54	96.52	21.59
5	5.57	-22.86	2.85	30	48.26	0.00		55	97.79	22.86
6	6.12	-21.59	3.49	31	50.80	1.50		56	99.06	24.13
7	6.84	-20.32	4.13	32	53.34	2.74		57	100.33	25.40
8	7.63	-19.05	4.45	33	55.88	3.49		58	101.60	26.67
9	8.19	-17.78	4.94	34	58.42	4.13		59	102.87	27.94
10	8.90	-16.51	5.48	35	60.96	4.45		60	103.38	29.21
11	10.02	-15.24	6.19	36	63.50	4.94		61	104.14	30.48
12	10.25	-13.97	6.67	37	66.04	5.48		62	105.41	31.75
13	11.12	-12.70	7.62	38	68.58	6.19		63	106.68	33.02
14	11.44	-12.07	8.26	39	71.12	6.67		64	107.95	34.29
15	12.12	-11.43	8.65	40	73.66	7.62		65	109.22	35.56
16	12.70	-9.92	8.89	41	76.20	8.26		66	110.49	36.83
17	15.24	-8.89	9.92	42	78.74	8.65		67	111.76	38.10
18	17.78	-8.65	11.43	43	81.28	8.89		68	114.30	39.37
19	20.32	-8.26	12.07	44	83.82	9.92		69	116.84	40.64
20	22.86	-7.62	12.70	45	86.36	11.43		70	119.38	41.91
21	25.40	-6.68	13.97	46	87.63	12.07		71	121.92	43.18
22	27.94	-6.19	16.51	47	88.90	12.70		72	124.46	44.20
23	30.48	-5.48	19.05	48	90.17	13.97		73	127.00	
24	33.02	-4.94	21.59	49	90.68	15.24		74	128.52	
25	35.56	-4.46	24.13	50	91.44	16.51				

^aBoundaries in centimeters.

Table 9. Interval boundaries for 2D DORT model for HFIR vessel

No.	z^a	r	No.	z	r	No.	r	No.	r
1	-60.82	0.00	36	1.00	22.18	71	43.44	106	116.90
2	-58.49	0.89	37	3.00	22.34	72	44.44	107	117.37
3	-56.17	1.55	38	5.00	22.50	73	45.44	108	117.83
4	-53.84	2.22	39	7.00	22.66	74	47.15	109	118.29
5	-51.51	2.88	40	9.00	22.82	75	48.86	110	118.76
6	-49.19	3.55	41	11.00	22.99	76	50.56	111	119.22
7	-46.86	4.26	42	13.00	23.15	77	52.27	112	119.54
8	-44.53	4.97	43	15.00	23.30	78	53.98	113	120.45
9	-42.20	5.69	44	17.00	23.46	79	56.48	114	121.36
10	-39.88	6.40	45	19.00	23.62	80	58.98	115	122.28
11	-37.55	6.77	46	21.00	23.97	81	61.48	116	123.19
12	-35.78	7.14	47	21.88	24.13	82	63.98	117	124.10
13	-34.02	7.15	48	22.75	24.76	83	66.48	118	125.02
14	-32.25	7.50	49	23.80	25.40	84	68.98	119	125.93
15	-30.48	8.50	50	24.85	26.03	85	71.48	120	126.84
16	-29.21	9.50	51	25.13	26.67	86	73.98	121	127.16
17	-27.94	10.50	52	25.40	27.31	87	76.48	122	127.66
18	-26.67	11.50	53	26.67	27.94	88	78.98	123	128.16
19	-25.40	12.50	54	27.94	28.58	89	81.48	124	128.66
20	-25.13	12.59	55	29.21	29.21	90	83.98	125	129.16
21	-24.85	12.60	56	30.48	29.85	91	86.48	126	131.16
22	-23.80	13.34	57	32.25	30.48	92	88.98	127	133.16
23	-22.75	14.41	58	34.02	31.11	93	91.48	128	137.24
24	-21.88	15.15	59	35.78	31.73	94	93.98	129	141.32
25	-21.00	15.16	60	37.55	32.35	95	96.48	130	145.40
26	-19.00	15.50	61	39.88	32.98	96	98.98	131	149.48
27	-17.00	16.50	62	42.20	33.98	97	101.48	132	153.56
28	-15.00	17.50	63	44.53	34.98	98	103.98	133	157.64
29	-13.00	18.50	64	46.86	35.98	99	106.48		
30	-11.00	19.50	65	49.19	36.99	100	108.98		
31	-9.00	20.50	66	51.51	38.10	101	111.48		
32	-7.00	20.99	67	53.84	39.21	102	113.98		
33	-5.00	21.00	68	56.17	40.32	103	114.98		
34	-3.00	21.77	69	58.49	41.43	104	115.98		
35	-1.00	22.02	70	60.82	42.44	105	116.44		

^a Boundaries in centimeters.

Use of a 2D model for HB-2 introduced a potential problem. As indicated in Fig. 10, because it wraps around the longitudinal axis of the beam tube (X axis), the 2D model treats the vessel as a sphere rather than a cylinder. As a result, “surface” locations above or below the horizontal midplane ($Z = 0$) are inboard of the actual surface, as shown in Fig. 10. This does not, however, introduce a significant error, assuming axisymmetry, for two reasons: (1) as indicated graphically later, the dpa-rate gradient in the X direction in the vicinity of the nozzle is very small, and (2) because of the actual cylindrical geometry of the core and vessel and the nonaxisymmetric design of the beryllium insert at the inboard end of the beam tube [16], the actual dpa rates in the vicinity of the nozzle might not be axisymmetric, as assumed with the use of a 2D model. This was investigated with a 3D discrete-ordinates model as well as a Monte Carlo model [16]. In both cases the dpa rates at 12:00 were less than those at 3:00, but only by ~5%. Thus, the 2D model for HB-2 was considered adequate.

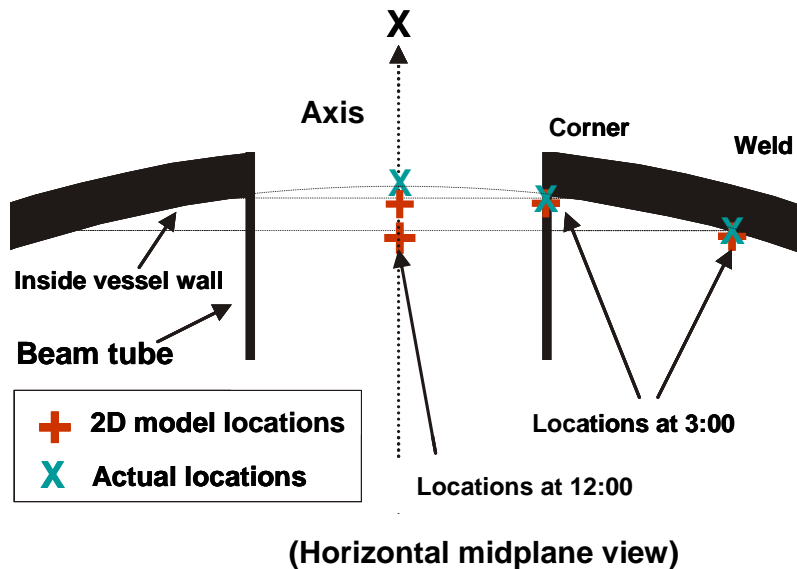


Fig. 10. Schematic of the offset locations at nozzle corner and weld at 12:00 positions caused by representation with a 2D model.

2.2.2 Specific Comments Regarding Input to the Structural Integrity Analysis

The geometric models for the calculation of dpa rates to be used as input to the structural integrity analysis [5] are those shown in Figs. 2, 3, and 5 for $t < 22.7$ EFPY and in Figs. 2 (Key 1) and 6 for $t > 22.7$ EFPY. As indicated in Figs. 2 and 6, Keys 5, 6, and 7 were not included in the HB-1 and -4 models. More recent calculations than those made for [5] indicate that the absence of Keys 1, 3, and 4 for $t < 22.7$ EFPY had a negligible effect on the outcome of the vessel structural integrity analysis results.

Key 5 was not included in the models because it is below the horizontal midplane and is located behind an ion chamber (IC3) and its lead shielding. The original intent with regard to Key 5 was to determine if displacement of water shielding (for neutrons) with lead would result in a higher dose in the vessel wall behind the chamber. A Key 5 capsule removed in 1983 indicated otherwise, and, as known now, gammas, rather than neutrons, dominate the dose at that location and would be shielded more effectively by the lead. Only one Key 5 capsule was removed for testing, and the others were transferred to Key 2W.

**3. CALCULATED (UPGRADE 2) NEUTRON AND GAMMA FLUXES AND dpa RATES
FOR THE SURVEILLANCE AND DOSIMETRY CAPSULE LOCATIONS
AND THE 31 REGIONS USED IN THE VESSEL
STRUCTURAL INTEGRITY ANALYSIS**

**3.1 CALCULATED dpa RATES (UPGRADE 2) FOR ALL SURVEILLANCE AND
DOSIMETRY CAPSULE LOCATIONS**

The geometric and analytic models used for these calculations are those described in Sect. 2 for application to Sect. 5 of the most recent vessel structural integrity analyses [5]. Neutron and gamma dpa rates are presented in Tables 10 – 15 for all of the surveillance-capsule Key locations and in Table 16 for the dosimetry-dedicated capsules located at the inner surface of the HB-2 nozzle. For $t > 22.7$ EFPY, the models included Keys 1, 2C, 2W, 3, and 4 and used the improved set of neutron dpa cross sections (“Upgrade 2”).

Table 10. Key 1 and 4 dpa rates (HB-4 original design, $t < 22.7$ EFPY (100 MW))

Position		Location XYZ (in.)	IJK cell no.	dpa rate (10^{-12}) s^{-1}	
Key 4	Key 1			Neutron	Gamma
1,5	6,10	42.80, -2.41, 4.35	57 17 9	1.238 (1.169) ^a	1.264
2,4	7,9	43.31, -4.17, 2.51	58 14 6	1.162 (1.103)	1.287
3	8	43.51, -4.81, 0.0	58 13 1	1.320 (1.231)	1.352
6,10	1,5	41.37, +2.41, 4.35	54 28 9	1.779 (1.713)	1.050
7,9	2,4	40.85, +4.17, 2.51	53 31 6	2.107 (2.042)	0.946
8	3	40.65, +4.81, 0.0	53 32 1	2.439 (2.368)	0.899

^a Upgrade 1 dpa rates in parentheses for comparison.

Table 11. Key 2, 2C, and 2W dpa rates (HB-2)^{a,b,c}

Key	Position in key	Location XR (in.)	JI cell no. ^d	dpa rate (10^{-12}) s^{-1}	
				Neutron ^d	Gamma
2	All	45.79, 7.02	(64 36), (64 37)	3.56	1.72
2C	All	38.94, 6.5	(49 26), (49 27)	153	10.1
2W	All	39.69, 12.0	(50 47), (51,47)	4.28	2.58

^a $t < 22.7$ EFPY for Key 2, and $t > 22.7$ EFPY for Keys 2C and 2W.

^b HB-2 original beam-tube model for $t < 22.7$ EFPY and enlarged beam tube model for $t > 22.7$ EFPY.

^c Improved neutron dpa cross sections for $t < 22.7$ EFPY and $t > 22.7$ EFPY.

^d I interval corresponds to radius, R, and J to location on longitudinal axis, X. For positions represented by multiple cell numbers, the dpa rate results are the average values for those cells.

Table 12. Key 3 dpa rates (HB-3)

Positions	Location XYZ (in.)	IJK cell no.	dpa rate (10^{-12}) s ⁻¹	
			Neutron	Gamma
1,5	45.51, -2.45, 4.35	51 15 9	2.498 (2.413) ^a	1.139
2,4	45.93, -4.24, 2.51	51 12 6	2.497 (2.385)	1.256
3	46.08, -4.89, 0.0	52 11 1	2.720 (2.610)	1.155
6,10	44.39, 2.45, 4.35	48 26 9	3.529 (3.415)	1.160
7,9	43.97, 4.24, 2.51	47 26 9	3.981 (3.844)	1.201
8	43.82, 4.89, 0.0	47 30 1	4.691 (4.542)	1.171

^a Upgrade 1 dpa rates in parentheses for comparison.

Table 13. Key 4 dpa rates^a (HB-4, modified design, $t > 22.7$ EFPY (100 MW))

Positions	Location XYZ (in.)	IJK cell no.	dpa rate (10^{-12}) s ⁻¹	
			Neutron	Gamma
1,5	36.44, -1.39, 4.28	50 26 17	16.39	3.453
2,4	36.44, -3.64, 2.65	50 16 (11,12) ^b	10.17	3.111
3	36.44, -4.50, 0.0	50 (14,15) 1	15.92	3.319
6,10	36.44, 1.39, 4.28	50 33 17	17.69	3.501
7,9	36.44, 3.64, 2.65	50 43 (11,12)	13.10	2.915
8	36.44, 4.50, 0.0	50 (44,45) 1	21.22	3.461

^a Model includes surveillance-capsule mount addition.

^b For positions represented by multiple cell numbers, the dpa rate results are the average values for those cells.

Table 14. Key 6 dpa rates (HB-1)^a

Positions	Location XYZ (in.)	IJK cell no.	dpa rate (10^{-12}) s ⁻¹	
			Neutron	Gamma
1	38.3, 10.5, 0.0	48 43 1	0.5142 (0.5027) ^b	1.828
2	36.8, 12.3, 0.0	45 47 1	0.4511 (0.4458)	1.973
3	35.4, 14.1, 0.0	42 51 1	0.3960 (0.3938)	1.750
4	33.9, 16.0, 0.0	39 54 1	0.3798 (0.3774)	1.718
5	31.0, 18.9, 0.0	36 60 1	0.3326 (0.3312)	1.816
6	29.2, 20.4, 0.0	35 63 1	0.2887 (0.2882)	1.743
7	27.4, 21.9, 0.0	33 66 1	0.2732 (0.2728)	1.760
8	25.6, 23.4, 0.0	31 69 1	0.2413 (0.2409)	2.055

^a Model includes surveillance-capsule mount addition.

^b Values in parentheses were obtained using original dpa cross sections. Otherwise, values reflect updated cross sections.

Table 15. Key 7 dpa rates (HB-4, original design, $t < 22.7$ EFPY (100 MW))

Positions	Location XYZ (in.)	IJK cell no.	dpa rate (10^{-12}) s^{-1}	
			Neutron	Gamma
1	26.2, 22.7, 0.0	32 68 1	0.2467 (0.2465) ^a	1.860
2	27.9, 21.0, 0.0	33 64 1	0.3393 (0.3375)	1.935
3	29.6, 19.4, 0.0	35 61 1	0.3474 (0.3454)	1.906
4	31.3, 17.8, 0.0	37 58 1	0.3479 (0.3461)	1.785
5	33.1, 16.2, 0.0	39 55 1	0.3437 (0.3422)	1.606
6	34.8, 14.6, 0.0	41 52 1	0.3848 (0.3826)	1.748
7	37.5, 11.6, 0.0	46 46 1	0.4262 (0.4198)	1.786
8	38.8, 9.7, 0.0	49 42 1	0.5016 (0.4894)	1.841

^a Upgrade 1 dpa rates in parentheses for comparison.

Table 16. dpa rates at HB-2 nozzle corner and weld dosimeters [$t > 22.7$ EFPY (100 MW)]

Dosimeter	Location XR (in.)	JI cell no. ^a	dpa rate (10^{-12}) s^{-1}	
			Neutron	Gamma
2D1C	46.44, 7.0	(64 28), (64 29)	74.9	3.56
2D2C	45.92, 7.0	(64 28), (64 29)	74.9	3.56
2D1W	46.44, 13.56	(62 51), (62 52) (61 51), (61 52)	2.05	1.31
2D2W	45.92, 13.56	(62 51), (62 52) (61 51), (61 52)	2.05	1.31
2D3W	44.44, 13.56	(62 51), (62 52) (61 51), (61 52)	2.05	1.31

^a I interval corresponds to radius, R, and J to location on longitudinal axis, X. For positions represented by multiple cell numbers, the dpa rate results are the average values for those cells.

3.2 CALCULATED dpa RATES (UPGRADE 2) FOR THE HFIR VESSEL 31 REGIONS USED IN THE VESSEL STRUCTURAL INTEGRITY ANALYSIS (SECT. 5 OF [5])

These calculations were performed with models that included Keys 1, 2, 3, and 4 for $t < 22.7$ EFPY and $t > 22.7$ EFPY and with the improved set of dpa cross sections. The results are presented in Table 17.

Table 17. Neutron and gamma calculated dpa rates for the 31 vessel regions considered in the vessel structural integrity study

Time period EFPY ^a	Region	Beam-tube or vessel location	x,y ^b	Table number ^c	dpa rates (10 ⁻¹² s ⁻¹)	
					Neutron	Gamma
<22.7	1,2,3	HB-2	69,37	5	3.06	1.13
	4,5	HB-2	68,46	5	1.21	1.20
	6,7	HB-2	64,63	5	0.270	1.11
>22.7	1,2,3	HB-2	65,29	6	61.2	3.8
	4,5	HB-2	64,37	6	17.3	1.7
	6,7	HB-2	63,52	6	2.53	1.0
>0	8,9,10	HB-3	49,29	7	6.07	1.07
	11,12	HB-3	48,31	7	3.46	0.92
	13,14	HB-3	45,39	7	0.802	1.28
HB-4	15,16,17	HB-1/4 ^d	55,31	4	3.08	0.927
<22.7	18,19	HB-1/4 ^d	54,33	4	1.80	0.776
HB-1 > 0	20,21	HB-1/4 ^d	52,41	4	0.546	1.34
>22.7	15,16,17	HB-4	62,44	8	9.43	2.09
	18,19	HB-4	61,47	8	3.90	1.52
	20,21	HB-4	58,55	8	0.702	1.09
>0	29	Cir. weld ^e	8,112	9	0.0405	0.652
	30,31	HMP ^f	35,112	9	0.0836	0.940

^aEffective full power years based on full power = 100 MW.

^bMesh indices along the model axes defining locations from appropriate model. For 2D beam-tube models, indices are for X and R axes, where R is the radial axis. For the 2D reactor model (for Regions 29, 30, and 31), the indices are for Z and R, where Z is the vertical axis of the reactor.

^cTable in this publication that shows mesh intervals for the appropriate model.

^dRegions shown for HB-4. Regions for HB-1 are 22–28 with same arrangement.

^eVessel circumferential weld below core.

^fVessel horizontal midplane.

3.3 CALCULATED NEUTRON AND GAMMA FLUXES AND dpa RATES PERTAINING TO THE DOSIMETRY OBTAINED FROM HFIR FUEL CYCLES 400 AND 401

3.3.1 Dosimeters and Their Locations

The dosimeters used for fuel cycles 400 and 401 and for which neutron and gamma fluxes and dpa rates were calculated are listed in Table 18. Their locations are indicated in Figs. 11 and 12 (Key 3) in this report and Fig. 3 (Keys 3 and 7) and (Key 2) in [3], as well as in the Z = 0 plane (horizontal midplane) of dpa-rate iso-plots in Figs. 13 (HB-2, $t > 22.7$ EFPY) and 14 (HB-3).

Iso-dpa-rate curves for the enlarged HB-4 model, showing the revised Key 4 surveillance-capsule mount, are also shown in Fig. 15. However, it is noted that dosimeters were not used in Key 4 during cycles 400 and 401.

The 2D (Z,R) model described in Sect. 2 was used to calculate the dpa rates at K7,P1, and its general location in that model, along with iso-dpa-rate curves, is shown in Fig. 16.

Table 19 (Key 2 dosimeters), Table 20 (Keys 2C and 2W), and Table 21 (Key 7) quantify the locations, compare those specified with the DORT model locations, and indicate the numbers of the cells for which an average value of dpa rate was obtained.

Table 18. Dosimetry-dedicated capsules used for HFIR fuel cycles 400 and 401

Key/dosimeter	Position in Key	Capsule ID	Capsule type	Fuel cycle
2C	1	DOS-8	B	400
	4	DOS-9	B	400
2W	8	DOS-1	A	400
	32	DOS-2	A	400
3	3	DOS-3	A	400
	8	DOS-4	A	400
	10	DOS-5	A	400
7	1	DOS-6	A	400
2C/2W	2D1C ^a	HRB2-1G	N/A ^b	400
	2D2C	HRB2-1G	N/A	400
	2D1W	HRB2-2G	N/A	400
	2D2W	HRB2-2G	N/A	400
	2D3W	HRB2-3G	N/A	400
	2D1C	HRB2-1A	N/A	401
	2D1W	HRB2-1A	N/A	401
	2D2C	HRB2-2A	N/A	401
	2D2W	HRB2-3A	N/A	401
	2D3W	HRB2-3A	N/A	401

^a2D1C, 2D2C, 2D1W, etc. are tubular capsules/dosimeters.

^bN/A = not applicable.

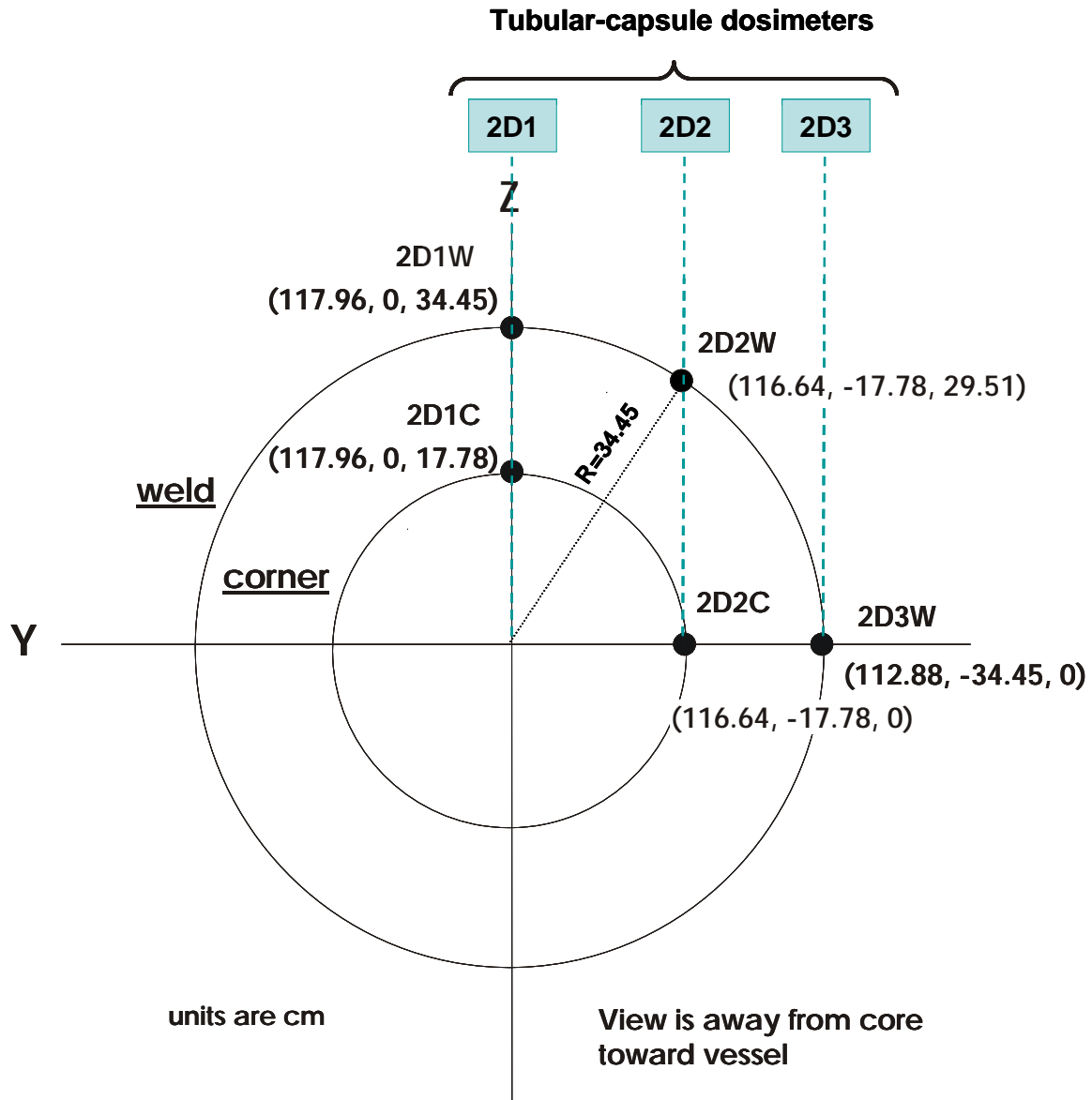


Fig. 11. Locations (x,y,z coordinates) for HB-2 tubular dosimeters 2D1C, 2D2C, 2D1W, 2D2W, and 2D3W. (+X-axis is perpendicular to image away from reader.)

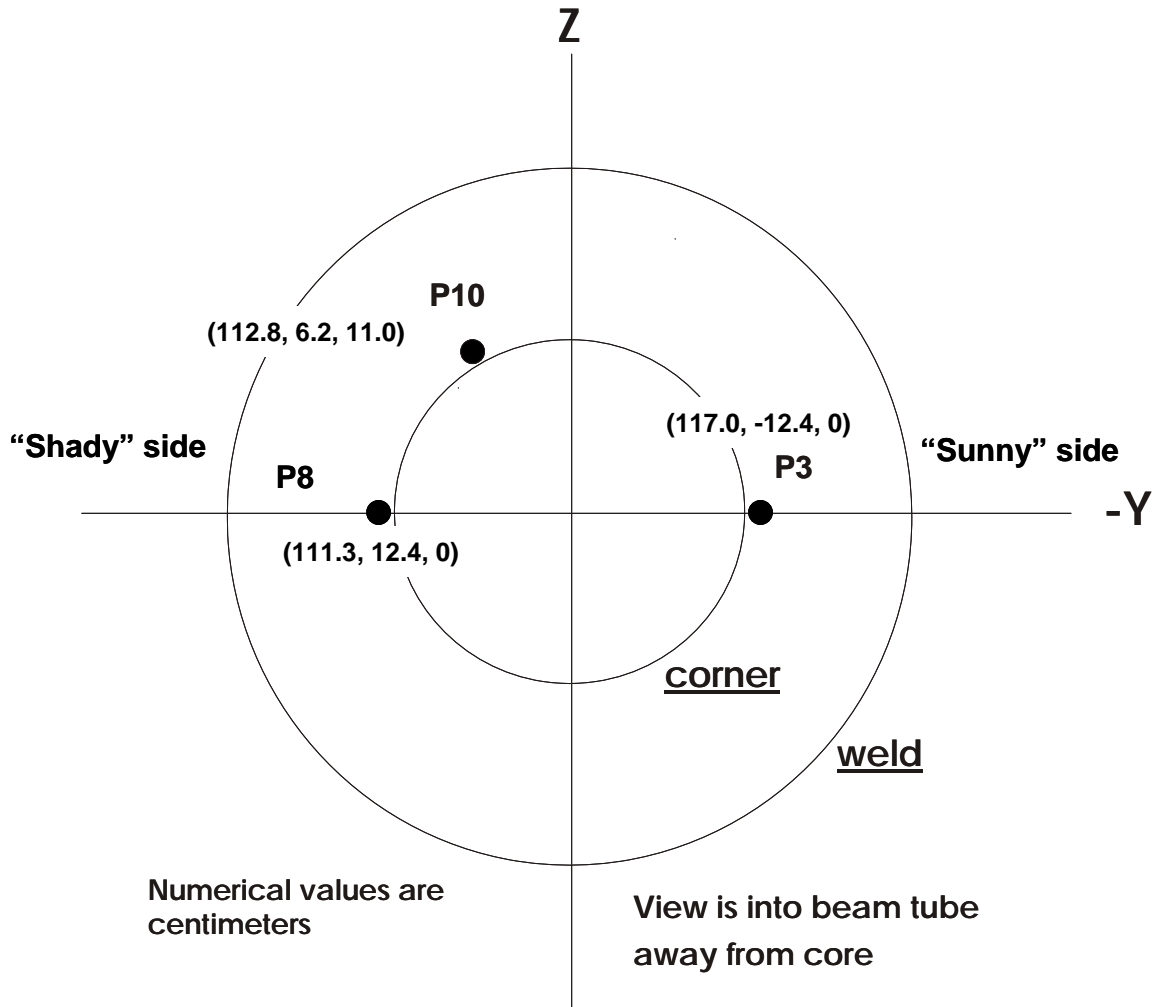


Fig. 12. Locations of dosimeters in (x,y,z) coordinate dimensions at HB-3. +X-axis is along longitudinal axis of beam tube (normal to page) away from the reactor core.

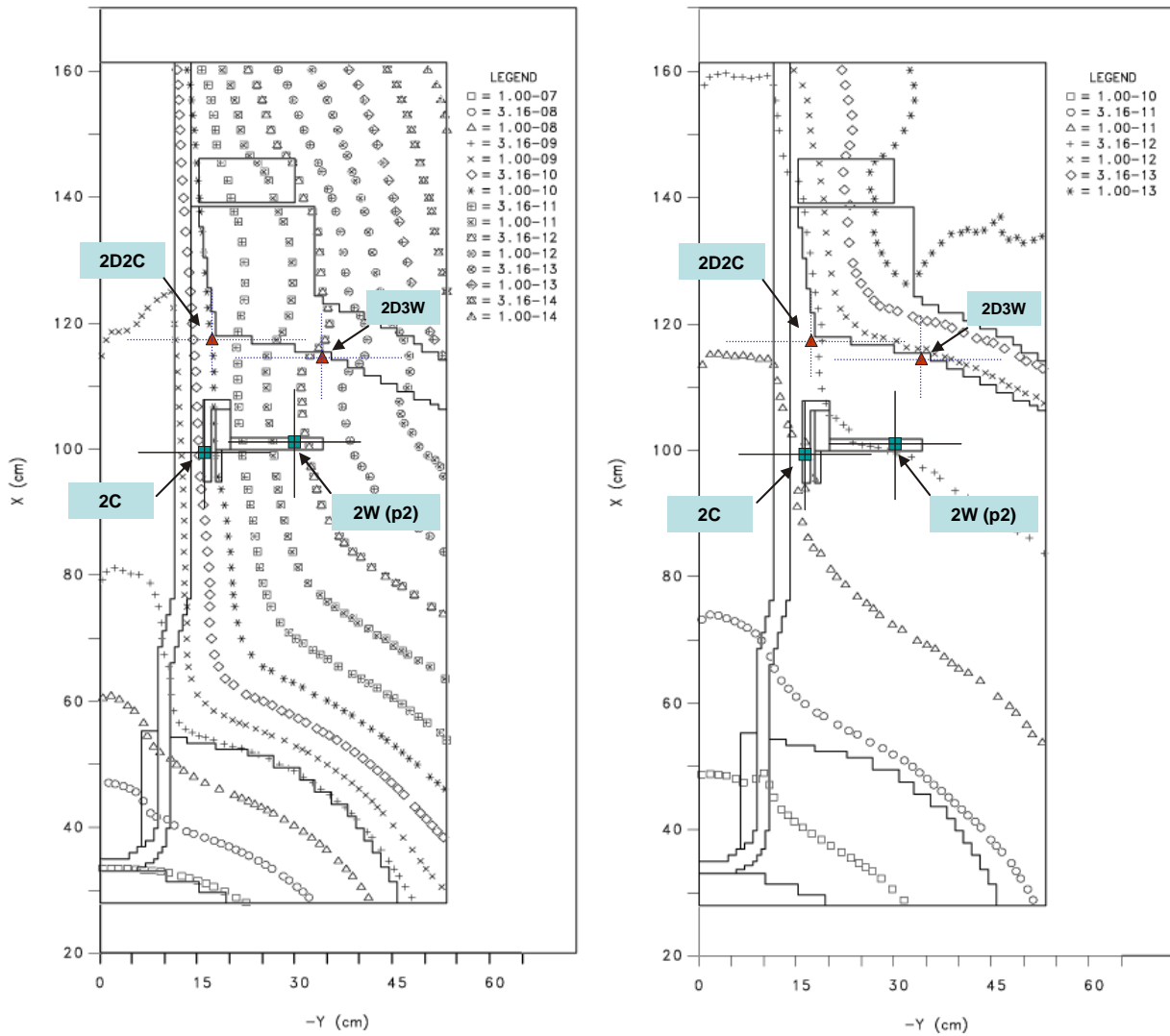


Fig. 13. Iso-plots of neutron (left) and gamma (right) dpa rates for HB-2 (modified, enlarged design) showing approximate axial and radial locations of dosimeters.

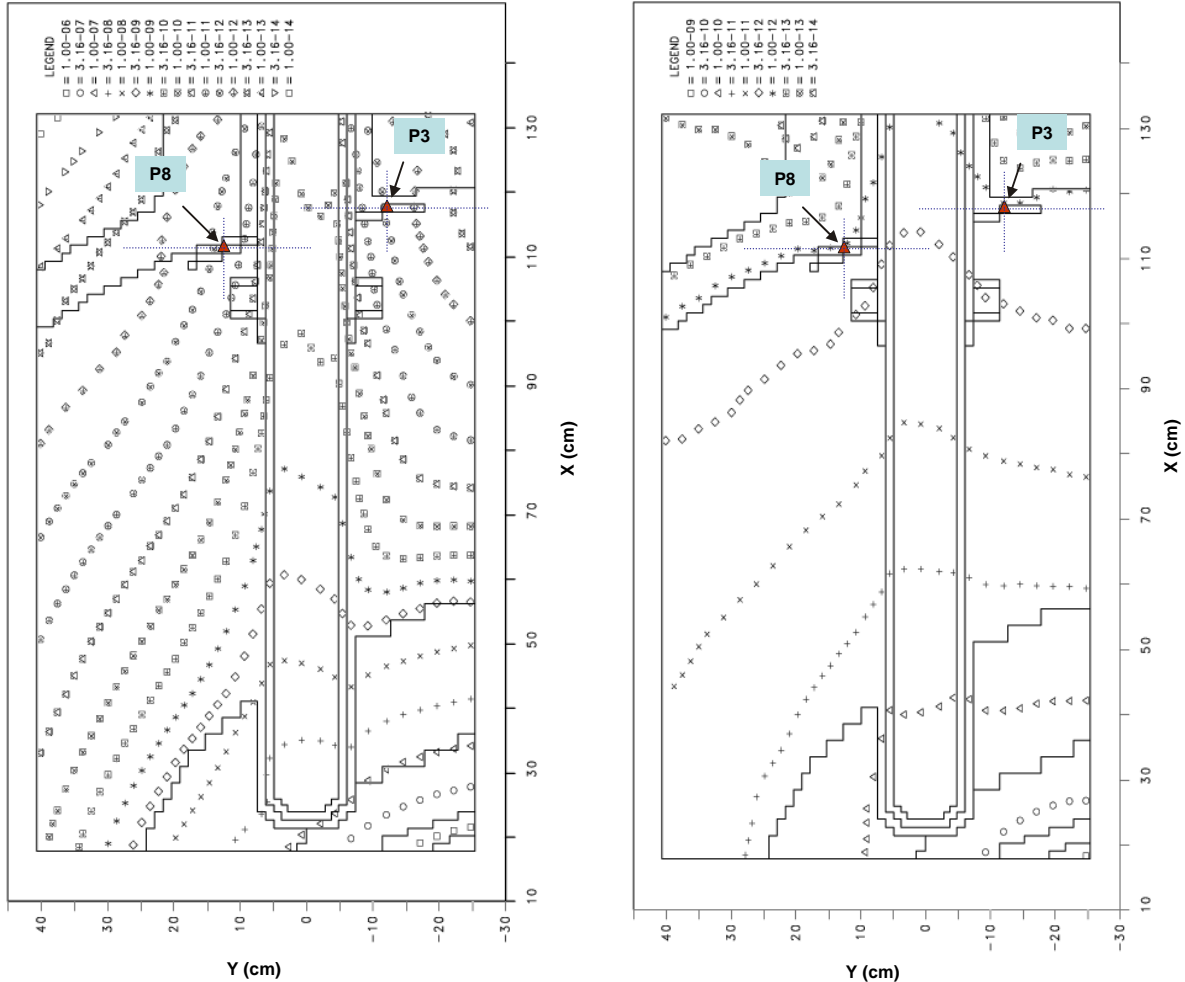


Fig. 14. Iso-plots of neutron (left) and gamma (right) dpa rates for HB-3 showing approximate locations of dosimeters (Key 3) in the reactor horizontal midplane ($Z = 0$).

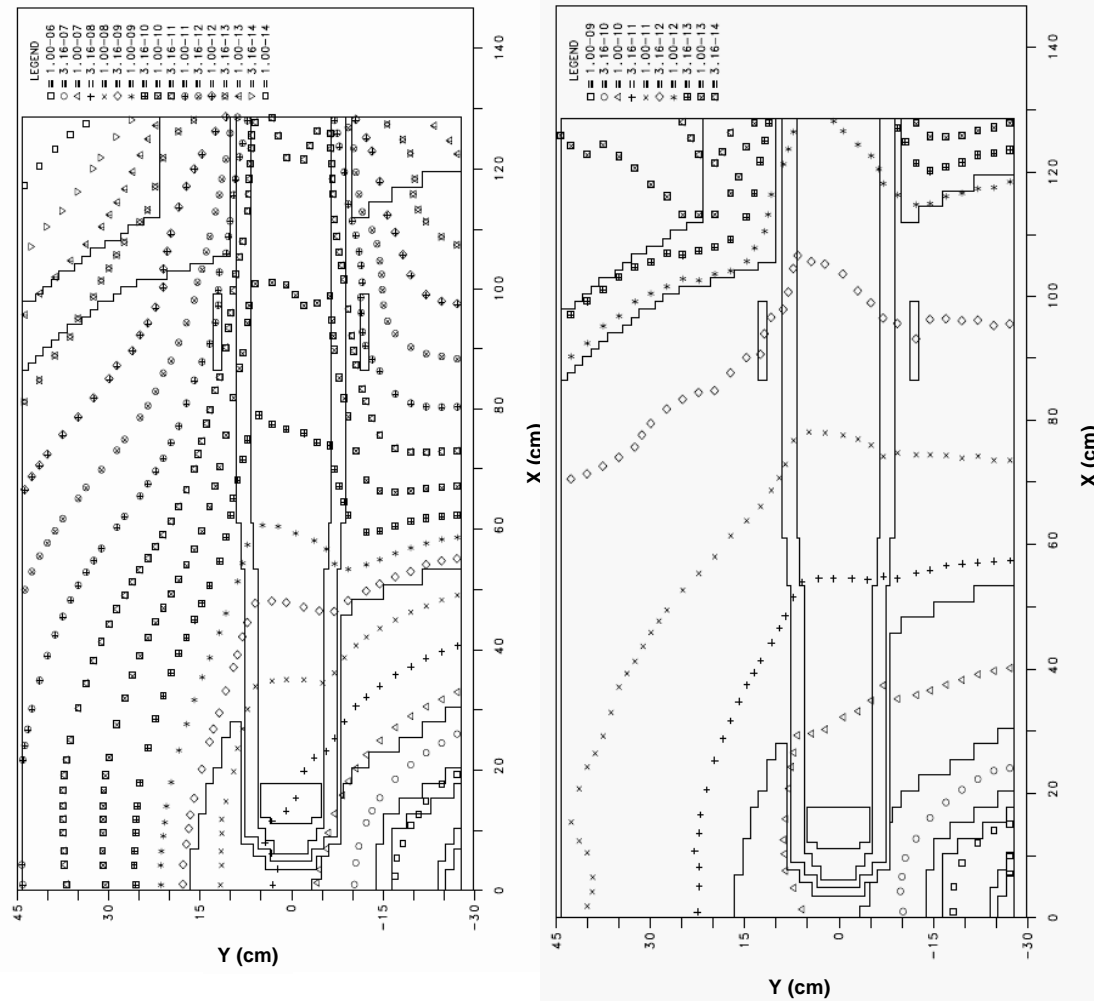


Fig. 15. Iso-plots of neutron (left) and gamma (right) dpa rates for HB-4 (modified, enlarged design).

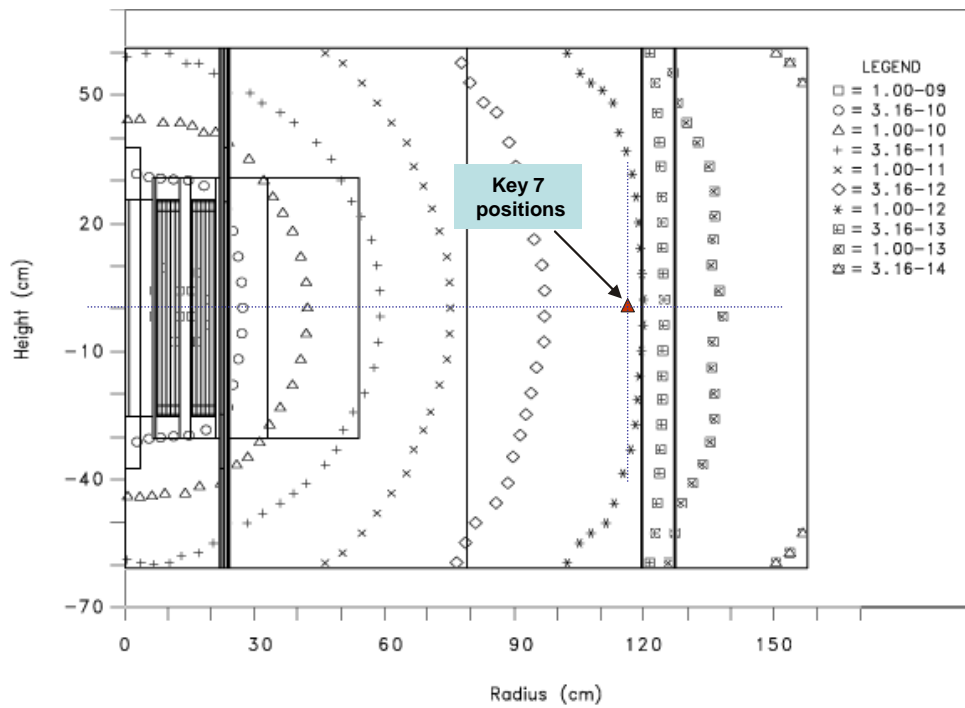
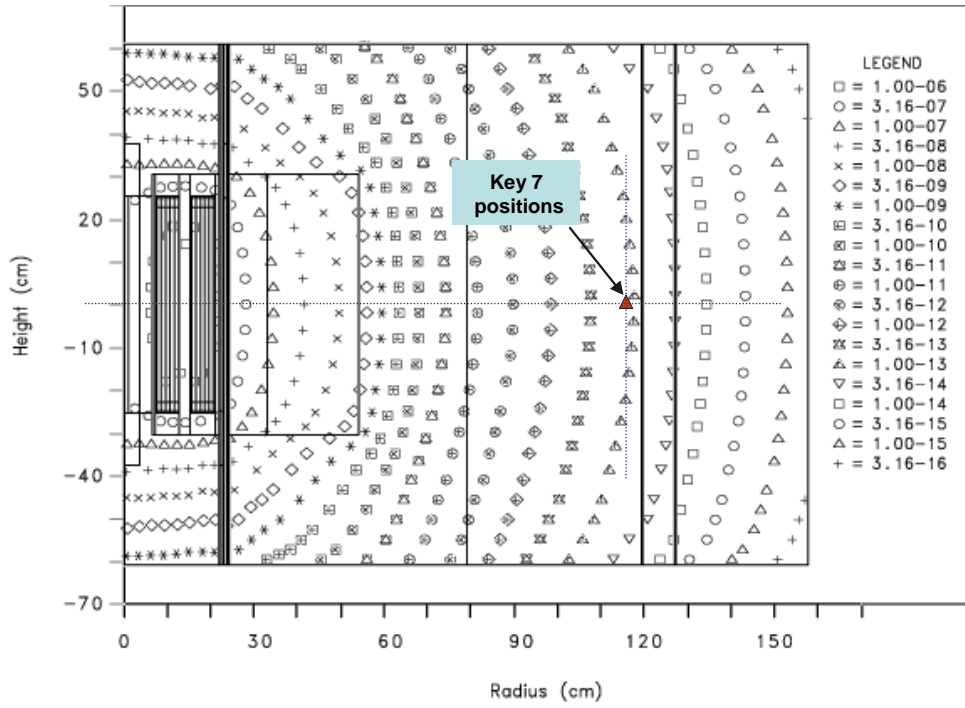


Fig. 16. Iso-plots of neutron (top) and gamma (bottom) dpa rates for the HFIR reactor model showing approximate location of Key 7 positions at the vessel wall.

Table 19. Actual vs DORT model locations of HB-2 nozzle and weld tubular dosimeters

Name	HB-2 (x,y,z) location [cm (in.)]			HB-2 2D model (r,x) location ^a [cm (in.)]		No. cells avgd.	DORT model cell IDs (x,r) ^c
	x	y	z	x	r		
2D1C	117.96 (46.44)	0 (0)	17.78 (7)	116.65 (45.92)	17.86 ^b (7.03)	2	(64,28),(64,29)
2D2C	116.64 (45.92)	-17.78 (-7)	0 (0)	116.65 (45.92)	17.86 ^b (7.03)	2	(64,28),(64,29)
2D1W	117.96 (46.44)	0 (0)	34.45 (13.56)	114.12 (44.93)	34.29 (13.50)	4	(62,51),(62,52) (61,51),(61,52)
2D2W	116.64 (45.92)	-17.78 (-7)	29.51 (11.62)	114.12 (44.93)	34.29 (13.50)	4	(62,51),(62,52) (61,51),(61,52)
2D3W	112.88 (44.44)	-34.45 (-13.56)	0 (0)	114.12 (44.93)	34.29 (13.50)	4	(62,51),(62,52) (61,51),(61,52)

^a Locations are averaged centers of cells. Dosimeter locations are axisymmetric; r is radius.

^b The boundary between meshes 28 and 29 in the radial dimension is exactly 17.78 cm. However, the average radius of the mesh centers is the slightly displaced value of 17.86 cm, as shown.

^c See Table 6.

Table 20. Actual vs DORT model locations of HB-2 capsules

Name (K,P)	HB-2 (x,r) location [cm (in.)]		HB-2 2D model (r,x) location ^a [cm (in.)]		No. cells avgd.	DORT model cell IDs (x,r) ^c
	x	r	x	r		
2C, 1-16	98.91 (38.94)	16.51 (6.5)	98.91 (38.94)	16.51 (6.5)	2	(49,26),(49,27)
2W, 1-32 (p1) ^b	100.8 (39.69)	31.75 (12.5)	100.8 (39.69)	31.88 (12.55)	2	(50,49), (51,49)
2W, 1-32 (p2)	100.8 (39.69)	30.48 (12)	100.8 (39.69)	30.35 (11.95)	2	(50,47), (51,47)
2W, 1-32 (p3)	100.8 (39.69)	29.21 (11.5)	100.8 (39.69)	29.31 (11.54)	4	(50,45), (51,45), (50,46), (51,46)

^a Locations are averaged centers of cells. Capsule locations are axisymmetric; r is radius.

^b For 2W, three dosimeter positions (p1,2,3) within each capsule are used.

^c See Table 6.

Table 21. Actual vs DORT model locations of vessel capsule

Name	Key 7 (x,y,z) location [cm (in.)] ^a			Reactor model (r,z) location ^b [cm (in.)]		DORT model cell ID (z,r)
	x	y	z	z	r	
P1	66.55 (26.2)	57.66 (22.7)	0.0 (0.0)	0.0 (0.0)	116.67 (45.93)	(35,105)

^a Based on HB-4 coordinate axes offset 38.35 cm from core center, $r = \sqrt{x^2 + (y + \text{"offset"})^2}$.

^b Center of cell.

3.3.2 Calculated Multigroup Neutron and Gamma Fluxes

Multigroup neutron and gamma fluxes and dpa cross sections are required as input to the conversion of dosimeter activities to dpa rates. The fluxes calculated for the dosimetry program discussed in [3] are presented in Tables 22 – 29, and the dpa cross sections are the “revised” ones in Table 2. (The flux values in Tables 22 – 29 are for a reactor power of 85 MW rather than 100 MW, which is used elsewhere in this report.) Because of the assumed axisymmetry for HB-2 (2Dl model), the calculated fluxes for 2D1C and 2D2C are the same, as are the values for 2D1W, 2D2W, and 2D3W. (The assumption of axisymmetry is supported by 3D discrete-ordinates and Monte Carlo calculations discussed in [16].) The calculations were performed for the beginning-of-cycle (BOC) and end-of-cycle (EOC)* conditions for all but K3, P3, 8, 10, for which only EOC calculations were made. The geometric and analytic models used in the calculations were the same as those described in Sects. 2.1 and 2.2 for calculation of dpa rates for [5] for $t > 22.7$ EFPY.

3.3.3 Calculated dpa Rates

The calculated dpa rates for each of the dosimeters are taken from Tables 11 (Key 2C, 2W), 12 (Key 3), 15 (Key 7), and 16 (HB-2 nozzle “corner” and “weld”) and are summarized in Table 30.

3.4 CALCULATED NEUTRON AND GAMMA dpa RATES PERTAINING TO HFIR DOSIMETRY OBTAINED IN 1993

The dosimetry program in 1993 [17] was similar to that conducted during HFIR fuel cycles 400 and 401 in that dosimetry materials capable of detecting gammas as well as neutrons were included. That dosimetry and its evaluation [18] established the apparent fact that gammas were responsible for the “accelerated” rate of embrittlement discovered in 1986 [19].

The dosimeters used in 1993 were in surveillance-type (dosimetry-dedicated) capsules located at Key 2, Position 9; Key 4, Positions 2 and 10; and Key 7, Position 5. These locations are illustrated in Fig. 4 of [6] and Figs. 17 and 18 of this report, the latter of which are cross sections at the horizontal midplane ($Z = 0$) of the HB-2 and HB-4 geometric models for $t < 22.7$ EFPY. The locations are quantified in Table 31.

The dpa rate calculations for these dosimeters were some of the earliest performed and did not physically include Keys 4 and 7 in the HB-4 model, even though the model was large enough [1]. Also at that time, the neutron dpa cross sections had not been updated (improved). The calculated dpa rates based on these early models are presented in Table 32 (dpa rates in parentheses). Updated values (Key 4 included in the HB-4 model and improved neutron dpa cross sections used in both models) are without parentheses (also see Tables 10, 11, and 15).

* EOC was simulated with control rods out but with BOC fuel and burnable poison loadings and distributions.

Table 22. Neutron fluxes for HB-2 nozzle corner and weld tubular dosimeters

Energy group	Upper Bndy. (eV)	NEUTRON FLUX (cm ⁻² .s ⁻¹)					
		CORNER (2D1C, 2D2C)			WELD (2D1W, 2D2W, 2D3W)		
		BOC	EOC	AVG.	BOC	EOC	AVG.
1	1.49E+07	1.36E+07	1.36E+07	1.36E+07	1.33E+06	1.33E+06	1.33E+06
2	1.22E+07	5.44E+07	5.48E+07	5.46E+07	3.87E+06	3.86E+06	3.87E+06
3	1.00E+07	1.56E+08	1.58E+08	1.57E+08	8.35E+06	8.27E+06	8.31E+06
4	8.19E+06	3.78E+08	3.82E+08	3.80E+08	1.66E+07	1.67E+07	1.66E+07
5	6.70E+06	7.67E+08	7.78E+08	7.73E+08	2.95E+07	2.99E+07	2.97E+07
6	5.49E+06	1.26E+09	1.28E+09	1.27E+09	4.51E+07	4.61E+07	4.56E+07
7	4.49E+06	1.58E+09	1.62E+09	1.60E+09	4.91E+07	5.04E+07	4.97E+07
8	3.68E+06	1.92E+09	1.98E+09	1.95E+09	6.11E+07	6.28E+07	6.19E+07
9	3.01E+06	2.39E+09	2.48E+09	2.43E+09	8.82E+07	9.09E+07	8.96E+07
10	2.47E+06	8.24E+08	8.54E+08	8.39E+08	2.94E+07	3.04E+07	2.99E+07
11	2.35E+06	8.25E+08	8.54E+08	8.39E+08	2.92E+07	3.02E+07	2.97E+07
12	2.23E+06	1.68E+09	1.74E+09	1.71E+09	5.34E+07	5.53E+07	5.44E+07
13	2.02E+06	4.20E+09	4.39E+09	4.29E+09	1.25E+08	1.29E+08	1.27E+08
14	1.65E+06	4.58E+09	4.80E+09	4.69E+09	1.35E+08	1.40E+08	1.38E+08
15	1.35E+06	4.59E+09	4.82E+09	4.71E+09	1.63E+08	1.70E+08	1.67E+08
16	1.11E+06	4.00E+09	4.20E+09	4.10E+09	1.65E+08	1.71E+08	1.68E+08
17	9.07E+05	4.85E+09	5.11E+09	4.98E+09	1.92E+08	2.00E+08	1.96E+08
18	7.43E+05	4.77E+09	5.03E+09	4.90E+09	2.56E+08	2.67E+08	2.61E+08
19	6.08E+05	3.21E+09	3.39E+09	3.30E+09	1.83E+08	1.92E+08	1.87E+08
20	5.23E+05	1.02E+09	1.08E+09	1.05E+09	5.26E+07	5.50E+07	5.38E+07
21	4.98E+05	4.04E+09	4.26E+09	4.15E+09	1.93E+08	2.01E+08	1.97E+08
22	3.88E+05	4.73E+09	5.00E+09	4.86E+09	2.74E+08	2.86E+08	2.80E+08
23	3.02E+05	2.28E+08	2.40E+08	2.34E+08	1.69E+07	1.77E+07	1.73E+07
24	2.99E+05	8.27E+07	8.73E+07	8.50E+07	6.01E+06	6.30E+06	6.16E+06
25	2.97E+05	1.67E+08	1.77E+08	1.72E+08	1.13E+07	1.18E+07	1.16E+07
26	2.95E+05	1.24E+09	1.31E+09	1.28E+09	6.30E+07	6.59E+07	6.45E+07
27	2.73E+05	3.27E+09	3.46E+09	3.36E+09	1.73E+08	1.81E+08	1.77E+08
28	2.24E+05	2.98E+09	3.15E+09	3.06E+09	1.35E+08	1.42E+08	1.38E+08
29	1.83E+05	2.81E+09	2.96E+09	2.89E+09	1.39E+08	1.46E+08	1.42E+08
30	1.50E+05	2.75E+09	2.91E+09	2.83E+09	1.36E+08	1.42E+08	1.39E+08
31	1.23E+05	4.20E+09	4.44E+09	4.32E+09	1.99E+08	2.08E+08	2.04E+08
32	8.65E+04	4.82E+09	5.10E+09	4.96E+09	2.30E+08	2.41E+08	2.35E+08
33	5.66E+04	7.97E+08	8.44E+08	8.20E+08	3.64E+07	3.81E+07	3.72E+07
34	5.25E+04	4.31E+09	4.56E+09	4.43E+09	1.90E+08	2.00E+08	1.95E+08
35	3.43E+04	1.75E+09	1.85E+09	1.80E+09	7.04E+07	7.37E+07	7.20E+07
36	2.85E+04	5.09E+08	5.39E+08	5.24E+08	2.01E+07	2.10E+07	2.06E+07
37	2.70E+04	3.85E+08	4.07E+08	3.96E+08	1.55E+07	1.62E+07	1.59E+07
38	2.61E+04	5.98E+08	6.33E+08	6.16E+08	3.20E+07	3.36E+07	3.28E+07
39	2.48E+04	5.38E+08	5.69E+08	5.53E+08	2.98E+07	3.13E+07	3.05E+07
40	2.36E+04	4.27E+09	4.52E+09	4.39E+09	1.79E+08	1.88E+08	1.84E+08
41	1.50E+04	4.83E+09	5.11E+09	4.97E+09	1.99E+08	2.09E+08	2.04E+08
42	9.12E+03	4.83E+09	5.11E+09	4.97E+09	1.85E+08	1.94E+08	1.89E+08
43	5.53E+03	3.97E+09	4.20E+09	4.08E+09	1.47E+08	1.54E+08	1.50E+08
44	3.71E+03	2.04E+09	2.16E+09	2.10E+09	7.47E+07	7.83E+07	7.65E+07
45	3.04E+03	1.53E+09	1.62E+09	1.57E+09	5.48E+07	5.75E+07	5.61E+07
46	2.61E+03	1.52E+09	1.62E+09	1.57E+09	5.31E+07	5.56E+07	5.43E+07
47	2.25E+03	1.05E+09	1.12E+09	1.08E+09	3.67E+07	3.84E+07	3.75E+07
48	2.04E+03	5.37E+09	5.70E+09	5.54E+09	1.86E+08	1.96E+08	1.91E+08
49	1.23E+03	5.53E+09	5.87E+09	5.70E+09	1.81E+08	1.90E+08	1.86E+08
50	7.49E+02	5.78E+09	6.13E+09	5.95E+09	1.81E+08	1.90E+08	1.85E+08
51	4.54E+02	6.02E+09	6.39E+09	6.21E+09	1.76E+08	1.85E+08	1.81E+08
52	2.75E+02	6.32E+09	6.71E+09	6.52E+09	1.78E+08	1.86E+08	1.82E+08
53	1.67E+02	6.62E+09	7.03E+09	6.82E+09	1.78E+08	1.87E+08	1.83E+08
54	1.01E+02	1.05E+10	1.12E+10	1.09E+10	2.69E+08	2.82E+08	2.76E+08
55	4.79E+01	1.13E+10	1.20E+10	1.16E+10	2.70E+08	2.84E+08	2.77E+08
56	2.26E+01	1.20E+10	1.28E+10	1.24E+10	2.71E+08	2.84E+08	2.77E+08
57	1.07E+01	1.28E+10	1.36E+10	1.32E+10	2.69E+08	2.83E+08	2.76E+08
58	5.04E+00	1.38E+10	1.47E+10	1.43E+10	2.70E+08	2.84E+08	2.77E+08
59	2.38E+00	1.56E+10	1.67E+10	1.61E+10	2.81E+08	2.95E+08	2.88E+08
60	1.13E+00	2.43E+10	2.60E+10	2.52E+10	3.98E+08	4.18E+08	4.08E+08
61	4.14E-01	2.04E+12	2.46E+12	2.25E+12	1.05E+10	1.13E+10	1.09E+10
TOTAL		2.28E+12	2.72E+12	2.50E+12	1.82E+10	1.93E+10	1.88E+10

Table 23. Gamma fluxes for HB-2 nozzle corner and weld tubular dosimeters

Energy group	Upper Bndy. (eV)	GAMMA FLUX (cm ⁻² ·s ⁻¹)					
		CORNER (2D1C, 2D2C)			WELD (2D1W, 2D2W)		
		BOC	EOC	AVG.	BOC	EOC	AVG.
1	1.40E+07	1.03E+07	1.15E+07	1.09E+07	1.24E+07	1.44E+07	1.34E+07
2	1.00E+07	4.20E+10	5.09E+10	4.64E+10	6.99E+09	8.46E+09	7.73E+09
3	8.00E+06	1.69E+11	2.14E+11	1.92E+11	4.19E+10	5.88E+10	5.03E+10
4	7.50E+06	2.29E+10	2.82E+10	2.55E+10	6.63E+09	8.83E+09	7.73E+09
5	7.00E+06	8.66E+10	1.10E+11	9.83E+10	4.83E+10	6.48E+10	5.66E+10
6	6.00E+06	8.69E+10	1.07E+11	9.68E+10	4.09E+10	5.01E+10	4.55E+10
7	5.00E+06	1.77E+11	2.11E+11	1.94E+11	7.96E+10	8.73E+10	8.35E+10
8	4.00E+06	2.28E+11	2.62E+11	2.45E+11	1.24E+11	1.30E+11	1.27E+11
9	3.00E+06	1.52E+11	1.71E+11	1.62E+11	8.39E+10	8.62E+10	8.50E+10
10	2.50E+06	6.64E+11	7.89E+11	7.27E+11	2.01E+11	2.23E+11	2.12E+11
11	2.00E+06	2.83E+11	3.15E+11	2.99E+11	1.75E+11	1.87E+11	1.81E+11
12	1.50E+06	4.02E+11	4.43E+11	4.22E+11	2.42E+11	2.60E+11	2.51E+11
13	1.00E+06	3.93E+11	4.34E+11	4.14E+11	2.25E+11	2.43E+11	2.34E+11
14	7.00E+05	1.80E+11	1.99E+11	1.90E+11	1.02E+11	1.10E+11	1.06E+11
15	6.00E+05	3.50E+11	4.01E+11	3.75E+11	1.75E+11	1.96E+11	1.86E+11
16	5.10E+05	3.90E+11	4.38E+11	4.14E+11	2.12E+11	2.32E+11	2.22E+11
17	4.00E+05	5.40E+11	6.08E+11	5.74E+11	2.82E+11	3.09E+11	2.96E+11
18	3.00E+05	1.97E+12	2.24E+12	2.11E+12	9.85E+11	1.08E+12	1.03E+12
19	1.50E+05	1.17E+12	1.34E+12	1.26E+12	5.67E+11	6.25E+11	5.96E+11
20	1.00E+05	8.54E+11	9.87E+11	9.21E+11	4.23E+11	4.67E+11	4.45E+11
21	7.00E+04	5.06E+11	5.87E+11	5.46E+11	3.35E+11	3.70E+11	3.53E+11
22	4.50E+04	6.95E+10	8.08E+10	7.51E+10	5.06E+10	5.59E+10	5.33E+10
23	2.00E+04	2.53E+08	2.94E+08	2.74E+08	1.86E+08	2.05E+08	1.96E+08
TOTAL		8.74E+12	1.00E+13	9.38E+12	4.41E+12	4.86E+12	4.63E+12

Table 24. Neutron and gamma fluxes for HB-2 Key 2C

Energy group	Upper Bnd. (eV)	NEUTRON FLUX (cm ⁻² s ⁻¹)		
		BOC	EOC	AVG.
1	1.49E+07	2.27E+07	2.28E+07	2.28E+07
2	1.22E+07	9.12E+07	9.18E+07	9.15E+07
3	1.00E+07	2.55E+08	2.58E+08	2.57E+08
4	8.19E+06	6.44E+08	6.52E+08	6.48E+08
5	6.70E+06	1.34E+09	1.36E+09	1.35E+09
6	5.49E+06	2.28E+09	2.33E+09	2.31E+09
7	4.49E+06	3.14E+09	3.23E+09	3.19E+09
8	3.68E+06	3.86E+09	4.00E+09	3.93E+09
9	3.01E+06	4.90E+09	5.08E+09	4.99E+09
10	2.47E+06	1.72E+09	1.79E+09	1.75E+09
11	2.35E+06	1.78E+09	1.85E+09	1.81E+09
12	2.23E+06	3.98E+09	4.15E+09	4.07E+09
13	2.02E+06	1.08E+10	1.13E+10	1.11E+10
14	1.65E+06	1.22E+10	1.28E+10	1.25E+10
15	1.35E+06	1.24E+10	1.31E+10	1.27E+10
16	1.11E+06	1.16E+10	1.22E+10	1.19E+10
17	9.07E+05	1.30E+10	1.37E+10	1.33E+10
18	7.43E+05	1.30E+10	1.38E+10	1.34E+10
19	6.08E+05	8.32E+09	8.80E+09	8.56E+09
20	5.23E+05	2.69E+09	2.85E+09	2.77E+09
21	4.98E+05	1.15E+10	1.22E+10	1.18E+10
22	3.88E+05	1.33E+10	1.41E+10	1.37E+10
23	3.02E+05	6.54E+08	6.93E+08	6.73E+08
24	2.99E+05	2.33E+08	2.47E+08	2.40E+08
25	2.97E+05	4.52E+08	4.80E+08	4.66E+08
26	2.95E+05	3.15E+09	3.34E+09	3.25E+09
27	2.73E+05	9.27E+09	9.83E+09	9.55E+09
28	2.24E+05	8.40E+09	8.92E+09	8.66E+09
29	1.83E+05	7.94E+09	8.43E+09	8.18E+09
30	1.50E+05	8.61E+09	9.14E+09	8.87E+09
31	1.23E+05	1.14E+10	1.21E+10	1.18E+10
32	8.65E+04	1.47E+10	1.56E+10	1.52E+10
33	5.66E+04	2.21E+09	2.35E+09	2.28E+09
34	5.25E+04	1.22E+10	1.29E+10	1.25E+10
35	3.43E+04	3.42E+09	3.63E+09	3.52E+09
36	2.85E+04	9.36E+08	9.96E+08	9.66E+08
37	2.70E+04	2.15E+09	2.29E+09	2.22E+09
38	2.61E+04	3.61E+09	3.83E+09	3.72E+09
39	2.48E+04	1.94E+09	2.07E+09	2.00E+09
40	2.36E+04	1.20E+10	1.28E+10	1.24E+10
41	1.50E+04	1.51E+10	1.61E+10	1.56E+10
42	9.12E+03	1.48E+10	1.58E+10	1.53E+10
43	5.53E+03	1.33E+10	1.41E+10	1.37E+10
44	3.71E+03	7.12E+09	7.58E+09	7.35E+09
45	3.04E+03	4.84E+09	5.15E+09	4.99E+09
46	2.61E+03	4.33E+09	4.60E+09	4.47E+09
47	2.25E+03	4.02E+09	4.28E+09	4.15E+09
48	2.04E+03	1.91E+10	2.03E+10	1.97E+10
49	1.23E+03	1.85E+10	1.97E+10	1.91E+10
50	7.49E+02	1.99E+10	2.12E+10	2.05E+10
51	4.54E+02	2.05E+10	2.18E+10	2.11E+10
52	2.75E+02	2.27E+10	2.43E+10	2.35E+10
53	1.67E+02	2.36E+10	2.51E+10	2.44E+10
54	1.01E+02	3.75E+10	4.00E+10	3.88E+10
55	4.79E+01	3.99E+10	4.26E+10	4.13E+10
56	2.26E+01	4.22E+10	4.52E+10	4.37E+10
57	1.07E+01	4.42E+10	4.74E+10	4.58E+10
58	5.04E+00	4.68E+10	5.03E+10	4.85E+10
59	2.38E+00	5.11E+10	5.51E+10	5.31E+10
60	1.13E+00	7.56E+10	8.18E+10	7.87E+10
61	4.14E-01	2.46E+12	3.03E+12	2.75E+12
TOTAL		3.22E+12	3.85E+12	3.54E+12

Energy group	Upper Bnd. (eV)	GAMMA FLUX (cm ⁻² s ⁻¹)		
		BOC	EOC	AVG.
1	1.40E+07	1.83E+07	2.03E+07	1.93E+07
2	1.00E+07	2.01E+11	2.46E+11	2.23E+11
3	8.00E+06	5.01E+11	6.26E+11	5.63E+11
4	7.50E+06	1.06E+11	1.30E+11	1.18E+11
5	7.00E+06	2.27E+11	2.88E+11	2.58E+11
6	6.00E+06	2.40E+11	2.95E+11	2.67E+11
7	5.00E+06	3.79E+11	4.57E+11	4.18E+11
8	4.00E+06	4.92E+11	5.79E+11	5.36E+11
9	3.00E+06	3.13E+11	3.61E+11	3.37E+11
10	2.50E+06	9.42E+11	1.12E+12	1.03E+12
11	2.00E+06	5.96E+11	6.80E+11	6.38E+11
12	1.50E+06	7.83E+11	8.77E+11	8.30E+11
13	1.00E+06	8.11E+11	9.11E+11	8.61E+11
14	7.00E+05	3.73E+11	4.18E+11	3.96E+11
15	6.00E+05	9.14E+11	1.07E+12	9.93E+11
16	5.10E+05	8.03E+11	9.08E+11	8.56E+11
17	4.00E+05	1.12E+12	1.27E+12	1.19E+12
18	3.00E+05	3.66E+12	4.17E+12	3.92E+12
19	1.50E+05	1.35E+12	1.55E+12	1.45E+12
20	1.00E+05	3.54E+11	4.09E+11	3.82E+11
21	7.00E+04	4.03E+10	4.68E+10	4.35E+10
22	4.50E+04	1.99E+09	2.43E+09	2.21E+09
23	2.00E+04	7.79E+07	9.57E+07	8.68E+07
TOTAL		1.42E+13	1.64E+13	1.53E+13

Table 25. Neutron fluxes for HB-2 Key 2W Positions 1, 2, and 3

Upper Energy group	Upper Bndy. (eV)	NEUTRON FLUX (cm ⁻² .s ⁻¹)								
		Position 1			Position 2			Position 3		
		BOC	EOC	AVG.	BOC	EOC	AVG.	BOC	EOC	AVG.
1	1.49E+07	4.62E+06	4.70E+06	4.66E+06	4.06E+06	4.12E+06	4.09E+06	3.56E+06	3.62E+06	3.59E+06
2	1.22E+07	1.42E+07	1.46E+07	1.44E+07	1.23E+07	1.25E+07	1.24E+07	1.05E+07	1.07E+07	1.06E+07
3	1.00E+07	3.18E+07	3.26E+07	3.22E+07	2.67E+07	2.73E+07	2.70E+07	2.21E+07	2.27E+07	2.24E+07
4	8.19E+06	6.58E+07	6.76E+07	6.67E+07	5.50E+07	5.61E+07	5.55E+07	4.46E+07	4.57E+07	4.51E+07
5	6.70E+06	1.15E+08	1.19E+08	1.17E+08	9.67E+07	9.90E+07	9.79E+07	7.72E+07	7.92E+07	7.82E+07
6	5.49E+06	1.63E+08	1.68E+08	1.66E+08	1.37E+08	1.41E+08	1.39E+08	1.08E+08	1.11E+08	1.09E+08
7	4.49E+06	1.71E+08	1.77E+08	1.74E+08	1.43E+08	1.47E+08	1.45E+08	1.10E+08	1.13E+08	1.11E+08
8	3.68E+06	2.08E+08	2.15E+08	2.12E+08	1.73E+08	1.78E+08	1.75E+08	1.31E+08	1.35E+08	1.33E+08
9	3.01E+06	2.82E+08	2.91E+08	2.87E+08	2.32E+08	2.40E+08	2.36E+08	1.76E+08	1.82E+08	1.79E+08
10	2.47E+06	9.19E+07	9.52E+07	9.36E+07	7.56E+07	7.83E+07	7.70E+07	5.67E+07	5.87E+07	5.77E+07
11	2.35E+06	9.08E+07	9.42E+07	9.25E+07	7.44E+07	7.70E+07	7.57E+07	5.53E+07	5.72E+07	5.63E+07
12	2.23E+06	1.69E+08	1.76E+08	1.73E+08	1.36E+08	1.41E+08	1.39E+08	1.00E+08	1.04E+08	1.02E+08
13	2.02E+06	3.98E+08	4.15E+08	4.06E+08	3.15E+08	3.27E+08	3.21E+08	2.27E+08	2.36E+08	2.31E+08
14	1.65E+06	4.19E+08	4.38E+08	4.29E+08	3.29E+08	3.43E+08	3.36E+08	2.34E+08	2.44E+08	2.39E+08
15	1.35E+06	4.43E+08	4.64E+08	4.53E+08	3.46E+08	3.61E+08	3.53E+08	2.44E+08	2.54E+08	2.49E+08
16	1.11E+06	3.79E+08	3.97E+08	3.88E+08	2.94E+08	3.07E+08	3.01E+08	2.05E+08	2.15E+08	2.10E+08
17	9.07E+05	4.40E+08	4.61E+08	4.51E+08	3.40E+08	3.56E+08	3.48E+08	2.37E+08	2.48E+08	2.43E+08
18	7.43E+05	4.64E+08	4.86E+08	4.75E+08	3.56E+08	3.73E+08	3.65E+08	2.46E+08	2.58E+08	2.52E+08
19	6.08E+05	3.09E+08	3.24E+08	3.16E+08	2.38E+08	2.49E+08	2.44E+08	1.64E+08	1.72E+08	1.68E+08
20	5.23E+05	9.03E+07	9.47E+07	9.25E+07	6.95E+07	7.28E+07	7.12E+07	4.80E+07	5.02E+07	4.91E+07
21	4.98E+05	3.37E+08	3.54E+08	3.46E+08	2.60E+08	2.73E+08	2.66E+08	1.80E+08	1.88E+08	1.84E+08
22	3.88E+05	4.04E+08	4.24E+08	4.14E+08	3.10E+08	3.25E+08	3.18E+08	2.13E+08	2.22E+08	2.18E+08
23	3.02E+05	2.17E+07	2.28E+07	2.22E+07	1.67E+07	1.75E+07	1.71E+07	1.14E+07	1.19E+07	1.16E+07
24	2.99E+05	7.73E+06	8.12E+06	7.92E+06	5.93E+06	6.21E+06	6.07E+06	4.04E+06	4.24E+06	4.14E+06
25	2.97E+05	1.49E+07	1.57E+07	1.53E+07	1.14E+07	1.20E+07	1.17E+07	7.83E+06	8.17E+06	8.00E+06
26	2.95E+05	9.25E+07	9.70E+07	9.47E+07	7.09E+07	7.43E+07	7.26E+07	4.88E+07	5.10E+07	4.99E+07
27	2.73E+05	2.69E+08	2.83E+08	2.76E+08	2.06E+08	2.16E+08	2.11E+08	1.41E+08	1.48E+08	1.44E+08
28	2.24E+05	2.16E+08	2.27E+08	2.21E+08	1.65E+08	1.73E+08	1.69E+08	1.13E+08	1.18E+08	1.16E+08
29	1.83E+05	2.22E+08	2.33E+08	2.27E+08	1.69E+08	1.77E+08	1.73E+08	1.16E+08	1.21E+08	1.18E+08
30	1.50E+05	2.02E+08	2.12E+08	2.07E+08	1.55E+08	1.62E+08	1.58E+08	1.05E+08	1.10E+08	1.08E+08
31	1.23E+05	3.01E+08	3.15E+08	3.08E+08	2.29E+08	2.40E+08	2.34E+08	1.56E+08	1.63E+08	1.60E+08
32	8.65E+04	3.42E+08	3.58E+08	3.50E+08	2.60E+08	2.73E+08	2.67E+08	1.77E+08	1.85E+08	1.81E+08
33	5.66E+04	5.11E+07	5.36E+07	5.24E+07	3.88E+07	4.07E+07	3.98E+07	2.64E+07	2.77E+07	2.71E+07
34	5.25E+04	2.87E+08	3.01E+08	2.94E+08	2.18E+08	2.29E+08	2.23E+08	1.48E+08	1.55E+08	1.52E+08
35	3.43E+04	6.85E+07	7.19E+07	7.02E+07	5.25E+07	5.50E+07	5.38E+07	3.60E+07	3.77E+07	3.68E+07
36	2.85E+04	1.84E+07	1.93E+07	1.88E+07	1.41E+07	1.48E+07	1.45E+07	9.68E+06	1.01E+07	9.90E+06
37	2.70E+04	4.21E+07	4.42E+07	4.31E+07	3.21E+07	3.37E+07	3.29E+07	2.18E+07	2.28E+07	2.23E+07
38	2.61E+04	7.51E+07	7.88E+07	7.69E+07	5.69E+07	5.97E+07	5.83E+07	3.81E+07	3.99E+07	3.90E+07
39	2.48E+04	4.40E+07	4.62E+07	4.51E+07	3.33E+07	3.49E+07	3.41E+07	2.23E+07	2.34E+07	2.28E+07
40	2.36E+04	2.61E+08	2.74E+08	2.67E+08	1.98E+08	2.08E+08	2.03E+08	1.34E+08	1.40E+08	1.37E+08
41	1.50E+04	3.08E+08	3.23E+08	3.16E+08	2.33E+08	2.45E+08	2.39E+08	1.58E+08	1.65E+08	1.61E+08
42	9.12E+03	2.70E+08	2.84E+08	2.77E+08	2.05E+08	2.15E+08	2.10E+08	1.39E+08	1.46E+08	1.43E+08
43	5.53E+03	2.31E+08	2.42E+08	2.37E+08	1.75E+08	1.84E+08	1.80E+08	1.18E+08	1.24E+08	1.21E+08
44	3.71E+03	1.21E+08	1.28E+08	1.24E+08	9.21E+07	9.66E+07	9.43E+07	6.21E+07	6.50E+07	6.36E+07
45	3.04E+03	8.13E+07	8.55E+07	8.34E+07	6.17E+07	6.47E+07	6.32E+07	4.17E+07	4.36E+07	4.26E+07
46	2.61E+03	7.04E+07	7.40E+07	7.22E+07	5.34E+07	5.60E+07	5.47E+07	3.62E+07	3.79E+07	3.71E+07
47	2.25E+03	6.40E+07	6.72E+07	6.56E+07	4.85E+07	5.09E+07	4.97E+07	3.28E+07	3.43E+07	3.35E+07
48	2.04E+03	3.03E+08	3.18E+08	3.11E+08	2.29E+08	2.41E+08	2.35E+08	1.54E+08	1.62E+08	1.58E+08
49	1.23E+03	2.81E+08	2.96E+08	2.88E+08	2.13E+08	2.23E+08	2.18E+08	1.43E+08	1.50E+08	1.47E+08
50	7.49E+02	2.91E+08	3.06E+08	2.98E+08	2.20E+08	2.30E+08	2.25E+08	1.48E+08	1.55E+08	1.51E+08
51	4.54E+02	2.71E+08	2.85E+08	2.78E+08	2.05E+08	2.15E+08	2.10E+08	1.38E+08	1.45E+08	1.42E+08
52	2.75E+02	2.99E+08	3.15E+08	3.07E+08	2.26E+08	2.37E+08	2.31E+08	1.51E+08	1.59E+08	1.55E+08
53	1.67E+02	3.02E+08	3.18E+08	3.10E+08	2.28E+08	2.39E+08	2.34E+08	1.52E+08	1.60E+08	1.56E+08
54	1.01E+02	4.62E+08	4.86E+08	4.74E+08	3.48E+08	3.65E+08	3.57E+08	2.32E+08	2.44E+08	2.38E+08
55	4.79E+01	4.72E+08	4.96E+08	4.84E+08	3.54E+08	3.72E+08	3.63E+08	2.36E+08	2.48E+08	2.42E+08
56	2.26E+01	4.80E+08	5.05E+08	4.92E+08	3.60E+08	3.78E+08	3.69E+08	2.40E+08	2.51E+08	2.45E+08
57	1.07E+01	4.87E+08	5.12E+08	4.99E+08	3.64E+08	3.83E+08	3.73E+08	2.42E+08	2.54E+08	2.48E+08
58	5.04E+00	4.99E+08	5.25E+08	5.12E+08	3.72E+08	3.91E+08	3.82E+08	2.47E+08	2.59E+08	2.53E+08
59	2.38E+00	5.33E+08	5.59E+08	5.46E+08	3.96E+08	4.16E+08	4.06E+08	2.62E+08	2.75E+08	2.68E+08
60	1.13E+00	7.76E+08	8.12E+08	7.94E+08	5.75E+08	6.03E+08	5.89E+08	3.80E+08	3.97E+08	3.88E+08
61	4.14E-01	2.15E+10	2.37E+10	2.26E+10	1.61E+10	1.77E+10	1.69E+10	1.09E+10	1.19E+10	1.14E+10
TOTAL		3.58E+10	3.86E+10	3.72E+10	2.70E+10	2.91E+10	2.81E+10	1.85E+10	1.97E+10	1.91E+10

Table 26. Gamma fluxes for HB-2 Key 2W Positions 1, 2, and 3

Energy group	Upper Bndy. (eV)	GAMMA FLUX (cm ⁻² ·s ⁻¹)								
		Position 1			Position 2			Position 3		
		BOC	EOC	AVG.	BOC	EOC	AVG.	BOC	EOC	AVG.
1	1.40E+07	2.49E+07	2.92E+07	2.70E+07	2.48E+07	2.90E+07	2.69E+07	2.37E+07	2.79E+07	2.58E+07
2	1.00E+07	9.80E+09	1.18E+10	1.08E+10	8.06E+09	9.72E+09	8.89E+09	6.14E+09	7.43E+09	6.79E+09
3	8.00E+06	8.02E+10	1.15E+11	9.74E+10	7.52E+10	1.08E+11	9.16E+10	6.98E+10	1.01E+11	8.54E+10
4	7.50E+06	1.10E+10	1.48E+10	1.29E+10	1.02E+10	1.38E+10	1.20E+10	8.98E+09	1.24E+10	1.07E+10
5	7.00E+06	1.02E+11	1.37E+11	1.20E+11	9.95E+10	1.33E+11	1.16E+11	9.60E+10	1.29E+11	1.12E+11
6	6.00E+06	8.16E+10	9.87E+10	9.02E+10	7.95E+10	9.57E+10	8.76E+10	7.53E+10	9.16E+10	8.34E+10
7	5.00E+06	1.69E+11	1.81E+11	1.75E+11	1.65E+11	1.76E+11	1.70E+11	1.55E+11	1.67E+11	1.61E+11
8	4.00E+06	2.73E+11	2.79E+11	2.76E+11	2.68E+11	2.74E+11	2.71E+11	2.53E+11	2.60E+11	2.56E+11
9	3.00E+06	1.90E+11	1.90E+11	1.90E+11	1.87E+11	1.88E+11	1.87E+11	1.76E+11	1.77E+11	1.77E+11
10	2.50E+06	5.16E+11	5.73E+11	5.44E+11	5.09E+11	5.63E+11	5.36E+11	4.67E+11	5.19E+11	4.93E+11
11	2.00E+06	4.11E+11	4.34E+11	4.22E+11	4.08E+11	4.33E+11	4.20E+11	3.83E+11	4.07E+11	3.95E+11
12	1.50E+06	5.76E+11	6.16E+11	5.96E+11	5.77E+11	6.13E+11	5.95E+11	5.43E+11	5.82E+11	5.62E+11
13	1.00E+06	5.34E+11	5.76E+11	5.55E+11	5.30E+11	5.68E+11	5.49E+11	5.04E+11	5.43E+11	5.23E+11
14	7.00E+05	2.38E+11	2.57E+11	2.48E+11	2.35E+11	2.53E+11	2.44E+11	2.25E+11	2.43E+11	2.34E+11
15	6.00E+05	4.24E+11	4.73E+11	4.48E+11	4.14E+11	4.61E+11	4.38E+11	3.92E+11	4.38E+11	4.15E+11
16	5.10E+05	4.69E+11	5.13E+11	4.91E+11	4.62E+11	5.03E+11	4.82E+11	4.40E+11	4.81E+11	4.60E+11
17	4.00E+05	6.14E+11	6.71E+11	6.43E+11	6.03E+11	6.60E+11	6.31E+11	5.76E+11	6.31E+11	6.04E+11
18	3.00E+05	2.05E+12	2.25E+12	2.15E+12	2.01E+12	2.21E+12	2.11E+12	1.94E+12	2.13E+12	2.04E+12
19	1.50E+05	8.21E+11	9.04E+11	8.63E+11	8.10E+11	8.92E+11	8.51E+11	7.91E+11	8.71E+11	8.31E+11
20	1.00E+05	2.71E+11	3.00E+11	2.85E+11	2.70E+11	2.99E+11	2.84E+11	2.71E+11	3.01E+11	2.86E+11
21	7.00E+04	6.15E+10	6.85E+10	6.50E+10	6.36E+10	7.12E+10	6.74E+10	6.53E+10	7.36E+10	6.94E+10
22	4.50E+04	1.20E+09	1.33E+09	1.26E+09	1.21E+09	1.36E+09	1.28E+09	1.29E+09	1.44E+09	1.37E+09
23	2.00E+04	1.02E+06	1.12E+06	1.07E+06	7.85E+05	8.70E+05	8.27E+05	6.48E+05	7.17E+05	6.83E+05
TOTAL		7.90E+12	8.67E+12	8.28E+12	7.79E+12	8.53E+12	8.16E+12	7.44E+12	8.17E+12	7.80E+12

Table 27. Neutron fluxes (EOC) for HB-3 Key 3 Positions 3, 8, and 10

Energy group	Upper Bndy. (eV)	NEUTRON FLUX (cm ² ·s ⁻¹)								
		Position 3			Position 8			Position 10		
		p1 ^a	p2	p3	p1	p2	p3	p1	p2	p3
1	1.49E+07	8.59E+05	9.34E+05	1.16E+06	2.68E+06	2.51E+06	2.91E+06	1.46E+06	1.68E+06	1.88E+06
2	1.22E+07	2.36E+06	2.53E+06	3.03E+06	6.67E+06	6.40E+06	7.43E+06	3.93E+06	4.55E+06	5.21E+06
3	1.00E+07	5.71E+06	6.81E+06	8.94E+06	2.50E+07	2.26E+07	2.76E+07	1.05E+07	1.35E+07	1.55E+07
4	8.19E+06	9.40E+06	1.11E+07	1.51E+07	3.03E+07	2.96E+07	3.57E+07	1.64E+07	2.00E+07	2.40E+07
5	6.70E+06	2.35E+07	2.95E+07	4.22E+07	7.57E+07	7.55E+07	9.85E+07	3.63E+07	4.86E+07	5.99E+07
6	5.49E+06	3.94E+07	5.08E+07	7.56E+07	1.08E+08	1.11E+08	1.50E+08	5.39E+07	7.29E+07	9.45E+07
7	4.49E+06	3.84E+07	5.05E+07	7.65E+07	8.87E+07	9.98E+07	1.34E+08	4.96E+07	6.96E+07	9.18E+07
8	3.68E+06	5.58E+07	7.43E+07	1.15E+08	1.18E+08	1.37E+08	1.92E+08	6.88E+07	9.83E+07	1.34E+08
9	3.01E+06	8.27E+07	1.09E+08	1.65E+08	1.59E+08	1.91E+08	2.60E+08	9.83E+07	1.40E+08	1.90E+08
10	2.47E+06	2.95E+07	3.94E+07	5.95E+07	5.64E+07	6.99E+07	9.57E+07	3.42E+07	5.01E+07	6.75E+07
11	2.35E+06	3.04E+07	4.07E+07	6.18E+07	5.75E+07	7.02E+07	9.83E+07	3.51E+07	5.17E+07	6.98E+07
12	2.23E+06	5.68E+07	7.63E+07	1.17E+08	1.03E+08	1.30E+08	1.80E+08	6.58E+07	9.71E+07	1.33E+08
13	2.02E+06	1.48E+08	2.04E+08	3.18E+08	2.57E+08	3.39E+08	4.86E+08	1.70E+08	2.58E+08	3.61E+08
14	1.65E+06	1.70E+08	2.36E+08	3.72E+08	2.90E+08	3.88E+08	5.50E+08	1.94E+08	2.99E+08	4.21E+08
15	1.35E+06	1.88E+08	2.57E+08	4.03E+08	3.13E+08	4.33E+08	5.90E+08	2.16E+08	3.33E+08	4.60E+08
16	1.11E+06	1.74E+08	2.37E+08	3.88E+08	2.80E+08	3.96E+08	5.55E+08	1.97E+08	3.12E+08	4.35E+08
17	9.07E+05	2.07E+08	2.84E+08	4.52E+08	3.37E+08	4.68E+08	6.50E+08	2.38E+08	3.69E+08	5.14E+08
18	7.43E+05	2.28E+08	3.03E+08	4.66E+08	3.63E+08	5.10E+08	6.90E+08	2.65E+08	4.00E+08	5.41E+08
19	6.08E+05	1.51E+08	2.01E+08	3.09E+08	2.45E+08	3.37E+08	4.54E+08	1.77E+08	2.67E+08	3.58E+08
20	5.23E+05	4.60E+07	6.23E+07	9.62E+07	7.42E+07	1.04E+08	1.41E+08	5.37E+07	8.17E+07	1.12E+08
21	4.98E+05	1.78E+08	2.43E+08	3.88E+08	2.91E+08	4.07E+08	5.68E+08	2.07E+08	3.23E+08	4.47E+08
22	3.88E+05	2.17E+08	2.89E+08	4.59E+08	3.43E+08	4.91E+08	6.63E+08	2.53E+08	3.89E+08	5.28E+08
23	3.02E+05	1.13E+07	1.45E+07	2.31E+07	1.72E+07	2.53E+07	3.27E+07	1.32E+07	2.00E+07	2.65E+07
24	2.99E+05	4.00E+06	5.17E+06	8.26E+06	6.21E+06	9.05E+06	1.17E+07	4.67E+06	7.15E+06	9.46E+06
25	2.97E+05	7.76E+06	1.02E+07	1.63E+07	1.21E+07	1.74E+07	2.29E+07	9.09E+06	1.39E+07	1.86E+07
26	2.95E+05	5.09E+07	7.01E+07	1.10E+08	8.35E+07	1.14E+08	1.61E+08	5.95E+07	9.18E+07	1.28E+08
27	2.73E+05	1.47E+08	1.98E+08	3.17E+08	2.32E+08	3.31E+08	4.54E+08	1.70E+08	2.65E+08	3.63E+08
28	2.24E+05	1.24E+08	1.72E+08	2.71E+08	2.04E+08	2.84E+08	3.99E+08	1.45E+08	2.25E+08	3.16E+08
29	1.83E+05	1.25E+08	1.69E+08	2.64E+08	2.02E+08	2.83E+08	3.89E+08	1.45E+08	2.25E+08	3.05E+08
30	1.50E+05	1.18E+08	1.63E+08	2.61E+08	1.90E+08	2.71E+08	3.86E+08	1.38E+08	2.16E+08	3.03E+08
31	1.23E+05	1.78E+08	2.44E+08	3.74E+08	2.91E+08	4.00E+08	5.60E+08	2.07E+08	3.21E+08	4.36E+08
32	8.65E+04	2.05E+08	2.81E+08	4.58E+08	3.31E+08	4.68E+08	6.70E+08	2.38E+08	3.75E+08	5.25E+08
33	5.66E+04	3.17E+07	4.45E+07	6.97E+07	5.22E+07	7.24E+07	1.03E+08	3.68E+07	5.78E+07	8.13E+07
34	5.25E+04	1.78E+08	2.46E+08	3.82E+08	2.92E+08	4.00E+08	5.72E+08	2.06E+08	3.23E+08	4.44E+08
35	3.43E+04	4.46E+07	7.59E+07	9.99E+07	8.64E+07	1.06E+08	1.69E+08	5.44E+07	8.57E+07	1.29E+08
36	2.85E+04	1.18E+07	2.15E+07	2.75E+07	2.43E+07	2.90E+07	4.70E+07	1.50E+07	2.35E+07	3.06E+07
37	2.70E+04	2.80E+07	3.77E+07	5.95E+07	4.38E+07	6.28E+07	8.91E+07	3.27E+07	5.05E+07	6.79E+07
38	2.61E+04	4.56E+07	5.47E+07	1.07E+08	6.23E+07	1.01E+08	1.32E+08	5.29E+07	8.34E+07	1.07E+08
39	2.48E+04	2.49E+07	3.19E+07	6.10E+07	3.72E+07	5.79E+07	7.76E+07	2.87E+07	4.66E+07	6.31E+07
40	2.36E+04	1.68E+08	2.37E+08	3.77E+08	2.78E+08	3.83E+08	5.58E+08	1.95E+08	3.09E+08	4.37E+08
41	1.50E+04	1.94E+08	2.71E+08	4.53E+08	3.21E+08	4.51E+08	6.58E+08	2.24E+08	3.58E+08	5.17E+08
42	9.12E+03	1.77E+08	2.62E+08	4.02E+08	3.04E+08	4.14E+08	6.23E+08	2.07E+08	3.30E+08	4.81E+08
43	5.53E+03	1.51E+08	2.17E+08	3.52E+08	2.52E+08	3.52E+08	5.37E+08	1.75E+08	2.80E+08	4.12E+08
44	3.71E+03	7.88E+07	1.11E+08	1.90E+08	1.30E+08	1.85E+08	2.84E+08	8.98E+07	1.46E+08	2.18E+08
45	3.04E+03	5.38E+07	7.97E+07	1.30E+08	9.10E+07	1.28E+08	1.98E+08	6.20E+07	1.02E+08	1.52E+08
46	2.61E+03	4.79E+07	7.54E+07	1.14E+08	8.43E+07	1.15E+08	1.79E+08	5.59E+07	9.11E+07	1.39E+08
47	2.25E+03	4.32E+07	6.13E+07	1.02E+08	7.17E+07	1.01E+08	1.55E+08	4.92E+07	8.03E+07	1.18E+08
48	2.04E+03	2.03E+08	2.90E+08	5.08E+08	3.33E+08	4.83E+08	7.47E+08	2.30E+08	3.83E+08	5.77E+08
49	1.23E+03	1.97E+08	2.91E+08	4.92E+08	3.26E+08	4.72E+08	7.36E+08	2.24E+08	3.73E+08	5.68E+08
50	7.49E+02	2.07E+08	3.03E+08	5.31E+08	3.41E+08	4.99E+08	7.81E+08	2.34E+08	3.94E+08	6.02E+08
51	4.54E+02	1.95E+08	3.08E+08	4.95E+08	3.37E+08	4.76E+08	7.69E+08	2.26E+08	3.77E+08	5.89E+08
52	2.75E+02	2.19E+08	3.24E+08	5.82E+08	3.60E+08	5.33E+08	8.65E+08	2.45E+08	4.20E+08	6.59E+08
53	1.67E+02	2.24E+08	3.40E+08	6.12E+08	3.71E+08	5.56E+08	9.03E+08	2.52E+08	4.37E+08	6.88E+08
54	1.01E+02	3.55E+08	5.39E+08	9.80E+08	5.82E+08	8.82E+08	1.45E+09	3.95E+08	6.89E+08	1.10E+09
55	4.79E+01	3.76E+08	5.78E+08	1.05E+09	6.15E+08	9.49E+08	1.55E+09	4.15E+08	7.36E+08	1.18E+09
56	2.26E+01	3.97E+08	6.17E+08	1.13E+09	6.51E+08	1.01E+09	1.66E+09	4.37E+08	7.85E+08	1.26E+09
57	1.07E+01	4.19E+08	6.57E+08	1.20E+09	6.81E+08	1.07E+09	1.77E+09	4.57E+08	8.32E+08	1.34E+09
58	5.04E+00	4.44E+08	7.11E+08	1.29E+09	7.24E+08	1.13E+09	1.92E+09	4.86E+08	8.86E+08	1.43E+09
59	2.38E+00	4.94E+08	7.97E+08	1.44E+09	8.13E+08	1.28E+09	2.14E+09	5.33E+08	9.79E+08	1.61E+09
60	1.13E+00	7.45E+08	1.22E+09	2.22E+09	1.22E+09	1.92E+09	3.26E+09	7.98E+08	1.49E+09	2.45E+09
61	4.14E-01	1.66E+10	3.07E+10	7.10E+10	3.15E+10	4.26E+10	9.43E+10	1.67E+10	3.23E+10	6.73E+10
TOTAL		2.54E+10	4.36E+10	9.30E+10	4.61E+10	6.39E+10	1.27E+11	2.67E+10	4.89E+10	9.22E+10

^a Position in capsule.

Table 28. Gamma fluxes (EOC) for HB-3 Key 3 Positions 3, 8, and 10

Energy group	Upper Bndy. (eV)	GAMMA FLUX (cm ⁻² ·s ⁻¹)								
		Position 3			Position 8			Position 10		
		p1 ^a	p2	p3	p1	p2	p3	p1	p2	p3
1	1.40E+07	1.92E+07	1.77E+07	1.81E+07	1.77E+07	1.27E+07	1.31E+07	1.74E+07	1.54E+07	1.54E+07
2	1.00E+07	9.31E+09	1.15E+10	1.72E+10	1.42E+10	1.68E+10	2.44E+10	9.11E+09	1.31E+10	1.86E+10
3	8.00E+06	5.19E+10	5.31E+10	6.39E+10	6.45E+10	5.67E+10	7.00E+10	4.71E+10	4.96E+10	5.79E+10
4	7.50E+06	8.32E+09	9.23E+09	1.21E+10	1.08E+10	1.13E+10	1.50E+10	8.16E+09	9.65E+09	1.23E+10
5	7.00E+06	5.73E+10	5.40E+10	5.91E+10	6.15E+10	4.92E+10	5.49E+10	6.48E+10	5.89E+10	6.05E+10
6	6.00E+06	5.35E+10	5.22E+10	5.80E+10	5.81E+10	4.88E+10	5.44E+10	5.17E+10	4.99E+10	5.37E+10
7	5.00E+06	4.88E+10	4.77E+10	5.43E+10	5.74E+10	4.80E+10	5.38E+10	5.56E+10	4.94E+10	5.07E+10
8	4.00E+06	1.38E+11	1.32E+11	1.44E+11	1.47E+11	1.16E+11	1.28E+11	1.28E+11	1.21E+11	1.26E+11
9	3.00E+06	7.64E+10	7.30E+10	7.86E+10	8.10E+10	6.61E+10	6.96E+10	7.28E+10	6.58E+10	6.81E+10
10	2.50E+06	1.62E+11	1.53E+11	1.72E+11	1.93E+11	1.53E+11	1.57E+11	2.03E+11	1.80E+11	1.82E+11
11	2.00E+06	1.88E+11	1.78E+11	1.91E+11	2.00E+11	1.63E+11	1.67E+11	1.97E+11	1.80E+11	1.84E+11
12	1.50E+06	2.28E+11	2.16E+11	2.31E+11	2.62E+11	2.14E+11	2.21E+11	2.44E+11	2.23E+11	2.24E+11
13	1.00E+06	2.30E+11	2.18E+11	2.38E+11	2.64E+11	2.13E+11	2.27E+11	2.42E+11	2.29E+11	2.33E+11
14	7.00E+05	1.02E+11	9.55E+10	1.05E+11	1.18E+11	9.82E+10	1.03E+11	1.07E+11	1.02E+11	1.05E+11
15	6.00E+05	1.93E+11	1.85E+11	2.03E+11	2.30E+11	2.02E+11	2.20E+11	2.10E+11	2.02E+11	2.10E+11
16	5.10E+05	2.08E+11	1.97E+11	2.17E+11	2.47E+11	2.09E+11	2.20E+11	2.26E+11	2.17E+11	2.23E+11
17	4.00E+05	2.70E+11	2.55E+11	2.84E+11	3.25E+11	2.71E+11	2.89E+11	2.92E+11	2.82E+11	2.92E+11
18	3.00E+05	9.37E+11	8.66E+11	9.90E+11	1.08E+12	8.55E+11	9.23E+11	9.79E+11	9.46E+11	9.78E+11
19	1.50E+05	3.72E+11	3.37E+11	4.18E+11	4.36E+11	2.92E+11	3.38E+11	3.71E+11	3.68E+11	3.95E+11
20	1.00E+05	1.12E+11	9.97E+10	1.41E+11	1.36E+11	6.80E+10	8.83E+10	1.07E+11	1.05E+11	1.21E+11
21	7.00E+04	2.36E+10	1.90E+10	3.21E+10	2.55E+10	8.89E+09	1.34E+10	2.31E+10	2.00E+10	2.41E+10
22	4.50E+04	4.44E+08	3.09E+08	6.34E+08	4.62E+08	1.50E+08	2.65E+08	4.50E+08	3.43E+08	4.74E+08
23	2.00E+04	6.35E+05	1.05E+06	2.41E+06	1.14E+06	1.39E+06	3.04E+06	6.35E+05	1.11E+06	2.26E+06
TOTAL		3.47E+12	3.25E+12	3.71E+12	4.01E+12	3.16E+12	3.44E+12	3.64E+12	3.47E+12	3.62E+12

^a Position in capsule.

Table 29. Neutron and gamma fluxes for reactor vessel wall

Energy group	Up. Bnd. (eV)	NEUTRON FLUX (cm ⁻² ·s ⁻¹)		
		BOC	EOC	AVG.
1	1.49E+07	7.88E+05	8.00E+05	7.94E+05
2	1.22E+07	1.81E+06	1.84E+06	1.82E+06
3	1.00E+07	2.93E+06	2.99E+06	2.96E+06
4	8.19E+06	4.62E+06	4.73E+06	4.68E+06
5	6.70E+06	5.99E+06	6.12E+06	6.06E+06
6	5.49E+06	6.34E+06	6.49E+06	6.41E+06
7	4.49E+06	4.72E+06	4.85E+06	4.79E+06
8	3.68E+06	4.56E+06	4.67E+06	4.62E+06
9	3.01E+06	5.11E+06	5.23E+06	5.17E+06
10	2.47E+06	1.40E+06	1.43E+06	1.42E+06
11	2.35E+06	1.28E+06	1.31E+06	1.30E+06
12	2.23E+06	2.10E+06	2.15E+06	2.13E+06
13	2.02E+06	3.94E+06	4.04E+06	3.99E+06
14	1.65E+06	3.67E+06	3.76E+06	3.72E+06
15	1.35E+06	3.45E+06	3.54E+06	3.49E+06
16	1.11E+06	2.71E+06	2.78E+06	2.74E+06
17	9.07E+05	3.25E+06	3.33E+06	3.29E+06
18	7.43E+05	2.88E+06	2.95E+06	2.91E+06
19	6.08E+05	1.95E+06	2.00E+06	1.97E+06
20	5.23E+05	6.02E+05	6.17E+05	6.10E+05
21	4.98E+05	2.35E+06	2.41E+06	2.38E+06
22	3.88E+05	2.59E+06	2.65E+06	2.62E+06
23	3.02E+05	1.16E+05	1.19E+05	1.17E+05
24	2.99E+05	4.25E+04	4.35E+04	4.30E+04
25	2.97E+05	8.87E+04	9.09E+04	8.98E+04
26	2.95E+05	6.97E+05	7.15E+05	7.06E+05
27	2.73E+05	1.73E+06	1.78E+06	1.76E+06
28	2.24E+05	1.56E+06	1.60E+06	1.58E+06
29	1.83E+05	1.43E+06	1.47E+06	1.45E+06
30	1.50E+05	1.33E+06	1.37E+06	1.35E+06
31	1.23E+05	2.10E+06	2.15E+06	2.12E+06
32	8.65E+04	2.26E+06	2.32E+06	2.29E+06
33	5.66E+04	3.78E+05	3.86E+05	3.82E+05
34	5.25E+04	2.02E+06	2.06E+06	2.04E+06
35	3.43E+04	8.34E+05	8.55E+05	8.44E+05
36	2.85E+04	2.39E+05	2.46E+05	2.42E+05
37	2.70E+04	1.57E+05	1.61E+05	1.59E+05
38	2.61E+04	2.20E+05	2.26E+05	2.23E+05
39	2.48E+04	2.19E+05	2.24E+05	2.21E+05
40	2.36E+04	1.91E+06	1.95E+06	1.93E+06
41	1.50E+04	2.05E+06	2.09E+06	2.07E+06
42	9.12E+03	2.00E+06	2.04E+06	2.02E+06
43	5.53E+03	1.57E+06	1.61E+06	1.59E+06
44	3.71E+03	7.82E+05	8.01E+05	7.92E+05
45	3.04E+03	5.84E+05	5.99E+05	5.92E+05
46	2.61E+03	5.83E+05	5.98E+05	5.90E+05
47	2.25E+03	3.88E+05	3.98E+05	3.93E+05
48	2.04E+03	1.94E+06	1.99E+06	1.96E+06
49	1.23E+03	1.93E+06	1.99E+06	1.96E+06
50	7.49E+02	1.94E+06	1.99E+06	1.96E+06
51	4.54E+02	1.94E+06	1.99E+06	1.96E+06
52	2.75E+02	1.94E+06	1.99E+06	1.96E+06
53	1.67E+02	1.94E+06	1.99E+06	1.96E+06
54	1.01E+02	2.90E+06	2.99E+06	2.94E+06
55	4.79E+01	2.91E+06	2.98E+06	2.94E+06
56	2.26E+01	2.91E+06	2.99E+06	2.95E+06
57	1.07E+01	2.92E+06	2.99E+06	2.95E+06
58	5.04E+00	2.97E+06	3.05E+06	3.01E+06
59	2.38E+00	3.16E+06	3.24E+06	3.20E+06
60	1.13E+00	4.68E+06	4.80E+06	4.74E+06
61	4.14E-01	2.40E+08	2.46E+08	2.43E+08
TOTAL		3.68E+08	3.78E+08	3.73E+08

Energy group	Up. Bnd. (eV)	GAMMA FLUX (cm ⁻² ·s ⁻¹)		
		BOC	EOC	AVG.
1	1.49E+07	1.95E+07	2.25E+07	2.10E+07
2	1.22E+07	6.63E+08	8.64E+08	7.64E+08
3	1.00E+07	2.18E+10	3.57E+10	2.88E+10
4	8.19E+06	4.26E+09	6.03E+09	5.14E+09
5	6.70E+06	6.63E+10	8.80E+10	7.71E+10
6	5.49E+06	4.51E+10	5.34E+10	4.92E+10
7	4.49E+06	8.37E+10	8.49E+10	8.43E+10
8	3.68E+06	1.48E+11	1.48E+11	1.48E+11
9	3.01E+06	1.04E+11	1.02E+11	1.03E+11
10	2.47E+06	2.22E+11	2.39E+11	2.31E+11
11	2.35E+06	2.25E+11	2.36E+11	2.30E+11
12	2.23E+06	3.29E+11	3.49E+11	3.39E+11
13	2.02E+06	3.04E+11	3.25E+11	3.14E+11
14	1.65E+06	1.34E+11	1.44E+11	1.39E+11
15	1.35E+06	1.96E+11	2.14E+11	2.05E+11
16	1.11E+06	2.61E+11	2.82E+11	2.72E+11
17	9.07E+05	3.51E+11	3.79E+11	3.65E+11
18	7.43E+05	1.32E+12	1.43E+12	1.38E+12
19	6.08E+05	9.10E+11	9.89E+11	9.50E+11
20	5.23E+05	8.92E+11	9.72E+11	9.32E+11
21	4.98E+05	9.84E+11	1.08E+12	1.03E+12
22	3.88E+05	1.76E+11	1.92E+11	1.84E+11
23	3.02E+05	6.64E+08	7.26E+08	6.95E+08
TOTAL		6.78E+12	7.35E+12	7.07E+12

Table 30. Calculated dpa rates for dosimeters used during HFIR fuel cycles 400 and 401

Key	Position in Key	General area	dpa rate (10^{-12}) s^{-1}	
			Neutron	Gamma
2C	1,4	HB-2	153	10.1
2W	8,32	HB-2	4.28	2.58
2C/2W	2D1C,2D2C ^a	HB-2	74.9	3.56
	2D1W,2D2W,2D3W ^a	HB-2	2.05	1.31
3	3	HB-3	2.72	1.16
	8	HB-3	4.69	1.17
	10	HB-3	3.53	1.16
7	1	HB-4	0.246	1.86
		^b	0.106	1.28

^a Tubular capsules.

^b Values obtained using vessel model.

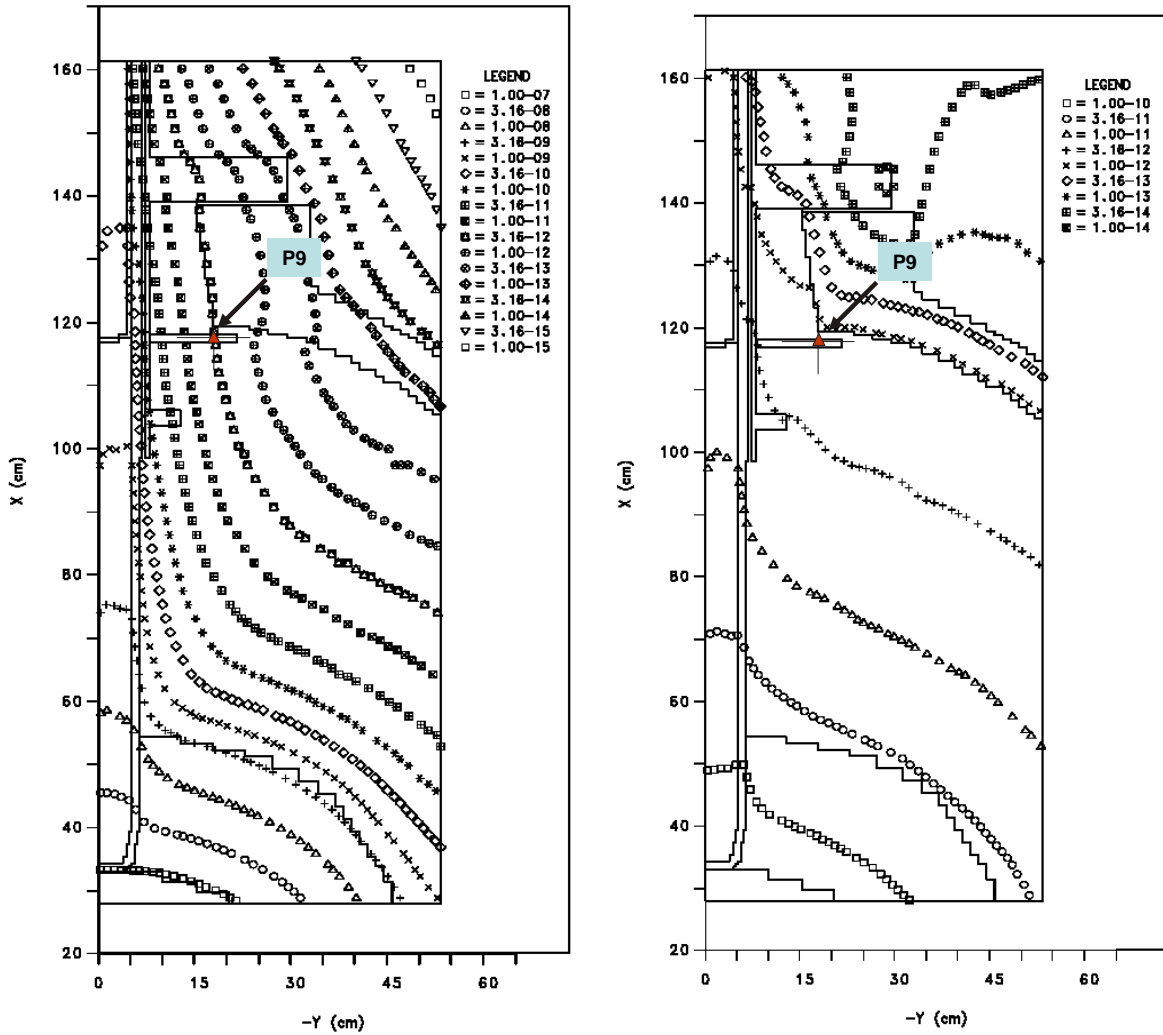


Fig. 17. Iso-plots of neutron (left) and gamma (right) dpa rates for HB-2 (original design) showing approximate location of the Key 2 radial dosimeter.

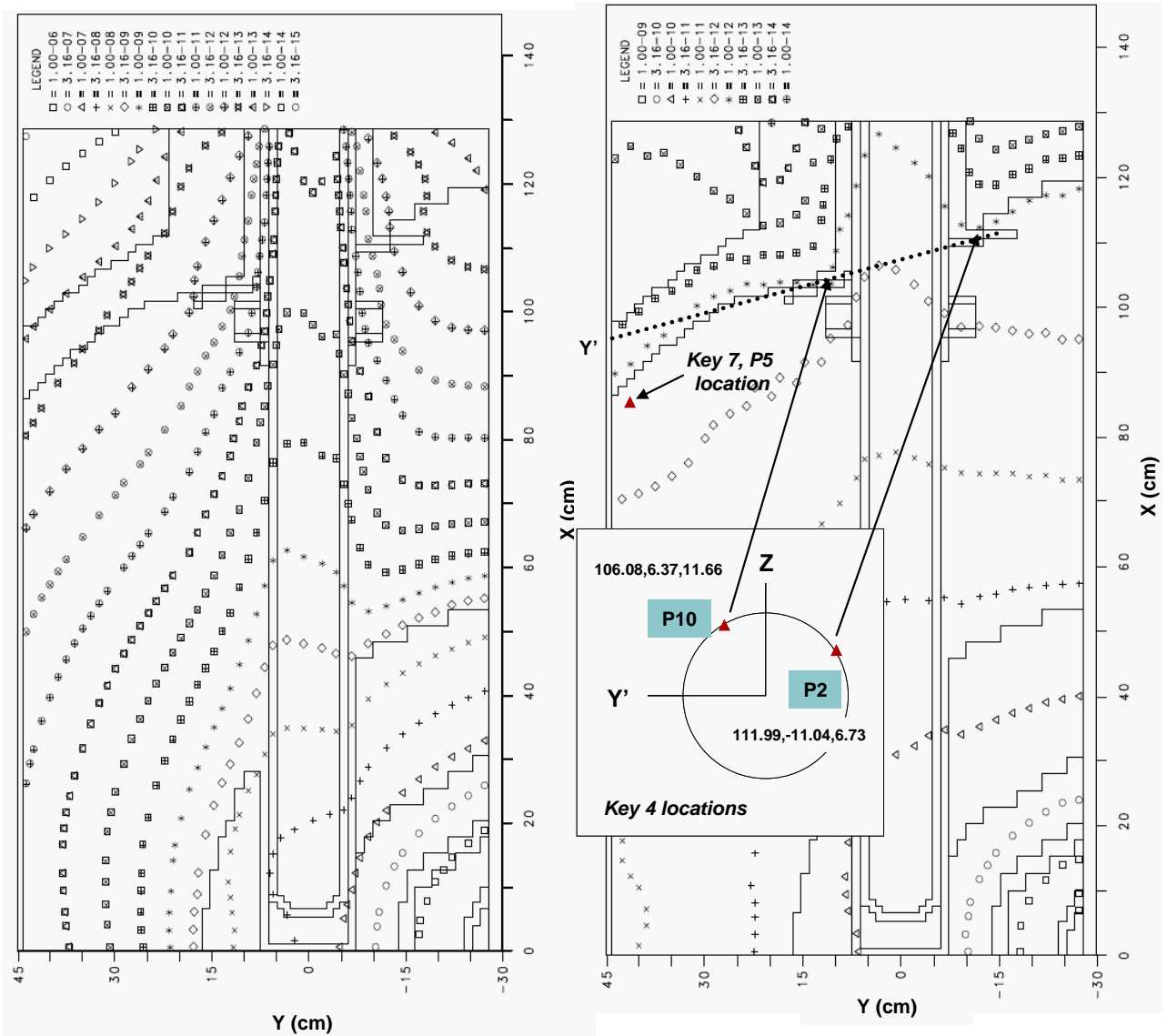


Fig. 18. Iso-plots of neutron (left) and gamma (right) dpa rates for HB-4 (original design). The plot is through the horizontal midplane, but the approximate locations of Key 4, Positions P2 and P10 are shown in the inset diagram on the right-hand figure. Key 4 position coordinates (X,Y,Z) are shown. Also, the approximate location for Key 7, Position P5 is shown. Calculations for Key 7, however, were performed using a model expanded in the Y dimension to 60.96 cm.

Table 31. Actual vs DORT/TORT model dosimeter locations for HB-2 and HB-4 (original designs)

Beam tube	Key/ position	Key (x,r) location [cm (in.)]		Model (x,r) location [cm (in.)]		Model cell ID (x,r)		
		x	r	x	r			
HB-2	K2,P9	116.4 (45.83)	17.8 (7.02)	116.3 (45.79)	17.8 (7.02)	(64,36),(64,37) ^a		
		Key (x,y,z) location [cm (in.)]			Model (x,y,z) location ^b [cm (in.)]		Model cell ID (x,y,z)	
		x	y	z	x	y		z
HB-4	K4,P2	110.01 (43.31)	-10.59 (-4.17)	6.38 (2.51)	109.86 (43.25)	-10.68 (-4.20)	6.745 (2.66)	(58,14,6)
	K4,P10	105.08 (41.37)	6.12 (-2.41)	11.05 (4.35)	104.78 (41.25)	6.745 (2.66)	10.68 (4.20)	(54,28,9)
	K7, P5	84.07 (33.1)	41.15 (16.2)	0.0 (0.0)	85.09 (33.5)	41.27 (16.3)	0.7125 (0.281)	(39,55,1)

^a Cell values are averaged.

^b Center of cell.

Table 32. Summary of calculated dpa rates for indicated HB-2 and HB-4 beam-tube locations for $t < 22.7$ EFPY (original designs)

Beam tube	Dosimeter Key location		dpa rates (10^{-12} s^{-1}) ^a	
	Key	Position	Neutron	Gamma
HB-2 ^b	2	9	3.556 (3.480) ^c	1.719 (1.445)
HB-4 ^b	4	2	1.162 (1.024) ^d	1.287 (1.434)
	4	10	1.779 (1.046)	1.050 (1.290)
	7	5	0.3437 (0.3422) ^e	1.606

^a dpa rate values for 100 MWt power level.

^b HB-2 and HB-4 original beam-tube designs.

^c Values in parentheses are dpa rates from Table 4 of [1], shown to one additional decimal place and obtained by dividing the normalized values by the normalization factors (neutron: 0.638, gamma: 1.76). They differ from the updated values due to neutron dpa rate cross-section revision, a shift in the Key mesh location, and specimen mount revisions.

^d HB-4 dpa rates in parentheses are from Table 5 of [1]. The model for these values does not include the specimen mount or revisions in the neutron dpa cross sections.

^e Value in parentheses for Key 7, Position 5, is the dpa rate without including the revisions in the neutron dpa cross sections.

4. DATA/CODE ARCHIVE AND QUALITY ASSURANCE

Models for the calculations discussed in this report comprise a revised subset of models developed for [1] and [2]. Appendix C of [1] describes the earlier models, discusses naming conventions, and provides additional explanation for reproducing the results. The primary revision to the calculation models is the updating of the dpa neutron cross sections, as discussed in Sect. 2.1. The earlier calculations had been performed on the Nuclear Science and Technology Division (NSTD) NAS computer system. Since then the NSTD CPILE computer system, in conjunction with the DOORS 3.2 code system, has been approved for quality-assurance-qualified HFIR calculations [8]. In consideration of these issues, it was deemed prudent to move the appropriate models and data to the CPILE computer and repeat the calculations. This was done, and it was noted that there were slight variations in the results when compared with the original NAS values (except for calculations for HB-4 for $t > 22.7$ EFY, for which it was noted that the original cross-section library lacked the appropriate scattering terms). The differences were small, typically $<2\%$ ($\sim 1\%$ for HB-2, which is the beam tube of most concern) and judged to be of no significant impact. Thus, the results for the earlier NAS computer calculations have been retained in this report to maintain consistency with other reports and avoid unnecessary confusion. It has also been noted that the file names and naming conventions in [1] and [2] are somewhat confusing. At the time the models were under development, efforts were made to reference model changes within the file names. Although this is an accepted and generally successful approach, because of the number of developmental revisions required, the file names grew long and cumbersome and had some confusing terminology. Therefore, at the same time the models were updated to CPILE, a simpler naming convention was implemented, and most file names were shortened. A simple directory structure was also implemented. An archive of the models is described in Appendix E.

In addition to the DOORS 3.2 software package, two additional codes have been used. These were the AXMIX code for cross-section mixing and the DTD code for transforming a boundary source from one 2D (DORT) calculation to another with a rotated and translated coordinate system. Quality-assurance approval for these codes on the CPILE system for HFIR safety-related analysis has been obtained [9, 10].

5. SUMMARY

This report, which is the second supplement to [1], records the set of dpa rates that was used in [5] to calculate measured-to-calculated (M/C) values, normalization factors, and normalized dpa rates that were used in Sect. 5 of [5] to evaluate the structural integrity of the HFIR pressure vessel. These upgraded unnormalized dpa rates are referred to as the “second upgrade.” The corresponding sets of M/C values and normalization factors were derived and recorded in [5]. The improvements associated with the second upgrade were the addition of the Keys to the geometric models and the substitution of an improved set of neutron dpa cross sections.

Following completion of the evaluation of vessel structural integrity included in [5], the models for calculating dpa rates were further upgraded with (1) inclusion of missing neutron scattering cross sections for the upgraded HB-4/Key 4–area analytic model, (2) the use of interpolation and curve fitting to “smooth” the calculated dpa-rate distribution, and (3) the use of an alternative computer (CPiLE) that is properly quality assured for HFIR safety issues. The corresponding set of dpa rates, referred to as the “third upgrade,” is documented in this report and was used, in the unnormalized form, in Appendix B of [5] for transposing dosimetry data.

Also documented in this report are the neutron and gamma fluxes corresponding to the “second upgrade” of dpa rates for neutron and gamma dosimeters irradiated during fuel cycles 400 and 401. These fluxes were used to help derive dpa values from the dosimeter activities, and these “measured” values of dpa were used in the calculation of the “2004” M/C and normalization factors [5].

Appendix D briefly addresses the use of the Monte Carlo approach as a supplement to or replacement for discrete-ordinates calculations in the future. A promising option with the Monte Carlo approach is the use of an advanced variance-reduction methodology, the Consistent Adjoint Driven Importance Sampling (CADIS) methodology, to accelerate results. A Monte Carlo model employing CADIS was used to calculate dpa rates for Key 5 (Appendix C), a location that presents difficulties for existing discrete-ordinates models.

6. REFERENCES

1. E. D. Blakeman, *Neutron and Gamma Fluxes and dpa Rates for the HFIR Vessel Beltline Region (Present and Upgrade Designs)*, ORNL/TM-13693, Oak Ridge National Laboratory, Oak Ridge, Tenn., September 2000.
2. E. D. Blakeman, *Neutron and Gamma Fluxes and dpa Rates for the HFIR Vessel Beltline Region (Present and Upgrade Designs), Supplement 1*, ORNL/TM-13693/S1, Oak Ridge National Laboratory, Oak Ridge, Tenn., December 2000.
3. I. Remec and C. A. Baldwin, *Analysis of HFIR Dosimetry Experiments Performed in Cycles 400 and 401*, ORNL/TM-2008/046, Oak Ridge National Laboratory, Oak Ridge, Tenn., September 2008.
4. R. K. Nanstad, "Final Report—2005 Charpy Impact Test Results for HFIR Surveillance Program," letter to Kevin A. Smith (ORNL), February 5, 2006.
5. R. D. Cheverton, R. K. Nanstad, C. A. Baldwin, E. D. Blakeman, T. L. Dickson, H. A. Kmiecik, and I. Remec, *Impact of 2004/2005 Dosimetry and Surveillance Data on the HFIR Vessel Radiation Embrittlement Trend Curve, Hydrostatic Proof Test Conditions, Pressure/Temperature Limits, and Life Extension*, ORNL/TM-2008/007, Oak Ridge National Laboratory, Oak Ridge, Tenn., August 2010.
6. R. D. Cheverton, R. K. Nanstad, E. D. Blakeman, and H. A. Kmiecik, *HFIR Pressure Vessel and Structural Component Materials Surveillance Program, Supplement 3*, ORNL/TM-1372/S3, Oak Ridge National Laboratory, Oak Ridge, Tenn., August 2010.
7. DOORS3.2, RSICC Computer Code Collection, CCC-650, Radiation Safety Information Computational Center, Oak Ridge National Laboratory, Oak Ridge, Tenn. (1998).
8. HFIR Safety-Related Software Baseline Revision Approval, SBPF-1300.1-DOORS-3.2a-cpile, December 14, 2005; Software Registry number 00963.
9. HFIR Safety-Related Software Baseline Revision Approval, SBPF-1300.1-AXMIX-cpile, February 7, 2006; Software Registry number 001331.
10. HFIR Safety-Related Software Baseline Revision Approval, SBPF-1300.1-DTD-cpile, February 7, 2006; Software Registry number 001327.
11. C. Y. Fu and D. T. Ingersoll, *VELM61 and VELM22: Multigroup Cross-Section Libraries for Sodium-Cooled Reactor Shield Analysis*, ORNL/TM-10302, Oak Ridge National Laboratory, Oak Ridge, Tenn., April 1987.
12. *ASTM Standard Practice for Characterizing Neutron Exposure in Iron and Low Alloy Steels in Terms of Displacement per Atom (DPA)*, E 693-94, Book of ASTM Standards, Section 12, Volume 12.02, Nuclear, Solar, and Geothermal Energy (1997).
13. F. W. Stallmann, *LSL-M2: A Computer Program for Least Squares Logarithmic Adjustment of Neutron Spectra*, NUREG/CR-4349 (ORNL/TM-9933), prepared for the U.S. Nuclear Regulatory Commission by Oak Ridge National Laboratory, Oak Ridge, Tenn., March 1986. Also distributed as report number PSR-233 by the Radiation Shielding Information Center (now the Radiation Safety Information Computational Center), Oak Ridge National Laboratory, July 1987.
14. N. P. Baumann, "Gamma-ray Induced Displacements in D2O Reactors," *Proc. Of the Seventh ASTM-EURATOM Symposium on Reactor Dosimetry*, Strasbourg, France, August 27–31, 1990.
15. R. D. Cheverton and T. L. Dickson, *HFIR Vessel Life Extension with Enlarged HB-2 and HB-4 Beam Tubes*, ORNL/TM-13698, Oak Ridge National Laboratory, Oak Ridge, Tenn., December 1998.
16. E. D. Blakeman, J. A. Bucholz, and R. D. Cheverton, *Calculation of dpa Rates at the HFIR HB-2 Beam Tube Nozzle Corner Using Three-Dimensional Discrete Ordinates and Monte Carlo Models*, ORNL/TM-2003/213, Oak Ridge National Laboratory, Oak Ridge, Tenn., June 2004.

17. K. Farrell, F. B. Cam, C. A. Baldwin, J. V. Pace III, W. R. Corwin, L. Robinson, F. F. Dyer, F. M. Haggag, F. W. Stallman, B. M. Oliver, and L. R. Greenwood, *The DOS 1 Neutron Dosimetry Experiment at the HB-4-A Key 7 Surveillance Site on the HFIR Pressure Vessel*, ORNL/TM-12511, Oak Ridge National Laboratory, Oak Ridge, Tenn., January 1994.
18. I. Remec, J. A. Wang, F. B. K. Kam, and K. Farrell, "Effects of Gamma-Induced Displacements on HFIR Pressure Vessel Materials," *J. Nucl. Mat.* **217**, 258–268 (1994).
19. R. D. Cheverton, J. G. Merkle, and R. K. Nanstad, editors, *Evaluation of HFIR Pressure-Vessel Integrity Considering Radiation Embrittlement*, ORNL/TM-10444, Oak Ridge National Laboratory, Oak Ridge, Tenn., April 1988.

APPENDIX A
dpa RATES USED FOR HFIR VESSEL STRUCTURAL INTEGRITY EVALUATIONS
SINCE THE ENLARGEMENT OF THE HB-2 AND HB-4 BEAM TUBES

Several sets of calculated dpa rates for neutrons and gammas have been developed as a result of upgrades in the geometric and analytical models and availability of new dosimetry data. The dosimetry data are used to normalize (correct) the calculated values of dpa rates before they are used in the vessel integrity analyses. The sets of dpa rates are defined by normalization factors as well as calculational models, and thus the same unnormalized dpa rates could be associated with two different “sets” of dpa rates, as is the case for Sets 2 and 3 defined below.

First Set:

The calculated values of dpa rate in this set were normalized using the dosimetry data from the 1993 dosimetry measurements [1]. Some of the dpa rates and a description of the models are included in [2].

This set, with a few preliminary gamma dpa rates, was used as input to [3, 4], the former of which was the first vessel integrity study with the enlarged beam tubes. All of the dpa rates used for the vessel 31 regions in [3] are included in Appendix E of [3].

A distinguishing feature of the geometric models used in [2] is that the only Key (surveillance capsule mount) included was Key 2 for $t < 22.7$ EFPY.

Second Set:

The second set of dpa rates was calculated using geometric models that included Keys 1, 2, 2C/W, 3, and 4 for $t < 22.7$ EFPY and > 22.7 EFPY, as appropriate, and normalization factors based on these calculated dpa rates and the 1993 dosimetry. This set of dpa rates was used in [5] and was nearly the same as Set 1, resulting in a gross understatement of some dpa rates for surveillance specimens removed and tested in 2005 [6].

Third Set:

This set included the unnormalized calculated dpa rates in Set 2 and the normalization factors based on the Set 2/Set 3 unnormalized calculated dpa values and the 2004 dosimetry data [7]. This set (Set 3) was used in the Sect. 4 analysis in [8]. The corresponding normalization factors are included in Table 3 of [8] under the column heading “Sect. 4.”

Fourth Set:

The calculated dpa rates used in Sect. 3 were updated by using an improved set of neutron dpa cross sections. The corresponding normalization factors, which are included in Table 3 of [8] under the column heading “Sect. 5,” are based on these new unnormalized dpa rates and the 2004 dosimetry data. These normalized dpa rates were used in the “Sect. 5” analysis in [8].

Fifth Set:

This set involves (1) interpolation and curve fitting of the unnormalized calculated dpa rates in Sect. 4 to cope with the geometric effects associated with the mesh-based numerical analysis method

(discrete ordinates) used, and (2) the addition of neutron scattering terms that were missing from the HB-4 model for $t > 22.7$ EFPY. Corresponding normalization factors were calculated using the 2004 dosimetry data [7] and the Set 5 unnormalized calculated dpa rates (see Appendices B and D in [9]).

The fifth set of dpa rates was used in Appendix B of [8] to transpose the dosimetry data to locations of specific surveillance capsules and was also used in [9] to calculate approximate values of dpa at specified times for removal of surveillance capsules for testing of Charpy V-notch specimens. It is intended that this set be used for future analysis.

It should be noted that the unnormalized dpa-rate first upgrade referred to in the text was used for dpa-rate Sets 2 and 3. Table A.1 provides a summary of all characteristics of the dpa-rate sets and dpa-rate upgrades.

Table A.1. Summary of conditions for dpa-rate sets

Set	Applied	Upgrade of calculated dpa rates	Essence of “upgrades”	Dosimetry for normalization
1	[3,4]	Original	None	1993
2	[5]	First	Added Keys 1, 2C/2W ($t > 22.7$ EFPY), 3, 4 ($t < 22.7$ EFPY), 4 ($t > 22.7$ EFPY)	1993
3	Sect. 4 [8]	First	SAME	2004
4	Sect. 5 [8]	Second	Improved neutron dpa cross sections	2004
5	App. B [8], [9]	Third	Interpolation, curve fitting, addition of neutron scattering terms for HB-4 ($t > 22.7$ EFPY).	2004

A.1 REFERENCES

1. I. Remec, J. A. Wang, F. B. K. Kam, and K. Farrell, "Effects of Gamma-Induced Displacements on HFIR Pressure Vessel Materials," *J. Nucl. Mat.* **217**, 258–268 (1994).
2. E. D. Blakeman, *Neutron and Gamma Fluxes and dpa Rates for the HFIR Vessel Beltline Region (Present and Upgrade Designs)*, ORNL/TM-13693, Oak Ridge National Laboratory, Oak Ridge, Tenn., September 2000.
3. R. D. Cheverton and T. L. Dickson, *HFIR Vessel Life Extension with Enlarged HB-2 and HB-4 Beam Tubes*, ORNL/TM-13698, Oak Ridge National Laboratory, Oak Ridge, Tenn., December 1998.
4. R. D. Cheverton and J. W. Bryson, *HFIR Vessel Pressure/Temperature Limits Corresponding to the Upgrade Design*, ORNL/TM-1999/181/R1, Oak Ridge National Laboratory, Oak Ridge, Tenn., March 2000.
5. R. D. Cheverton, R. K. Nanstad, and E. D. Blakeman, *HFIR Pressure Vessel and Structural Components Materials Surveillance Program, Supplement 2*, ORNL/TM-1372/S2, Oak Ridge National Laboratory, Oak Ridge, Tenn., August 1999.
6. R. K. Nanstad, "Final Report—2005 Charpy Impact Test Results for HFIR Surveillance Program," letter to Kevin A. Smith (ORNL), February 5, 2006.
7. I. Remec and C. A. Baldwin, *Analysis of HFIR Dosimetry Experiments Performed in Cycles 400 and 401*, ORNL/TM-2008/046, Oak Ridge National Laboratory, Oak Ridge, Tenn., September 2008.
8. R. D. Cheverton, R. K. Nanstad, C. A. Baldwin, E. D. Blakeman, T. L. Dickson, H. A. Kmiecik, and I. Remec, *Impact of 2004/2005 Dosimetry and Surveillance Data on the HFIR Vessel Radiation Embrittlement Trend Curve, Hydrostatic Proof Test Conditions, Pressure/Temperature Limits, and Life Extension*, ORNL/TM-2008/007, Oak Ridge National Laboratory, Oak Ridge, Tenn., August 2010.
9. R. D. Cheverton, R. K. Nanstad, E. D. Blakeman, and H. A. Kmiecik, *HFIR Pressure Vessel and Structural Component Materials Surveillance Program, Supplement 3*, ORNL/TM-1372/S3, Oak Ridge National Laboratory, Oak Ridge, Tenn., August 2010.

APPENDIX B
MESH-INTERVAL-BASED INTERPOLATION PROCESS FOR
CALCULATION OF dpa RATES

A simple linear interpolation scheme for determining displacements-per-atom-per-second (dpa) rates (or other quantities of interest) at a specified location from a discrete mesh calculation is shown in Fig. B.1. It depicts only one dimension, whereas the actual interpolation should be performed in up to three dimensions. In the scheme as shown, the calculated values are assumed to occur at the center of the mesh intervals, as depicted as $x_{1,c}$ and $x_{2,c}$ for the two intervals. The line joining the top centers of the two histogram values is assumed to be the dpa rate curve, and the value d_D at the dosimetry point x_D is, by linear interpolation, given by

$$d_D = \frac{\Delta_{1D}}{\Delta_{12}} (d_2 - d_1) + d_1,$$

where the Δ terms are defined as shown in Fig. B.1.

If the dosimetry point, x_D , is located at one of the mesh point centers, $x_{1,c}$ or $x_{2,c}$, then Δ_{1D} is either zero or Δ_{12} , and d_D is the dpa rate value within one of the mesh cells (i.e., either d_1 or d_2 , respectively). Similarly, if x_D is located halfway between the two interval centers (at the interval boundary if the

intervals are the same width), $\Delta_{1D} = \frac{\Delta_{12}}{2}$ and the above expression simplifies to

$$d_D = \frac{d_1 + d_2}{2},$$

which is simply the average of the mesh interval values. It follows that if the dosimeter point is sufficiently close to either a mesh cell center or the boundary between two equal-sized mesh cells (or average of two centers if not equal), then the interpolated value can be approximated by either the value for the appropriate mesh cell or the averaged value for two adjacent mesh cells.

The above approach addresses only one dimension. For higher-dimensional spaces, proportionally more mesh cells are involved (e.g., up to four mesh cells for a two-dimensional interpolation).

It must also be emphasized that the assumption that the value for a mesh cell is located at the center is in itself an approximation because the value cannot in fact be localized anywhere except over the entire mesh cell. The best approach to achieve finer resolution is to decrease the mesh interval size at the point of interest. However, care must be taken because this change must be incorporated over the entire extent of the other orthogonal dimensions (e.g., a change in an X dimension mesh occurs over the entire extent of the Y and Z model dimensions).*

* This effect would not occur if the discontinuous mesh option was used. However, this option is not available for the DORT two-dimensional transport code and is limited and seldom used in the TORT three-dimensional one.

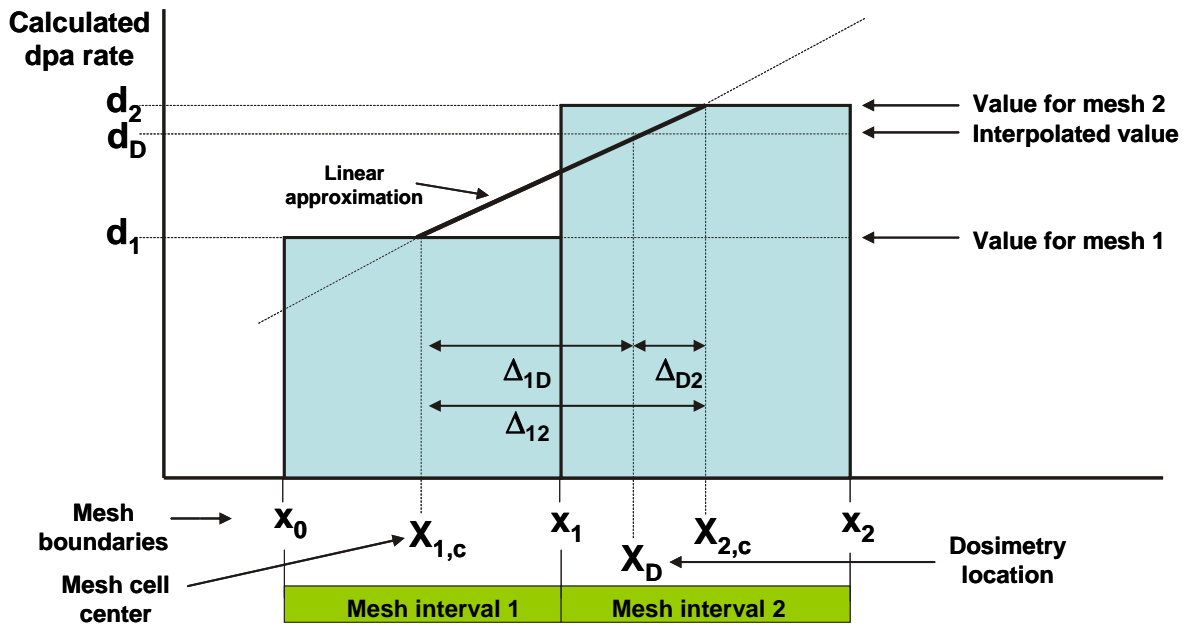


Fig. B.1. Linear interpolation scheme for estimation of dpa rate at specified location from discrete mesh calculations. Only one dimension is shown. Values for each mesh cell are assumed to be located at the mesh cell center.

APPENDIX C
REVISED dpa RATE CALCULATIONS PERFORMED USING THE
OAK RIDGE NATIONAL LABORATORY CPILE COMPUTER AND INCORPORATING
INTERPOLATION AND CURVE-FITTING ENHANCEMENTS

C.1 THE THIRD UPGRADE

As mentioned in the introduction to this report, the third upgrade included (1) application of interpolation and curve fitting of the calculated dpa rates (displacements-per-atom-per-second) to improve their accuracy, (2) addition of neutron scattering terms that were missing for the enlarged HB-4 beam-tube analytic model, and (3) use of an alternate computer (CPILE) that has been quality-assurance approved in conjunction with the DOORS 3.2 software system* for the performance of High Flux Isotope Reactor (HFIR) safety-related calculations.

Interpolated dpa rates, which depend on the gradients with neighboring cells, more nearly correspond to the specified locations, and the additional application of curve fitting provides a more realistic distribution curve from which dpa rates can be selected for a specific location.

Calculated dpa rates corresponding to the third upgrade have not yet been used in the vessel structural integrity analysis but were applied in Appendix B in [1] and [2]. In this report the third upgrade has been applied to the calculation of a set of dpa rates for all Keys and dosimeters described in [1] and for the 31 vessel regions used in the vessel integrity analysis [1, 2, 3].

A convention used for calculations in this appendix is shown in Fig. C.1, which depicts a beam line from the perspective of sighting through the beam line away from the core and toward the vessel wall. From this perspective the +Y axis is to the left and +Z is up. Angular changes are assumed to be positive in the clockwise direction, and 0 degrees is at the 12 o'clock position. For plots it is useful to use negative angles, which correspond to angles greater than 180 degrees in the third and fourth quadrant. Because of vertical symmetry with respect to the $Z = 0$ plane, it is not necessary to plot redundant values for the second and third quadrants. Thus, plots of dpa rate vs angle will run from -90 to +90 degrees.

* Separate QA was performed for the AXMIX and DTD codes which are not officially contained within the DOORS software system.

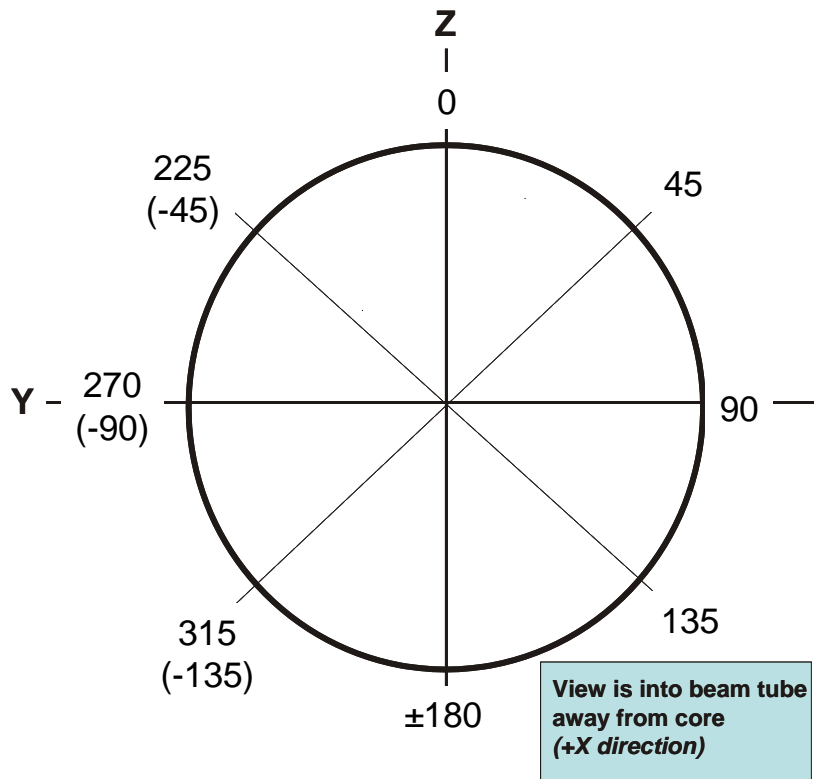


Fig. C.1. Convention for specifying angles for capsule locations in a beam tube. The perspective is looking into the beam tube toward the vessel wall. Thus, the positive X-axis direction projects into the image plane.

C.2 CALCULATED VALUES OF dpa RATE (UPGRADE 3) FOR ALL SURVEILLANCE-CAPSULE AND DOSIMETER-DEDICATED CAPSULE LOCATIONS

C.2 depicts plots of the calculated neutron dpa rate for angular positions at 5-degree increments for Key 3 (HB-3). Uninterpolated and interpolated values, obtained by applying the mesh-interval interpolation described in Appendix A, are shown in the top plot. The bottom plot includes not only the interpolated data, but also least squares fits of the interpolated data to a straight line and to a sine curve. The straight-line fit was considered an initial possibility and is shown more for reference purposes. The sine-curve fit is considered appropriate because it enables a smooth, zero-slope transition at 90 and 270 (-90) degrees, as required by the vertical symmetry, and in general correlates well to the dpa rate vs angle relationship. The straight-line fit, shown for comparison, is in general close to the sine-curve fit but is inappropriate because it has discontinuous slopes at 90 and 270 (-90) degrees (seen if entire angular plot is shown). Curve fitting of the interpolated data is intended to further smooth out “bumps” in the data resulting from effects of the discrete mesh. However, for Key 3 the interpolated neutron dpa rate vs angle curve is sufficiently smooth, so the curve-fit data were not used. Similar plots are shown in Fig. C.3 for the gamma dpa rate. Note that the interpolated gamma dpa rate vs angle plot contains significant scatter. Thus, the sine-curve-fit data were used. Neutron and gamma dpa rates at the Key 3 position locations are shown in Fig. C.4. The uninterpolated and interpolated values are shown for the neutron dpa rate, and the uninterpolated, interpolated, and sine-curve-fit values are shown for the gamma dpa rates.

Similar plots are shown in Figs. C.5 – C.7 for Key 4 (HB-4, original design), which show calculated dpa rates for times (t) less than 22.7 effective full-power years (EFPY). Note that the sine-curve-fitted data were used only for the gamma dpa rates. Plots shown in Figs. C.8 – C.10 are equivalent plots, also for Key 4 (HB-4, modified design), for times greater than 22.7 EFPY. The sine-curve fits were used for the neutron and gamma dpa rates for this case.

Calculated neutron and gamma dpa rates for Key 6 are shown in Fig. C.11. Positions in Keys 6 and 7 are not arranged in a circular pattern. Therefore, an angular depiction was not used. Interpolated values are shown for neutron and gamma Key positions. Key 7 values are shown in Figs. C.12 and C.13 for times before and after 22.7 EFPY (HB-4, original and modified designs, respectively). For Keys 6 and 7, models extended in the +Y direction were used to include all the positions. Because HB-1 is the same as HB-4 (original design), the HB-4 model was used for Key 6 calculations.

Tables C.1 – C.6 list the Key position neutron and gamma dpa rates shown in plots in Figs. C.4, C.7, and C.10 – C.13. Uninterpolated, interpolated, and sine-curve-fit (if used) values are listed.

The “best-case” values (either interpolated or interpolated and sine-curve fitted) from Tables C.1 – C.6 are summarized in Table C.7. Also included are values for HB-2 for times before and after 22.7 EFPY. Thus, data shown in Table C.7 are for Keys 2, 3, 4, 6, and 7 for times before and after 22.7 EFPY. Angles are expressed in Table C.7 only in the positive sense, and the use of negative angles, conveniently used for the plots, is dispensed with. Note that values at all points other than at the horizontal midplane ($Z = 0$) are applicable to two Key locations, one above and one below the horizontal midplane.

Results for Key 5 calculated by an Oak Ridge National Laboratory Monte Carlo model of HFIR using an advanced variance-reduction methodology ([4] and Appendix D) are also given in Table C.7. Because of its location between HB-4 and HB-3, its vertical location (-9 in.) from the midplane, and the need to include an ion chamber with lead shielding, it was not otherwise considered practical to modify the existing HB-4 model to include the Key 5 positions.

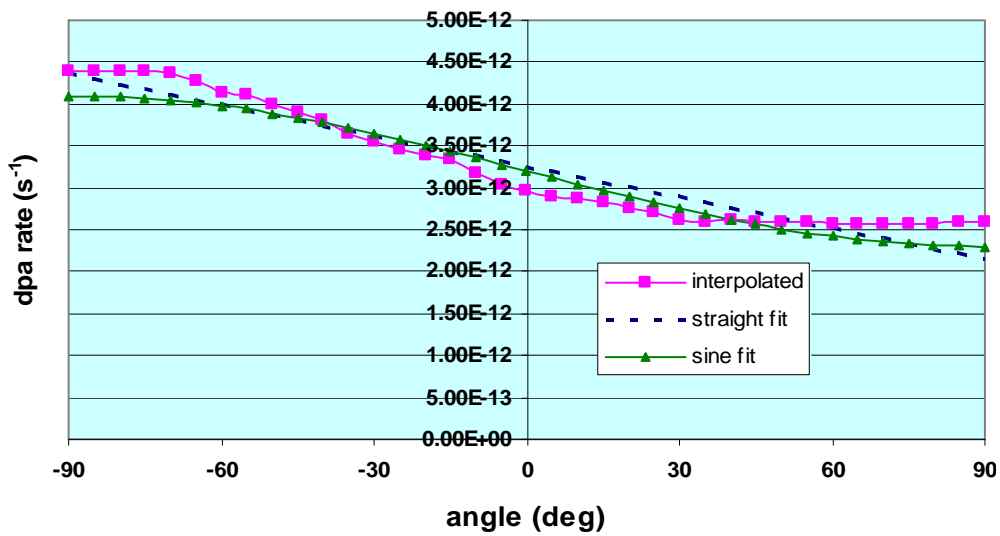
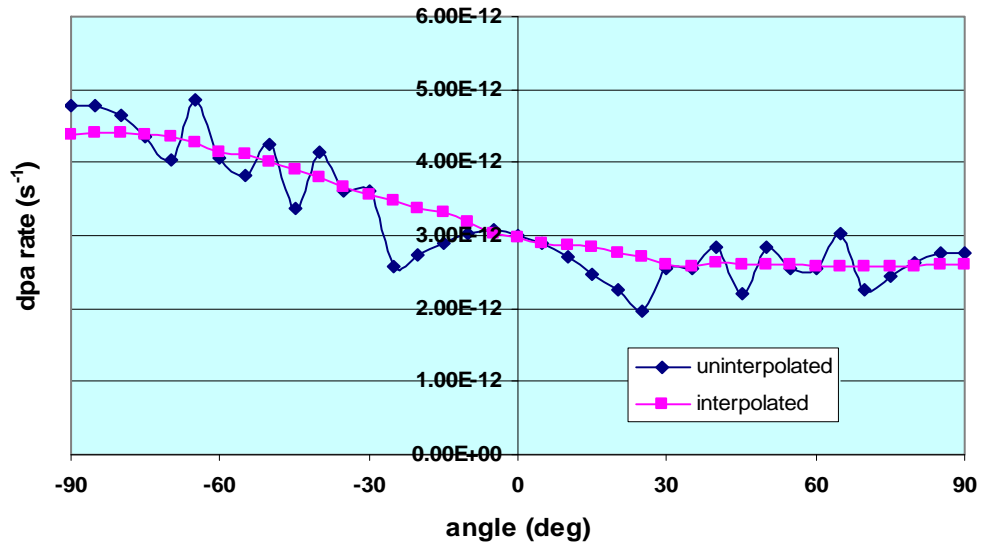


Fig. C.2. Key 3 (HB-3) neutron dpa rate vs angle showing uninterpolated and interpolated data (top) and interpolated data with straight-line and sine-curve fits (bottom).

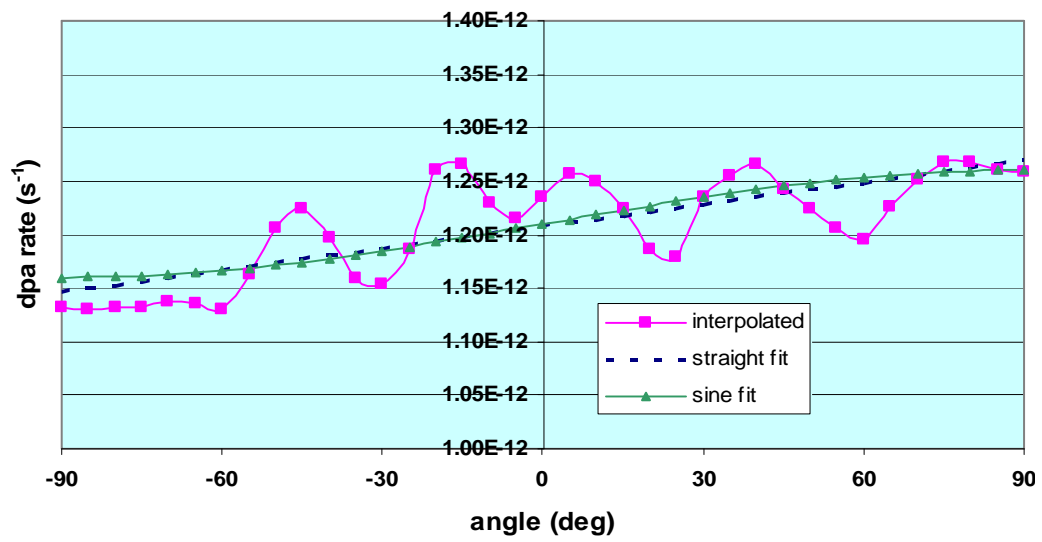
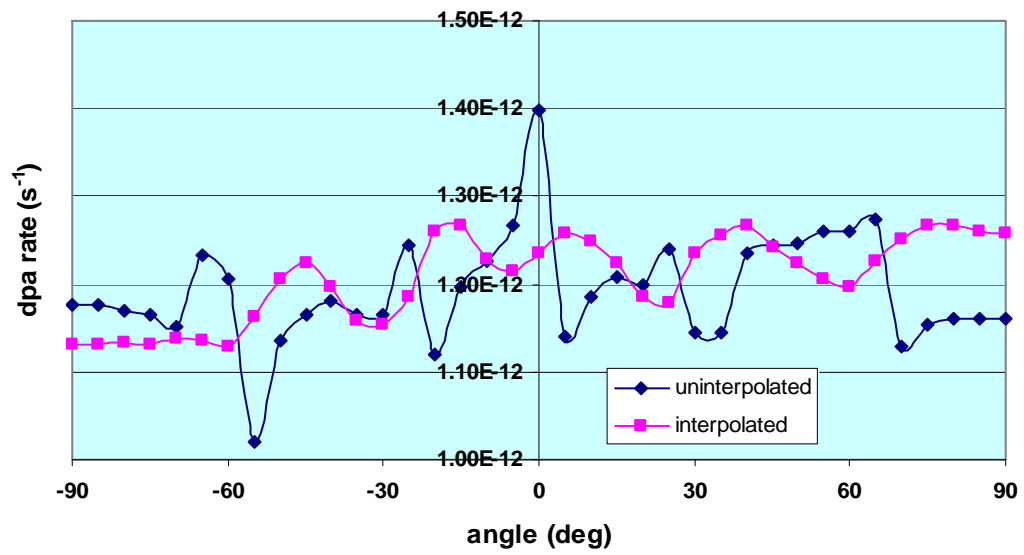


Fig. C.3. Key 3 (HB-3) gamma dpa rate vs angle showing uninterpolated and interpolated data (top), and interpolated data with straight-line and sine-curve fits (bottom).

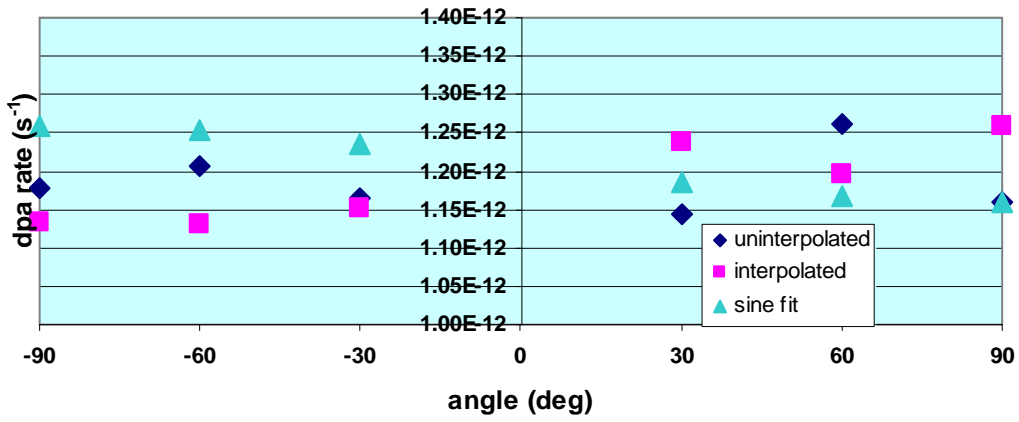
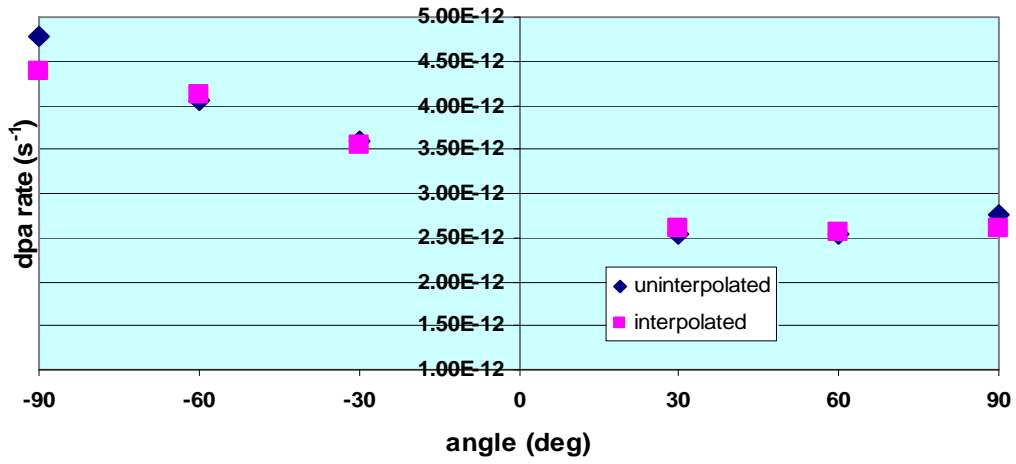


Fig. C.4. Key 3 (HB-3) neutron (top) and gamma (bottom) dpa rates for Key positions plotted vs angle showing uninterpolated, interpolated, and sine-curve-fit (where used) data.

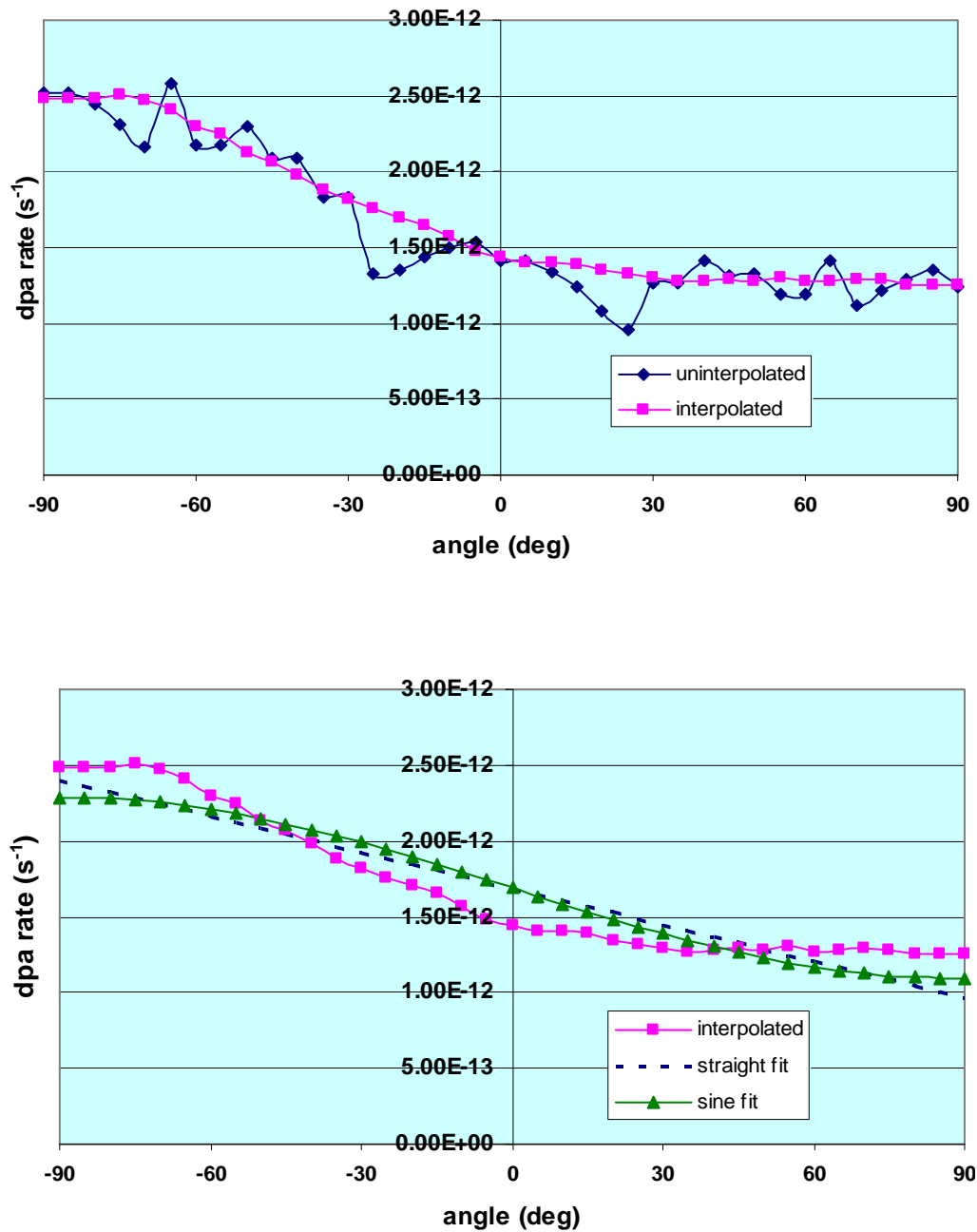


Fig. C.5. Key 4 (HB-4 original design) neutron dpa rate vs angle showing uninterpolated and interpolated data (top) and interpolated data with straight-line and sine-curve fits (bottom). Values are for $t < 22.7$ EFPY.

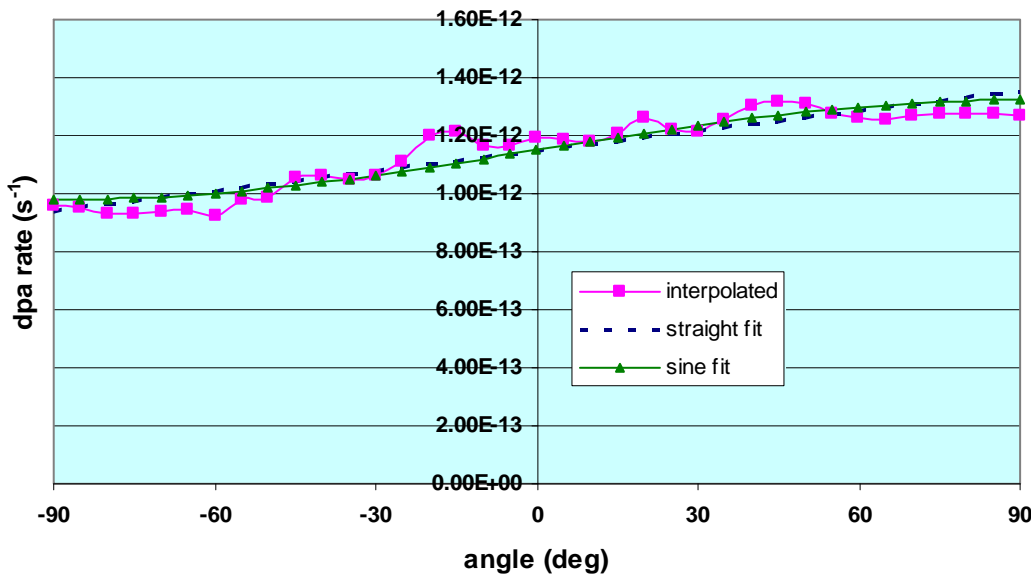
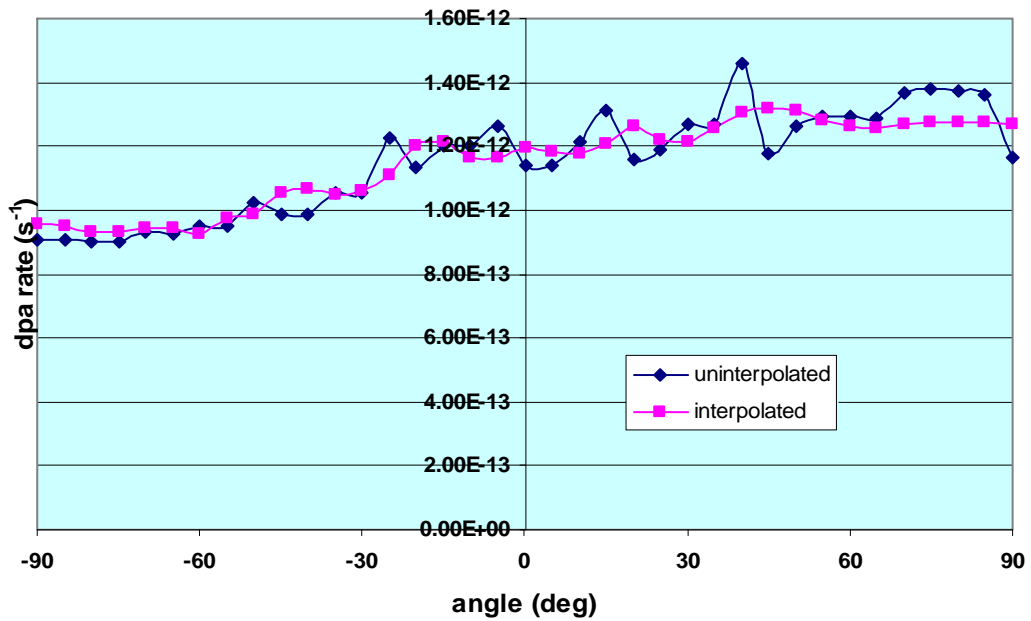


Fig. C.6. Key 4 (HB-4 original design) gamma dpa rate vs angle showing uninterpolated and interpolated data (top) and interpolated data with straight-line and sine-curve fits (bottom). Values are for $t < 22.7$ EFPY.

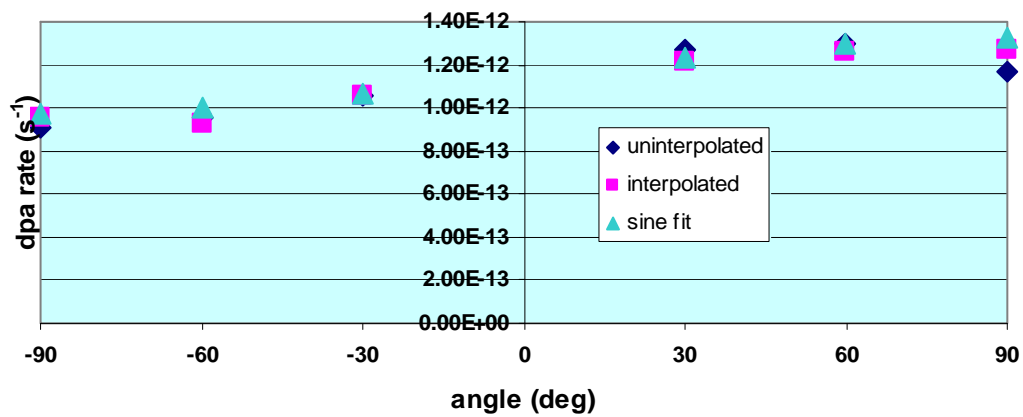
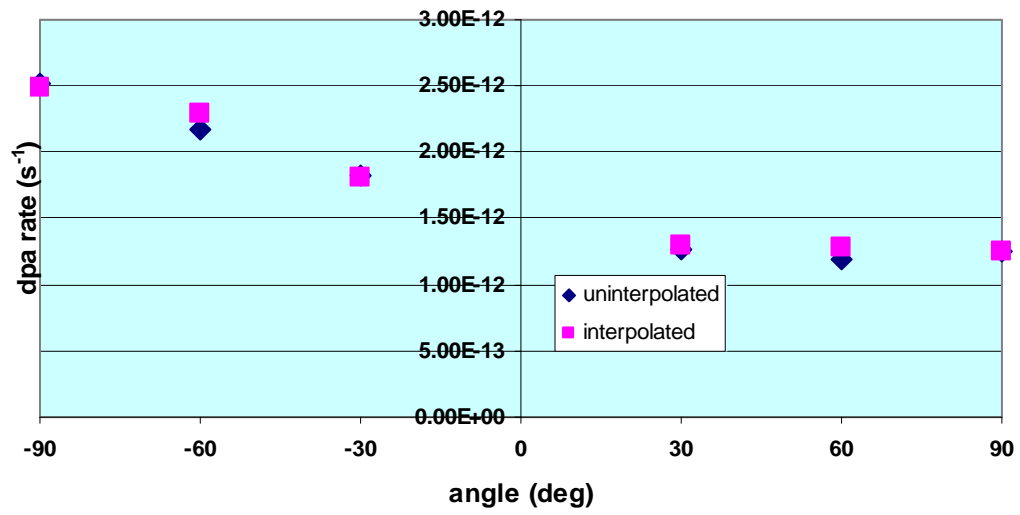


Fig. C.7. Key 4 (HB-4 original design) neutron (top) and gamma (bottom) dpa rates for Key positions plotted vs angle showing uninterpolated, interpolated, and sine-curve-fit (where used) data.

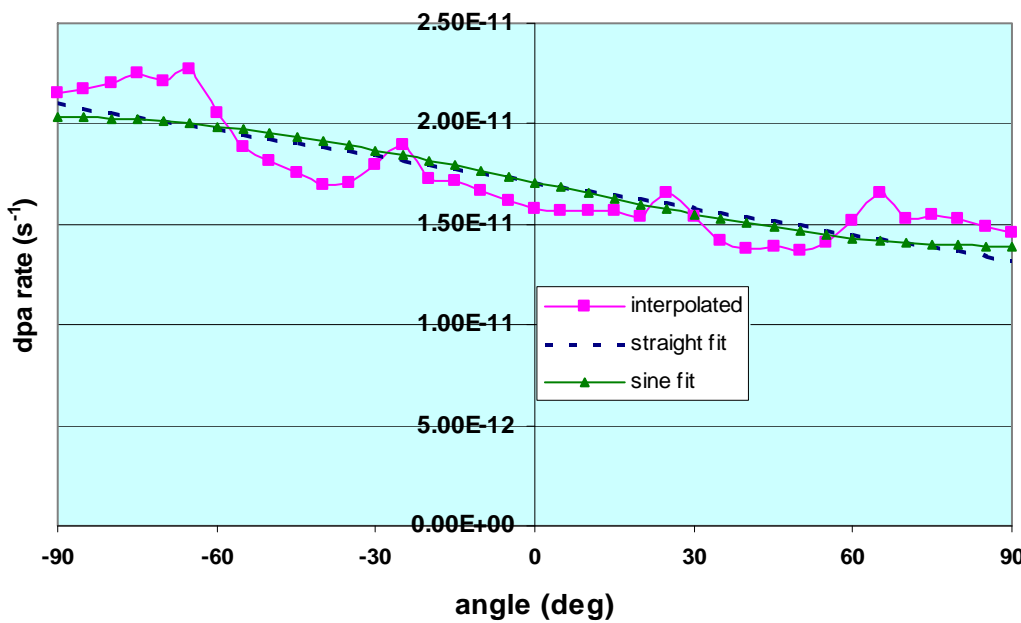
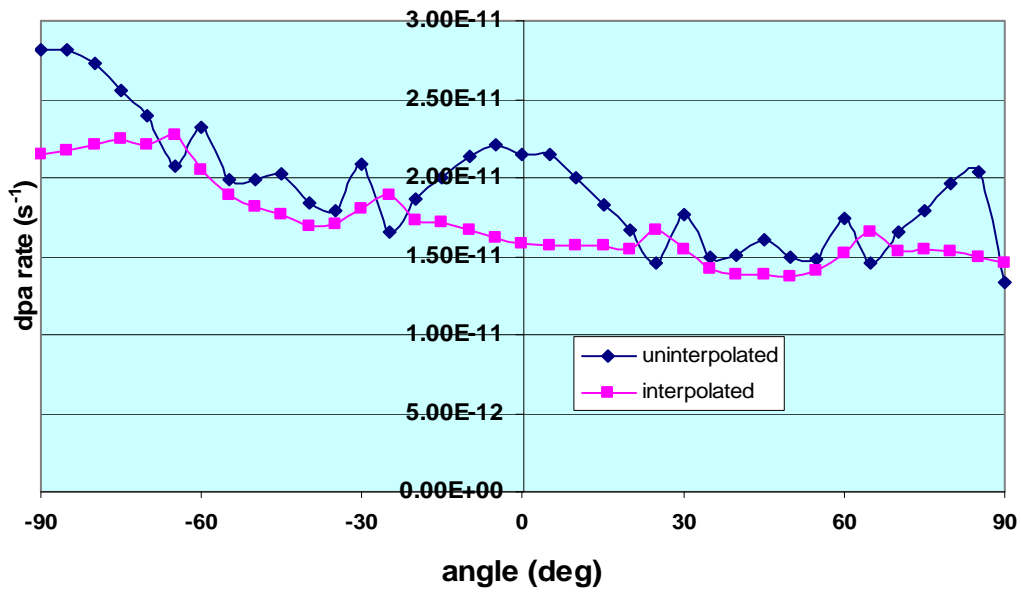


Fig. C.8. Key 4 (HB-4 modified design) neutron dpa rate vs angle showing uninterpolated and interpolated data (top) and interpolated data with straight-line and sine-curve fits (bottom). Values are for $t > 22.7$ EFPY.

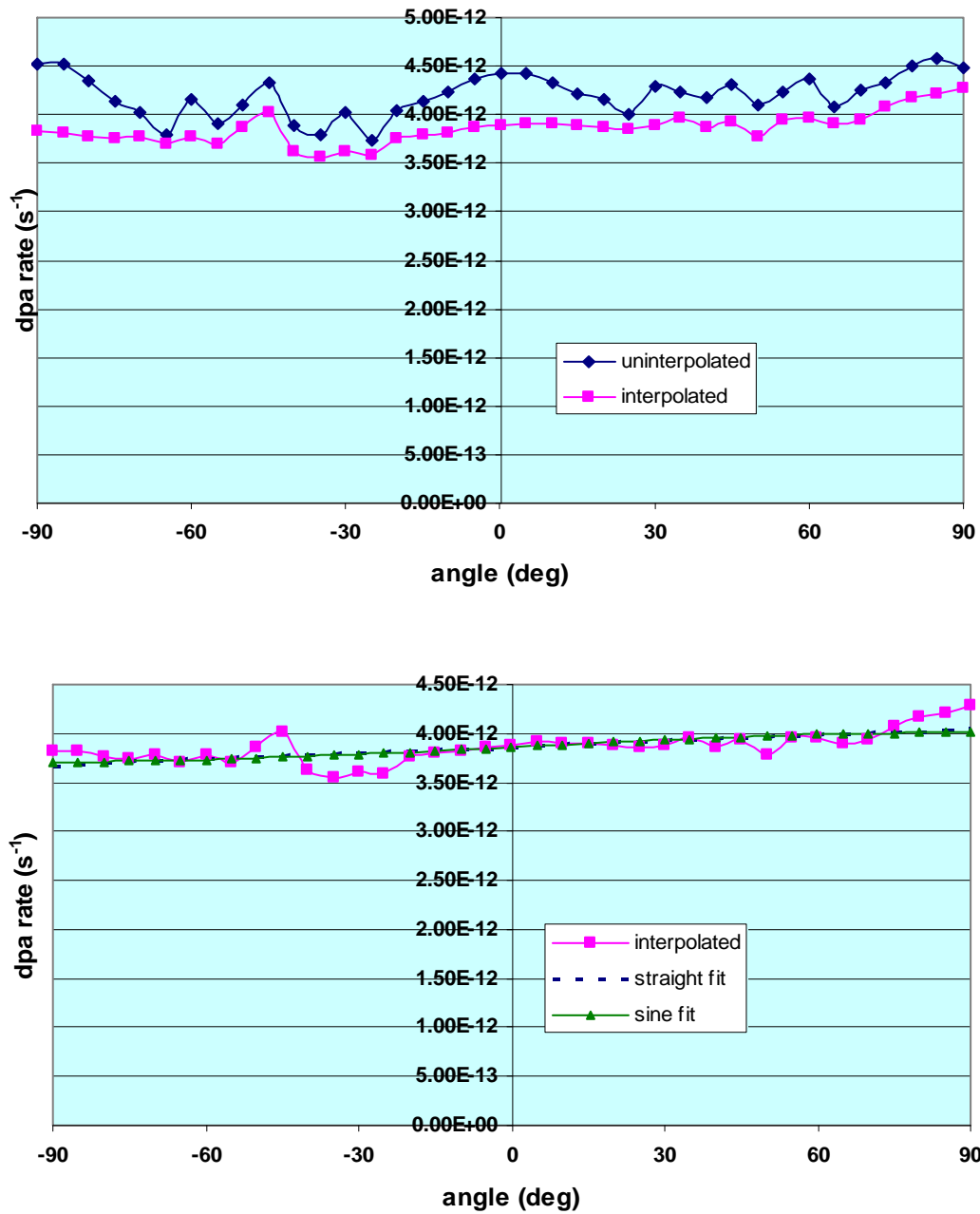


Fig. C.9. Key 4 (HB-4 modified design) gamma dpa rate vs angle showing uninterpolated and interpolated data (top) and interpolated data with straight-line and sine-curve fits (bottom). Values are for $t > 22.7$ EFPY.

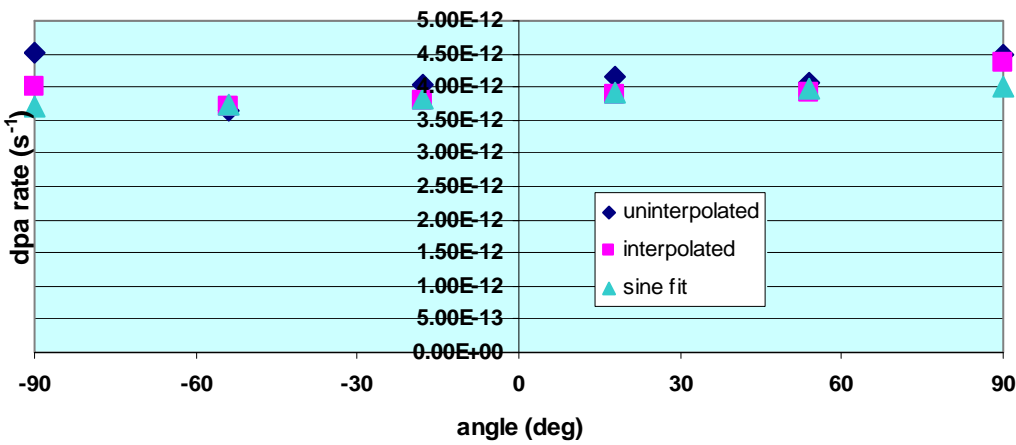
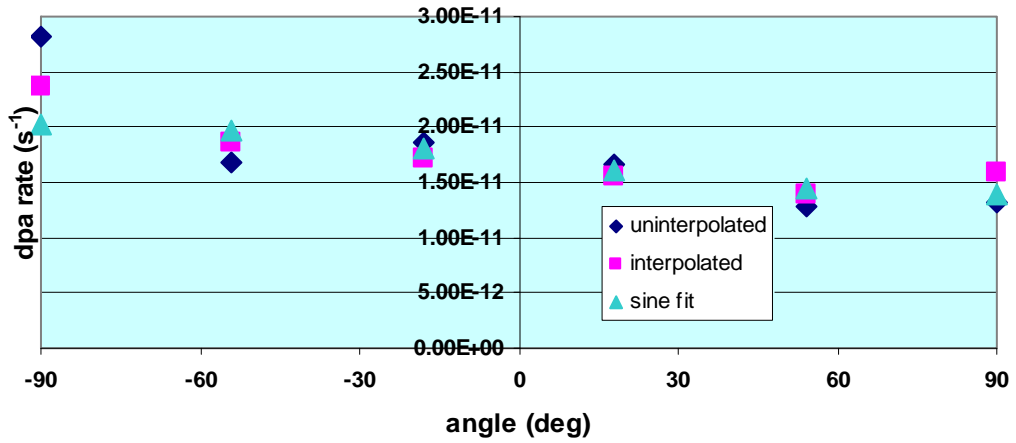


Fig. C.10. Key 4 (HB-4 modified design) neutron (top) and gamma (bottom) dpa rates for Key positions plotted vs angle showing uninterpolated, interpolated, and sine-curve-fit (where used) data. Values are for $t > 22.7$ EFY.

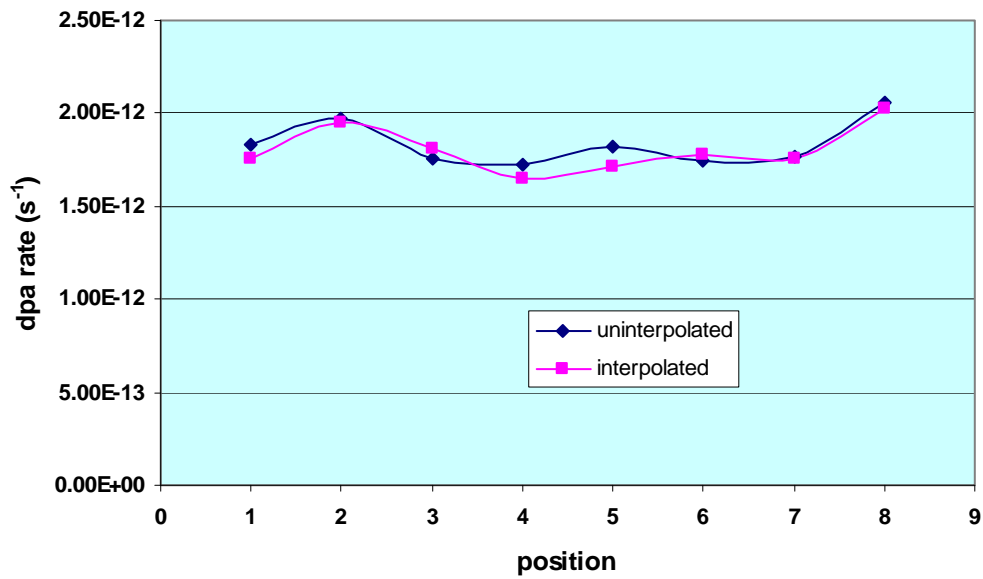
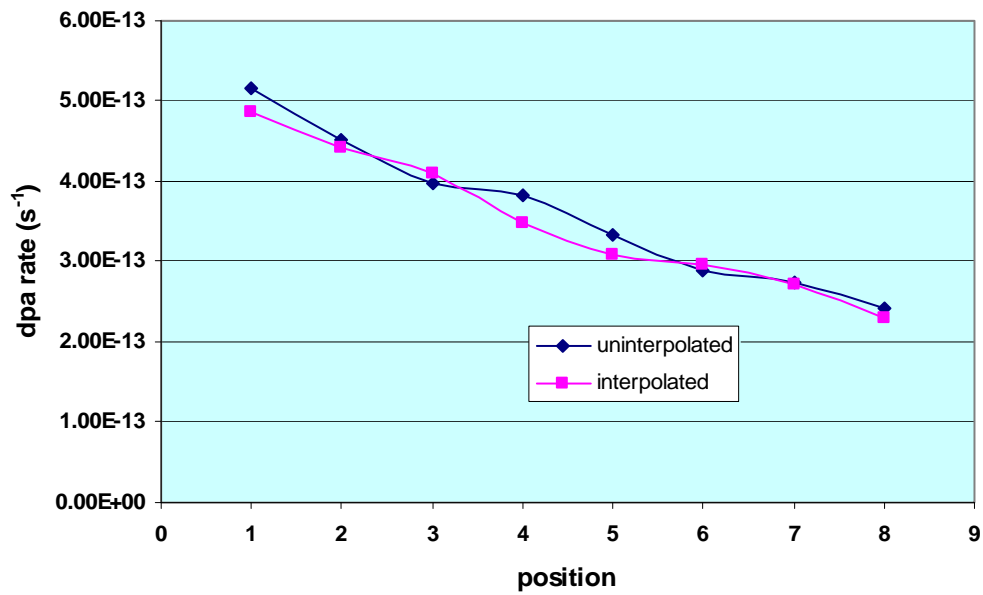


Fig. C.11. Key 6 (HB-1 [4] original extended design) neutron (top) and gamma (bottom) dpa rates for Key positions showing uninterpolated and interpolated data.

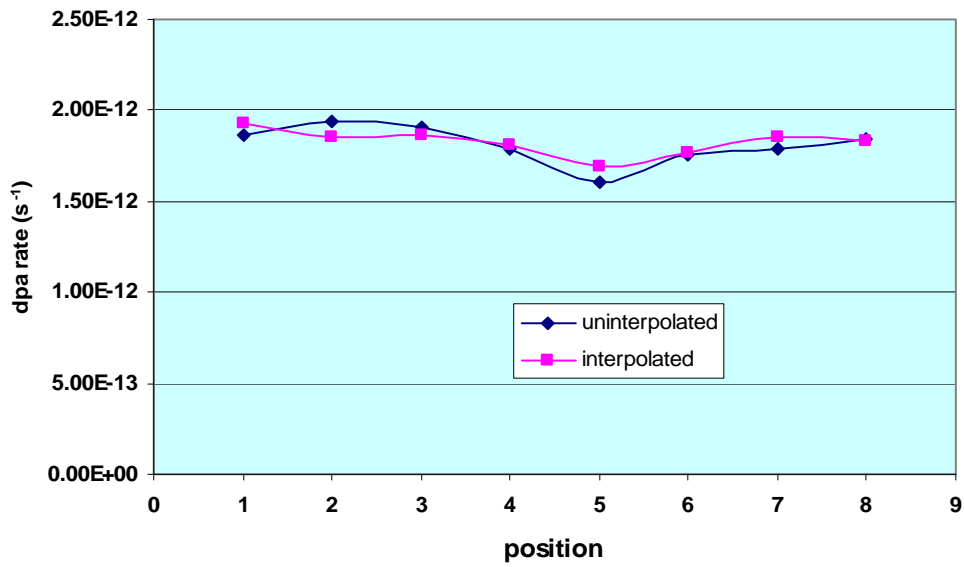
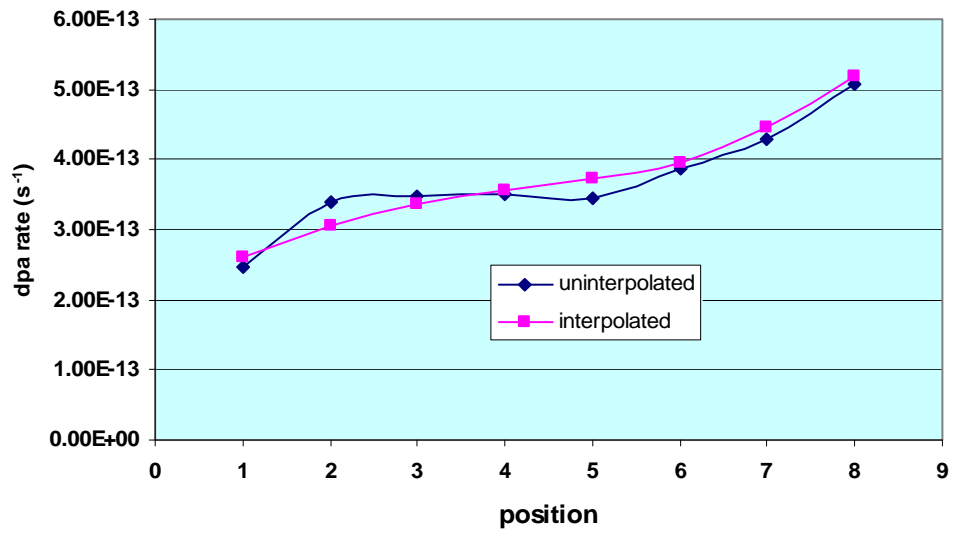


Fig. C.12. Key 7 (HB-4 original extended design) neutron (top) and gamma (bottom) dpa rates for Key positions showing uninterpolated and interpolated data.

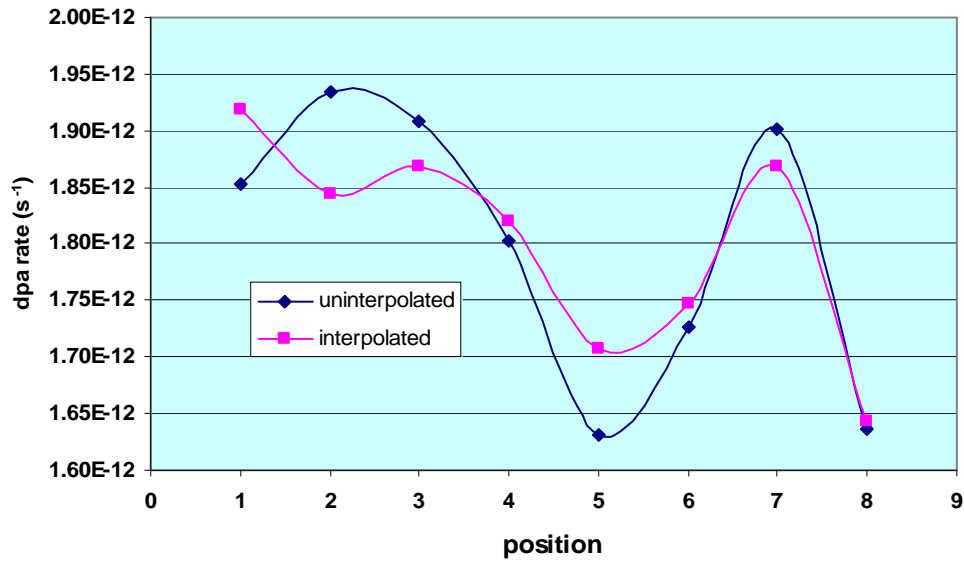
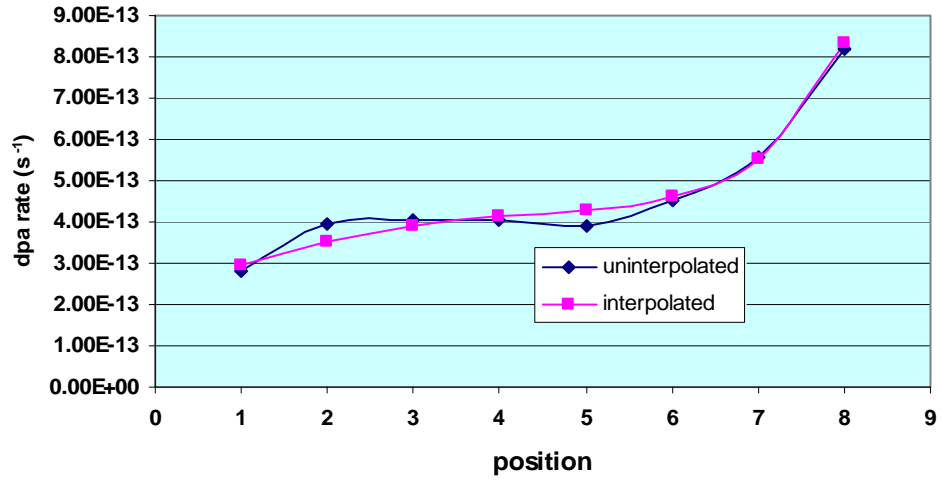


Fig. C.13. Key 7 (HB-4 modified extended design) neutron (top) and gamma (bottom) dpa rates for Key positions showing uninterpolated and interpolated data.

Table C.1. Calculated neutron and gamma dpa rates for Key 3 (HB-3) surveillance capsule positions

Pos.	Angle (deg.)	Location (X,Y,Z) (in.)	Model mesh no.	dpa rate (10^{-12} s^{-1})				
				Neutron		Gamma		
				Uninterp.	Interp.	Uninterp.	Interp.	Interp. and fit (sine)
1,5	30, 150	45.51,-2.45,4.35	51,15,9	2.54	2.61	1.14	1.24	1.24
2,4	60, 120	45.93,-4.24,2.51	51,12,6	2.54	2.56	1.26	1.20	1.25
3	90	46.08,-4.89, 0	52,11,1	2.77	2.60	1.16	1.26	1.26
6,10	210, 330	44.39,2.45,4.35	48,26,9	3.60	3.55	1.17	1.15	1.19
7,9	240, 300	43.97,4.24,2.51	47,29,6	4.06	4.13	1.21	1.13	1.17
8	270	43.82,4.89, 0	47,30,1	4.79	4.40	1.18	1.13	1.16

Table C.2. Calculated neutron and gamma dpa rates for Key 4 surveillance capsule positions (original HB-4 and Key 4 designs, $t < 22.7$ EFPY)

Pos.	Angle (deg.)	Location (X,Y,Z) (in.)	Model mesh no.	dpa rate (10^{-12} s^{-1})				
				Neutron		Gamma		
				Uninterp.	Interp.	Uninterp.	Interp.	Interp. and fit (sine)
1,5	30, 150	42.8, -2.41,4.35	57,17,9	1.27	1.30	1.27	1.21	1.24
2,4	60, 120	43.31,-4.17,2.51	58,14, 6	1.19	1.27	1.30	1.26	1.30
3	90	43.4, -4.81,0	58,13 1	1.25	1.25	1.16	1.27	1.32
6,10	210, 330	41.37,2.41,4.35	54,28,9	1.83	1.81	1.06	1.06	1.06
7,9	240, 300	40.85,4.17,2.65	53,31 6	2.17	2.30	0.953	0.924	1.00
8	270	40.65,4.81,0	53,32,1	2.52	2.49	0.906	0.959	0.978

Table C.3. Calculated neutron and gamma dpa rates for Key 4 surveillance capsule positions (modified HB-4 and Key 4 designs, $t > 22.7$ EFPY)

Pos	Angle (deg.)	Location (X,Y,Z) (in.)	Model mesh no.	dpa rate (10^{-12} s^{-1})					
				Neutron			Gamma		
				Uninterp.	Interp.	Interp. and fit (sine)	Uninterp.	Interp.	Interp. and fit (sine)
1,5	18, 162	36.44,-1.4,4.28	50,26,17	16.7	15.6	16.1	4.16	3.87	3.91
2,4	54, 126	36.44,-3.6,2.65	50,16,12	12.8	13.9	14.5	4.07	3.93	3.98
3	90	36.44,-4.5,0	50,14,1	13.3	16.0	13.9	4.48	4.37	4.01
6,10	198, 342	36.44,1.39, 4.28	50,33,17	18.6	17.2	18.1	4.05	3.79	3.81
7,9	234, 306	36.44,3.64,2.65	50,43,12	16.8	18.6	19.7	3.64	3.71	3.74
8	270	36.44,4.5, 0	50,44,1	28.1	23.8	20.3	4.52	3.99	3.71

Table C.4. Calculated neutron and gamma dpa rates for Key 6 (HB-1 [4], original extended design) surveillance capsule positions

Position	Location (X,Y,Z) (in.)	Model mesh no.	dpa rate (10^{-12} s^{-1})			
			Neutron		Gamma	
			Uninterp.	Interp.	Uninterp.	Interp.
1	38.3, 10.5, 0	48,43,1	0.517	0.485	1.83	1.76
2	36.8, 12.3, 0	45,47,1	0.453	0.441	1.98	1.95
3	35.4, 14.1, 0	42,51,1	0.397	0.409	1.75	1.81
4	33.9, 16.0, 0	39,54,1	0.382	0.349	1.72	1.64
5	31.0, 18.9, 0	36,60,1	0.334	0.308	1.82	1.72
6	29.2, 20.4, 0	35,63,1	0.290	0.296	1.75	1.78
7	27.4, 21.9, 0	33,66,1	0.275	0.271	1.76	1.76
8	25.6, 23.4, 0	31,69,1	0.242	0.229	2.05	2.03

Table C.5. Calculated neutron and gamma dpa rates for Key 7 (HB-4, original extended design) surveillance capsule positions

Position	Location (X,Y,Z) (in.)	Model mesh no.	dpa rate (10^{-12} s^{-1})			
			Neutron		Gamma	
			Uninterp.	Interp.	Uninterp.	Interp.
1	26.2, 22.7, 0	32,68,1	0.247	0.261	1.86	1.93
2	27.9, 21.0, 0	33,64,1	0.340	0.306	1.94	1.85
3	29.6, 19.4, 0	35,61,1	0.349	0.336	1.91	1.87
4	31.3, 17.8, 0	37,58,1	0.349	0.357	1.79	1.81
5	33.1, 16.2, 0	39,55,1	0.345	0.372	1.61	1.70
6	34.8, 14.6, 0	41,52,1	0.388	0.394	1.75	1.76
7	37.5, 11.6, 0	46,46,1	0.429	0.445	1.79	1.85
8	38.8, 9.7, 0	49,42,1	0.506	0.520	1.84	1.83

Table C.6. Calculated neutron and gamma dpa rates for Key 7 (HB-4, modified extended design) surveillance capsule positions

Position	Location (X,Y,Z) (in.)	Model mesh no.	dpa rate (10^{-12} s^{-1})			
			Neutron		Gamma	
			Uninterp.	Interp.	Uninterp.	Interp.
1	26.2, 22.7, 0	37,82,1	0.280	0.293	1.85	1.92
2	27.9, 21.0, 0	38,78,1	0.396	0.354	1.94	1.84
3	29.6, 19.4, 0	40,75,1	0.407	0.389	1.91	1.87
4	31.3, 17.8, 0	42,72,1	0.405	0.414	1.80	1.82
5	33.1, 16.2, 0	44,69,1	0.392	0.429	1.63	1.71
6	34.8, 14.6, 0	46,66,1	0.451	0.460	1.73	1.75
7	37.5, 11.6, 0	52,60,1	0.560	0.554	1.90	1.87
8	38.8, 9.7, 0	55,56,1	0.821	0.832	1.64	1.64

Table C.7. Summary of calculated (unnormalized) neutron and gamma dpa rates for HFIR surveillance capsule Keys for times before and after 22.7 EFPY (3rd upgrade)

Key 1 ($t > 0$) (HB-1)^a						
Position^b	Angle (deg.)^c	Location (X,Y,Z) (in.)^d	Model mesh no.^e	dpa rate (10^{-12} s^{-1})		
				Neutron	Gamma	Total
1,5	30, 150	41.37, 2.41, \pm 4.35	54, 28, 9	1.81	1.06	2.88
2,4	60, 120	40.85, 4.17, \pm 2.51	53, 31, 6	2.30	1.00	3.30
3	90	40.65, 4.81, 0	53, 32, 1	2.49	0.978	3.46
6,10	210, 330	42.80, -2.41, \mp 4.35	57, 17, 9	1.30	1.24	2.54
7,9	240, 300	43.31, -4.17, \mp 2.51	58, 14, 6	1.27	1.30	2.57
8	270	43.51, -4.81, 0	58, 13, 1	1.25	1.32	2.57
Key 2 ($0 < t < 22.7$ EFPY) (HB-2, original design)						
Position^f	Angle (deg.)	Location (X,R) (in.)	Model mesh no.	dpa rate (10^{-12} s^{-1})		
				Neutron	Gamma	Total
N/A	N/A	45.79, 7.02	64, 37	3.82	1.52	5.35
Key/Dosimeter 2C, 2W, 2D1C&2D2C, 2D1W ($t > 22.7$ EFPY) (HB-2, modified design)						
Key, dosimeter^g	Angle (deg.)	Location (X,R) (in.)	Model mesh no.	dpa rate (10^{-12} s^{-1})		
				Neutron	Gamma	Total
K2C	N/A	38.94, 6.5	(49,26),(49,27)	155.0	10.2	165.2
K2W	N/A	39.69, 12.0	(50,47),(51,47)	4.36	2.59	6.95
2D1C & 2D2C	N/A	(46.44 & 45.92), 7.0	(64,28),(64,29)	75.8	3.60	79.4
2D1W,2D2W,2D3W	N/A	46.44, 13.56	(62,51),(62,52) (61,51),(61,52)	2.10	1.31	3.41
Key 3 ($t > 0$ EFPY) (HB-3)						
Position	Angle (deg.)	Location (X,Y,Z) (in.)	Model mesh no.	dpa rate (10^{-12} s^{-1})		
				Neutron	Gamma	Total
1,5	30, 150	45.51, -2.45, \pm 4.35	51, 15, 9	2.61	1.24	3.84
2,4	60, 120	45.93, -4.24, \pm 2.51	51, 12, 6	2.56	1.25	3.81
3	90	46.08, -4.89, 0	52, 11, 1	2.60	1.26	3.86
6,10	210, 330	44.39, 2.45, \mp 4.35	48, 26, 9	3.55	1.19	4.73
7,9	240, 300	43.97, 4.24, \mp 2.51	47, 29, 6	4.13	1.17	5.29
8	270	43.82, 4.89, 0	47, 30, 1	4.40	1.16	5.56
Key 4 ($0 < t < 22.7$ EFPY) (HB-4, original design)						
Position	Angle (deg.)	Location (X,Y,Z) (in.)	Model mesh no.	dpa rate (10^{-12} s^{-1})		
				Neutron	Gamma	Total
1,5	30, 150	42.80, -2.41, \pm 4.35	57, 17, 9	1.30	1.24	2.54
2,4	60, 120	43.31, -4.17, \pm 2.51	58, 14, 6	1.27	1.30	2.57
3	90	43.51, -4.81, 0	58, 13, 1	1.25	1.32	2.57
6,10	210, 330	41.37, 2.41, \mp 4.35	54, 28, 9	1.81	1.06	2.88
7,9	240, 300	40.85, 4.17, \mp 2.51	53, 31, 6	2.30	1.00	3.30
8	270	40.65, 4.81, 0	53, 32, 1	2.49	0.978	3.46
Key 4 ($t > 22.7$ EFPY) (HB-4, modified design)						
Position	Angle (deg.)	Location (X,Y,Z) (in.)	Model mesh no.	dpa rate (10^{-12} s^{-1})		
				Neutron	Gamma	Total
1,5	18, 162	36.44, -1.39, \pm 4.28	50, 26, 17	16.1	3.91	20.0
2,4	54, 126	36.44, -3.64, \pm 2.65	50, 16, 12	14.5	3.98	18.5
3	90	36.44, -4.50, 0	50, 14, 1	13.9	4.01	17.9
6,10	198, 342	36.44, 1.39, \mp 4.28	50, 33, 17	18.1	3.81	21.9
7,9	234, 306	36.44, 3.64, \mp 2.65	50, 43, 12	19.7	3.74	23.4
8	270	36.44, 4.50, 0	50, 44, 1	20.3	3.71	24.0

Table C.7 (continued)

Key 5 ($t < 22.7$ EFY) (Monte Carlo model) ^h						
Position	Angle (deg.)	Location (X,Y,Z) (in.)	Model mesh no.	dpa rate (10^{-12} s ⁻¹)		
				Neutron	Gamma	Total
1	N/A	46.2, -8.1, -9.0	N/A	0.082	0.615	0.697
2	N/A	46.5, -10.5, -9.0	N/A	0.080	0.340	0.420
3	N/A	46.6, -12.8, -9.0	N/A	0.083	0.230	0.313
4	N/A	46.7, -15.1, -9.0	N/A	0.085	0.157	0.242
5	N/A	46.6, -17.4, -9.0	N/A	0.083	0.202	0.285
6	N/A	46.5, -19.7, -9.0	N/A	0.084	0.359	0.443
7	N/A	46.2, -20.1, -9.0	N/A	0.090	0.685	0.775
Key 6 ($t > 0$ EFY) (HB-1 [4], original design, extended model) ⁱ						
Position	Angle (deg.)	Location (X,Y,Z) (in.)	Model mesh no.	dpa rate (10^{-12} s ⁻¹)		
				Neutron	Gamma	Total
1	N/A	38.3, 10.5, 0	48, 43, 1	0.485	1.76	2.24
2	N/A	36.8, 12.3, 0	45, 47, 1	0.441	1.95	2.39
3	N/A	35.4, 14.1, 0	42, 51, 1	0.409	1.81	2.22
4	N/A	33.9, 16.0, 0	39, 54, 1	0.349	1.64	1.99
5	N/A	31.0, 18.9, 0	36, 60, 1	0.308	1.72	2.02
6	N/A	29.2, 20.4, 0	35, 63, 1	0.296	1.78	2.07
7	N/A	27.4, 21.9, 0	33, 66, 1	0.271	1.76	2.03
8	N/A	25.6, 23.4, 0	31, 69, 1	0.229	2.03	2.26
Key 7 ($0 < t < 22.7$ EFY) (HB-4, original design, extended model) ⁱ						
Position	Angle (deg.)	Location (X,Y,Z) (in.)	Model mesh no.	dpa rate (10^{-12} s ⁻¹)		
				Neutron	Gamma	Total
1	N/A	26.2, 22.7, 0	32, 68, 1	0.261	1.93	2.19
2	N/A	27.9, 21.0, 0	33, 64, 1	0.306	1.85	2.16
3	N/A	29.6, 19.4, 0	35, 61, 1	0.336	1.87	2.20
4	N/A	31.3, 17.8, 0	37, 58, 1	0.357	1.81	2.16
5	N/A	33.1, 16.2, 0	39, 55, 1	0.372	1.70	2.07
6	N/A	34.8, 14.6, 0	41, 52, 1	0.394	1.76	2.16
7	N/A	37.5, 11.6, 0	46, 46, 1	0.445	1.85	2.29
8	N/A	38.8, 9.7, 0	49, 42, 1	0.520	1.83	2.35
Key 7 ($t > 22.7$ EFY) (HB-4, modified design, extended model) ⁱ						
Position	Angle (deg.)	Location (X,Y,Z) (in.)	Model mesh no.	dpa rate (10^{-12} s ⁻¹)		
				Neutron	Gamma	Total
1	N/A	26.2, 22.7, 0	37, 82, 1	0.293	1.92	2.21
2	N/A	27.9, 21.0, 0	38, 78, 1	0.354	1.84	2.20
3	N/A	29.6, 19.4, 0	40, 75, 1	0.389	1.87	2.26
4	N/A	31.3, 17.8, 0	42, 72, 1	0.414	1.82	2.23
5	N/A	33.1, 16.2, 0	44, 69, 1	0.429	1.71	2.14
6	N/A	34.8, 14.6, 0	46, 66, 1	0.460	1.75	2.21
7	N/A	37.5, 11.6, 0	52, 60, 1	0.554	1.87	2.42
8	N/A	38.8, 9.7, 0	55, 56, 1	0.832	1.64	2.48

^a The model for HB-1 is the same as the original (unenlarged) model for HB-4.

^b Models are assumed to be symmetric above and below the horizontal midplane such that points that differ in only the sign of the Z coordinate are the same.

^c Angles are measured clockwise from the 12 o'clock position from the perspective of sighting along the beam tube toward the outside of the vessel (+X direction). This convention is observed for all beam tubes.

^d The models are symmetric above and below the Z = 0 plane. Negative Z coordinate values therefore refer to surveillance capsule position angles between 90 and 270 degrees. When sighting along the beam tube toward the outside of the vessel (+X direction), the +Y direction is to the left for beam tubes HB-2, -3, and -4. For HB-1, the +Y direction is to the right.

^e Mesh interval numbers are for the appropriate three- or two-dimensional beam-tube model. These define the model mesh cell in which the Key location falls. However, dpa rates are determined by interpolation with values from surrounding mesh cells. For HB-2, values are averages for cells specified.

^f Because HB-2 models are two-dimensional (axial [X] and radial [R]), there is no differentiation between azimuthal Key positions. (Position and angle designations are designated as N/A [not applicable]).

^g Key 2C/2W has two capsules approximately in line with the nozzle corner (C) and nozzle weld (W). Dosimeters 2D1C, 2D2C, and 2D1W are attached to Key 2C/2W.

^h Location is with respect to HB-4.

ⁱ The model has been extended in the +Y direction to accommodate the Key 6 or 7 position.

C.3 CALCULATED dpa RATES (UPGRADE 3) FOR THE 31 REGIONS USED IN THE VESSEL STRUCTURAL INTEGRITY ANALYSIS

Similar updated calculations have been performed for the 31 regions considered in the vessel integrity study and described in [2]. Numerical model mesh cell locations for the regions are shown in Table C.8. Figure C.14 is a schematic view of the relative locations of the corner, annulus, and weld for a typical beam tube located at radii r_i , r_a , and r_w , respectively, and shows the inside contour of a beam tube nozzle with a discrete ordinates mesh superimposed.

Values shown in Table C.8 for the HB-2 model for time prior to 22.7 EFPY (original design) are for a somewhat updated version of the model that was used in previous analyses. In the updated model the mesh spacing has been retained, but the vessel wall has been repositioned (moved closer to the origin by ~1–2 cm) so that the wall/water interfaces at the corner, annulus, and weld locations in the model better correspond to the actual beam-tube values.

Results are shown, with comparison to previous results (see Table 17 in main report), in Table C.9. Updated dpa rate values are given for uninterpolated and interpolated results. For the uninterpolated values, the following approach was used. The dpa rate is the value that corresponds to the model mesh cell in which the corner, annulus, or weld location falls. This is assumed to be the mesh cell in the nozzle wall adjacent to the water along the X direction (aligned with the beam-tube axis) and enclosing the radial dimension specified for the corner, annulus, or weld. The interpolated values are the dpa rates interpolated to the wall/water interface (in the X direction) and the actual radial location for the corner, annulus, or weld. Note that the wall/water interface in the X direction may not exactly correspond to the actual location because some errors are introduced by using a rectangular-mesh model (also, the model mesh locations may differ somewhat from those in Table 17 in the main report). This approach is shown schematically in Fig. C.14, and it is also shown how the mesh can be offset slightly from the actual nozzle surface location. For the interpolated values, interpolation is performed to the points shown by the linear approximation described in Appendix B. In general, the interpolated dpa rate value is greater than the uninterpolated value because the location has effectively been moved from the center of a mesh interval (used in previous analyses) to a point closer to the core and/or the beam-tube radial center. This increase in value is especially true for the corner in which the interpolated location is always closer to the core and to the beam-tube radial center than that which was assumed in earlier analyses. This is evident in Fig. C.11 and Table C.9. Neutron dpa rates for HB-4 (modified design, >22.7 EFPY) are elevated in the updated results for an additional reason—the addition of the cross-section scattering terms that had been omitted. In addition to the increase at the corner due to the interpolation approach, the dpa rates moderately increased due to this latter effect, as can also be seen in Table C.9.

Table C.8. Locations of corner, annulus, and weld regions in beam-tube coordinates and numerical models

Time period EFPY ^a	Region	Beam-tube or vessel location	Name	Location [cm (in.)] ^b		Model location X ^c (cm)	Model mesh no.
				Radius	X		
<22.7	1,2,3	HB-2	Corner	17.78 (7)	117.9 (46.4)	118.1	67, 37
	4,5	HB-2	Annulus	23.62 (9.3)	116.9 (46.0)	116.8	65, 46
	6,7	HB-2	Weld	38.1 (15)	113.6 (44.5)	113.0	62, 66
>22.7	1,2,3	HB-2	Corner	17.78 (7)	117.9 (46.4)	117.9	65, 29
	4,5	HB-2	Annulus	23.62 (9.3)	116.9 (46.0)	116.6	64, 37
	6,7	HB-2	Weld	38.1 (15)	113.0 (44.5)	114.1	62, 54
>0	8,9,10	HB-3	Corner	10.16 (4)	113.4 (44.6)	113.0	49,29,1
	11,12	HB-3	Annulus	13.46 (5.3)	112.3 (44.2)	111.8	48,31,1
	13,14	HB-3	Weld	25.4 (10)	107.3 (42.2)	108.0	45,40,1
HB-4 < 22.7 HB-1 > 0	15,16,17	HB-1/4 ^d	Corner	10.16 (4)	105.4 (41.5)	105.4	55, 31, 1
	18,19	HB-1/4 ^d	Annulus	13.46 (5.3)	104.1 (41.0)	104.1	54, 33, 1
	20,21	HB-1/4 ^d	Weld	25.4 (10)	100.3 (39.5)	100.3	52, 42, 1
>22.7	15,16,17	HB-4	Corner	10.16 (4)	105.4 (41.5)	105.4	62, 44, 1
	18,19	HB-4	Annulus	13.46 (5.3)	104.1 (41.0)	104.1	61, 47, 1
	20,21	HB-4	Weld	25.4 (10)	100.3 (39.5)	100.3	58, 56, 1
>0	29	Weld ^e	Weld	119.54 (47.06) ^f	43.18 (-17)	43.37	8, 112
	30,31	HMP ^g	Weld	119.54 (47.06)	0	0	35, 112

^aEffective full-power years based on full power = 100 MW.

^bFor HB-1, -3, and -4, the location is assumed to be in the beam-tube horizontal midplane (Z = 0) on the “shady” side. In this case the radius corresponds to the +Y value (at Z = 0) that extends to the nozzle inside surface. X is the distance from the beam-tube origin to the inside of the nozzle surface value at the radius location. For HB-2, which is symmetric, the radius refers to the radial distance to the corner, annulus, or weld.

^cFor all the beam-tube models, X is the distance from the beam-tube model origin along the beam-tube axis to the water/vessel surface interface and may vary slightly from the actual location due to approximations in the discrete-ordinates model required to model a rounded surface. Also, the model mesh numbers differ somewhat from earlier values (Table 17 in the main report).

^dRegions shown are for HB-4. Regions 22–28 (original design) are for HB-1 with the same arrangement.

^eVessel circumferential (girth) weld below core.

^fFor the vessel weld and horizontal midplane, the radius is the inner radius of the vessel wall (beyond the thin stainless steel liner), and X is the vertical location (Z) of the weld with respect to the midline. Mesh numbers are listed with the X mesh first.

^gVessel seam weld at horizontal midplane.

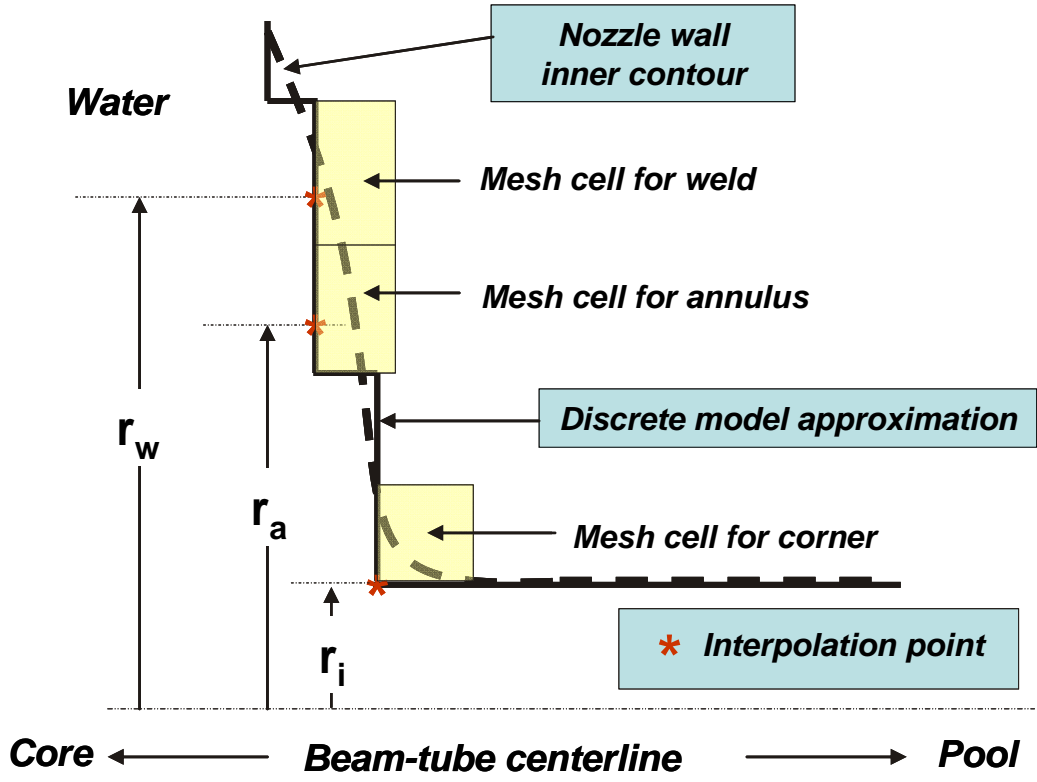


Fig. C.14. Schematic showing locations of corner, annulus, and weld for a beam tube with a discrete-ordinates mesh overlaying the geometry. Locations are assumed to be on the inside surface of the nozzle.

Table C.9. Calculated neutron and gamma dpa rates for the 31 vessel regions considered in the vessel structural integrity study: previous reported values (2nd upgrade) and updated values using the CPILE computer system and interpolation, and including Keys in models (3rd upgrade)

Time period EFY ^a	Region	Beam-tube or vessel location	dpa rates (10 ⁻¹² s ⁻¹)					
			Neutron			Gamma		
			Previous	Updated		Previous	Updated	
				Uninterp.	Interp.		Uninterp.	Interp.
<22.7	1,2,3	HB-2	3.06	3.41	3.62	1.13	1.12	1.20
	4,5	HB-2	1.21	1.42	1.37	1.20	1.32	1.37
	6,7	HB-2	0.270	0.220	0.232	1.11	1.09	1.20
>22.7	1,2,3	HB-2	61.2	62.0	74.6	3.8	3.83	3.73
	4,5	HB-2	17.3	17.6	16.8	1.7	1.74	1.88
	6,7	HB-2	2.53	1.58	1.29	1.0	1.03	1.11
>0	8,9,10	HB-3	6.07	6.19	8.03	1.07	1.08	1.28
	11,12	HB-3	3.46	3.54	3.46	0.92	0.92	1.01
	13,14	HB-3	0.802	0.722	0.662	1.28	1.21	1.35
HB-4, <22.7	15,16,17	HB-1/4 ^b	3.08	3.17	4.33	0.927	0.934	1.14
	18,19	HB-1/4 ^b	1.80	1.86	1.86	0.776	0.782	0.881
HB-1, >0	20,21	HB-1/4 ^b	0.546	0.462	0.469	1.34	1.16	1.27
>22.7	15,16,17	HB-4	9.43	12.31	20.69	2.09	2.12	2.35
	18,19	HB-4	3.90	4.89	4.89	1.52	1.12	1.18
	20,21	HB-4	0.702	0.831	0.749	1.09	1.25	1.33
>0	29	Weld ^c	0.0405	0.0409	0.0423	0.652	0.652	0.729
	30,31	HMP ^d	0.0836	0.0846	0.0877	0.940	0.939	1.047

^aEffective full-power years based on full power = 100 MW.

^bRegions shown are for HB-4. Regions 22–28 are for HB-1 with the same arrangement.

^cVessel circumferential (girth) weld below core.

^dVessel seam weld at horizontal midplane.

C.4 REFERENCES

1. R. D. Cheverton, R. K. Nanstad, C. A. Baldwin, E. D. Blakeman, T. L. Dickson, H. A. Kmiecik, and I. Remec, *Impact of 2004/2005 Dosimetry and Surveillance Data on the HFIR Vessel Radiation Embrittlement Trend Curve, Hydrostatic Proof Test Conditions, Pressure/Temperature Limits, and Life Extension*, ORNL/TM-2008/007, Oak Ridge National Laboratory, Oak Ridge, Tenn., August 2010.
2. R. D. Cheverton, R. K. Nanstad, E. D. Blakeman, H. A. Kmiecik, *HFIR Pressure Vessel and Structural Components Materials Surveillance Program – Supplement 3*, ORNL/TM-1372/53, August 2010.
2. R. D. Cheverton and T. L. Dickson, *HFIR Vessel Life Extension with Enlarged HB-2 and HB-4 Beam Tubes*, ORNL/TM-13698, Oak Ridge National Laboratory, Oak Ridge, Tenn., December 1998.
3. E. D. Blakeman, *Calculation of dpa Rates at HFIR Key 5 and HB-2 Nozzle Corner Using an Existing MCNP Monte Carlo Model Incorporating the CADIS/ADVANTG Variance-Reduction Method*, unpublished Oak Ridge National Laboratory report sent by email to H. Kmiecik, June 17, 2009.

APPENDIX D MONTE CARLO METHOD ANALYSIS

A limited number of calculations have also been performed for determination of displacements-per-atom-per-second (dpa) rates at the HB-2 nozzle corner using a Monte Carlo-methodology High Flux Isotope Reactor (HFIR) model [1, 2] based on the well-established Monte Carlo N-Particle Transport Code (MCNP) [3]. This model was also used to perform shielding calculations for HB-3 [4]. Results for the discrete-ordinates HB-2 analysis have been compared with those from the Monte Carlo model and were found to be in reasonable agreement. As explained below, this outcome is encouraging. The discrete-ordinates method requires the simultaneous solution of a large number of linear equations and is referred to as a “deterministic” approach. The Monte Carlo method, on the other hand, is a “statistical” approach in which particles are simulated and tracked through the geometry. The two methodologies are based on entirely separate and fundamentally different approaches and do not share common data sets. For this reason, when the methods are used together, one as a check for the other, and the results show agreement, the overall confidence in the outcome is increased.

An advantage of the Monte Carlo approach is that the geometric representation can be made reasonably exact because it is not a mesh-based approach. Models are three dimensional, and a single model can incorporate the reactor and all of the beam tubes in complete detail, which has been done [2]. However, because of the statistical nature of the methodology and the need to simulate large numbers of particles* to achieve reasonable convergence, the Monte Carlo method is very computationally intensive, especially for large and detailed models such as currently exists for HFIR. Fortunately, a method has recently been developed that uses an automatically-generated discrete-ordinates adjoint-source model to enable considerable speedup of the calculation for a corresponding Monte Carlo model [5, 6]. The discrete-ordinates model uses the energy-sensitive response (e.g., dpa cross-section multipliers) as a source and calculates the adjoint flux at all mesh locations in the model. The adjoint flux at a specific location and energy (phase space) is a measure of the relative importance of particles at that phase space with regard to ultimately contributing to the response of interest. Subsequent Monte Carlo calculations can then use these adjoint fluxes to bias particle transport such that particles are literally guided to the region of interest.

The above method, referred to as the Consistent Adjoint Driven Importance Sampling (CADIS) methodology, has been successfully implemented at Oak Ridge National Laboratory on a very large pressurized-water reactor model [7]. Furthermore, some preliminary calculations[†] have indicated that it should also be successful on the current HFIR model. The bottom line with this approach is that Monte Carlo calculations can be run much more efficiently using CADIS than using standard methods of variance reduction. Thus, with the option of using the CADIS methodology, the fact that computer speed is continually increasing (thus, decreasing the penalty for a greater computational demand of the Monte Carlo method), and the existence of a highly detailed HFIR model, the implementation of the Monte Carlo approach using the CADIS methodology as an alternative or as a supplement to the current discrete ordinates approach should be considered as a viable option for future efforts.

* Monte Carlo calculations specialized to specific locations such as the HB-2 nozzle region can be performed more efficiently using biasing methods (referred to as “variance reduction”) that enhance particle transport to those locations while reducing transport to locations that are of little or no concern. (The contributions from these particles are adjusted such that the final result is valid. This is called the “fair game.”) Still, the computational demand required to perform well-converged calculations for HFIR can be quite large.

[†] These calculations show promise but have not yet been fully evaluated.

D.1 REFERENCES

1. E. D. Blakeman, J. A. Bucholz, and R. D. Cheverton, *Calculation of dpa Rates at the HFIR HB-2 Beam Tube Nozzle Corner Using Three-Dimensional Discrete Ordinates and Monte Carlo Models*, ORNL/TM-2003/213, Oak Ridge National Laboratory, Oak Ridge, Tenn., June 2004.
2. D. E. Peplow, *A Computational Model of the High Flux Isotope Reactor for the Calculation of Cold Source, Beam Tube, and Guide Hall Nuclear Parameters*, ORNL/TM-2004/237, Oak Ridge National Laboratory, Oak Ridge, Tenn., November 2004.
3. X-5 Monte Carlo Team, *MCNP – A General Monte Carlo N-Particle Transport Code*, Version 5, Volume I: Overview and Theory, LA-UR-03-1987, Los Alamos National Laboratory, Los Alamos, N.M. (2003).
4. J. A. Bucholz, *Source Terms for HFIR Beam Tube Shielding Analyses, and a Complete Shielding Analysis of the HB-3 Tube*, ORNL/TM-13720, Oak Ridge National Laboratory, Oak Ridge, Tenn., 2000.
5. J. C. Wagner, “Acceleration of Monte Carlo Shielding Calculations with an Automated Variance Reduction Technique and Parallel Processing,” Ph.D. dissertation, Pennsylvania State University, University Park, Pa., 2002.
6. J. C. Wagner, “An Automated Deterministic Variance Reduction Generator for Monte Carlo Shielding Applications,” American Nuclear Society/Radiation Protection & Shielding Division 12th Biennial Topical Meeting, Santa Fe, N.M., April 14–18, 2002.
7. E. D. Blakeman, D. E. Peplow, J. C. Wagner, B. D. Murphy, and D. E. Mueller, *PWR Facility Dose Modeling Using MCNP5 and the CADIS/ADVANTG Variance-Reduction Methodology*, ORNL/TM-2007/133, Oak Ridge National Laboratory, Oak Ridge, Tenn., September 2007.

**APPENDIX E
COMPUTER MODEL DESCRIPTIONS AND ARCHIVE**

The directory structure for the software calculation models is shown in Fig. E.1. Models for the reactor (rx) and each beam tube (HB-2, -3, and -4 [the “original” HB-4 is the same as HB-1]) are contained in separate directories. For HB-2 and -4, models for the original and modified (enlarged) designs are also contained in separate subdirectories for the appropriate beam tube. The cross-section library files, which include the AXMIX mixing files, are in the directory “lib.” Documentation that provides guidelines for running the software is in the “doc” directory. The “tmp” directory is typically empty but is required as a temporary storage area when the software is run and is therefore included in the structure. Finally, the “misc” directory contains additional files required by certain utility codes and necessary for formatting data. Table E.1 provides a listing and brief description of the archived files. Table E.2 provides a cross index to earlier equivalent files. Table E.3 provides an updated file-naming convention.

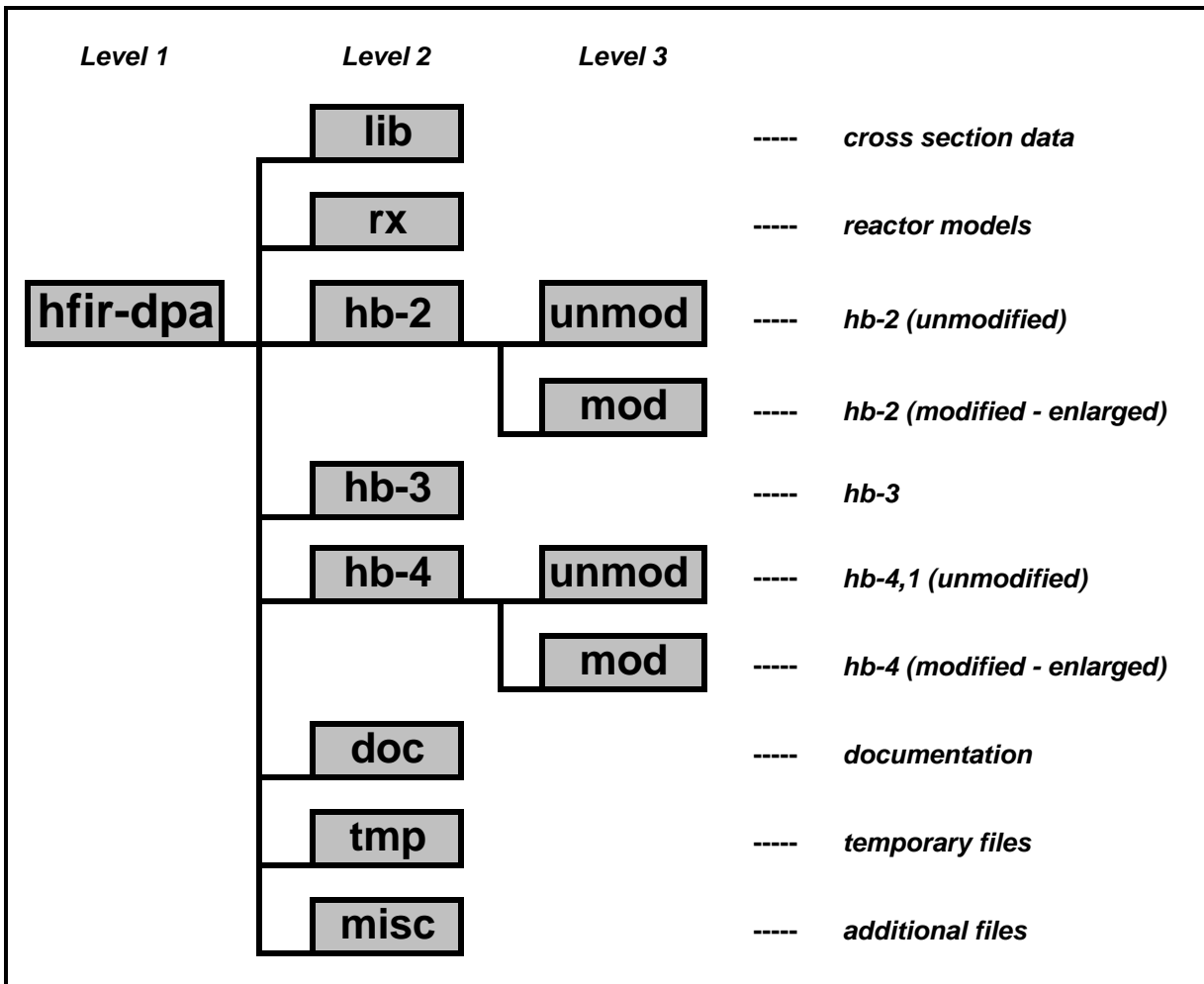


Fig. E.1. Directory structure for High Flux Isotope Reactor displacements-per-atom-per-second (dpa) model files. The original HB-4 design is equivalent to the HB-1 design.

Table E.1. Summary of files for beam-tube dpa rate analysis

Directories and files (executable/input/output)	Description
<i>Directory: lib</i>	
axmerge.i <i>Input:</i> velm61.bin, velm61fe.bin <i>Output:</i> velm61_merged.bin axmix_hfr.sh <i>Output:</i> hfrvelm.9_07.lib	Merges two binary velm61 files Binary velm61 cross sections Merged binary cross sections Produces mixture cross-section file Mixture cross sections
<i>Directory: rx</i>	
dort_rx_k1.sh <i>Output:</i> dort_rx_k1.p3flx dort_rx_k2.sh <i>Output:</i> dort_rx_k.fdpch dort_rx_k.fdpch.mod dort_rx_fs.sh & dort_rx_fs.dg.sh <i>Outputs:</i> p3flx.fs.100M, p3flx.fs.100M.dg, dirflx.fs.100M, & dirflx.fs.100M.dg flxadd_rx.f isoplot_rx.dpa	Calculation to produce fission densities Output fluxes Similar run to output fission densities Fission density ASCII file Fission density ASCII file edited to add extra intervals for fs run Neutron/gamma and delayed gamma reactor flux DORT calculations Scalar and directional flux files Utility program to add neutron/gamma and delayed gamma flux files Writes dpa rate values
<i>Directory: hb-2</i>	
visa.sh & visa.dg.sh <i>Outputs:</i> visa.srce, visa.dg.srce	Visa input to reorder directional flux file and calculate boundary source Boundary sources
<i>Directory: hb-2/unmod</i>	
dtd_hb-2U.sh & dtd_hb-2U.dg.sh <i>Outputs:</i> dtd_hb-2U.srce & dtd_hb-2U.dg.srce dort_hb-2U.sh & dort_hb-2U.dg.sh <i>Outputs:</i> dort_hb-2U.p3flx & dort_hb-2U.dg.p3flx flxadd_hb-2U.f isoplot_hb-2U.dpa	Writes boundary sources for DORT in rotated coordinate system Rotated coordinates boundary sources Neutron/gamma and delayed gamma HB-2 DORT calculations Scalar flux files Utility program to add neutron/gamma and delayed gamma flux files Outputs/plots dpa rate values
<i>Directory: hb-2/mod</i>	
dtd_hb-2M.sh & dtd_hb-2M.dg.sh <i>Outputs:</i> dtd_hb-2M.srce & dtd_hb-2M.dg.srce dort_hb-2M.sh & dort_hb-2M.dg.sh <i>Outputs:</i> dort_hb-2M.p3flx & dort_hb-2M.dg.p3flx flxadd_hb-2M.f rip_hb2.f isoplot_hb-2M.dpa	Writes boundary sources in rotated coordinate system Rotated coordinates boundary sources Neutron/gamma and delayed gamma HB-2 DORT calculation inputs Scalar flux files Utility program to add neutron/gamma and delayed gamma flux files Utility program to read flux files and calculate dpa rates; includes interpolation For modified and original HB-2 designs Writes dpa rate values

Table E.1 (continued)

<i>Directory: hb-3</i>	
visa_hb-3.sh & visa_hb-3.dg.sh <i>Outputs:</i> visa_hb-3.srce, visa_hb-3.dg.srce torsed_hb-3.sh & torsed_hb-3.dg.sh <i>Outputs:</i> torsed_hb-3.srce & torsed_hb-3.dg.srce match_hb-3.f & match_hb-3.dg.f tort_hb-3.sh & tort_hb-3.dg.sh <i>Outputs:</i> tort_hb-3.res & tort_hb-3.dg.res respadd_hb-3.f xtorid_hb-3.res.z isoplot_hb-3.dpa.z	Visa input to calculate boundary source Boundary sources Writes boundary sources for TORT in rotated coordinate system Rotated coordinates boundary sources Utility codes to write distributed source Neutron/gamma and delayed gamma TORT dpa response calculations dpa rates Utility program to add neutron/gamma and delayed gamma dpa response files Writes dpa for selected plane Writes dpa rates at horizontal midplane
<i>Directory: hb-4</i>	
visa_hb-4.sh & visa_hb-4.dg.sh <i>Outputs:</i> visa_hb-4.srce, visa_hb-4.dg.srce	Visa input to calculate boundary source Boundary sources
<i>Directory: hb-4/unmod</i>	
torsed_hb-4U.sh & torsed_hb-4U.dg.sh <i>Outputs:</i> torsed_hb-4U.srce & torsed_hb-4U.dg.srce match_hb-4U.f & match_hb-4U.dg.f tort_hb-4U.sh & tort_hb-4U.dg.sh <i>Outputs:</i> tort_hb-4U.res & tort_hb-4U.dg.res respadd_hb-4U.f xtorid_hb-4U.z isoplot_hb-4U.dpa.z	Writes boundary sources for TORT in rotated coordinate system Rotated coordinates boundary sources Utility codes to write distributed source Neutron/gamma and delayed gamma TORT dpa response calculations dpa rates Utility program to add neutron/gamma and delayed gamma dpa response files Writes dpa for selected plane Writes dpa rates at horizontal midplane
<i>Directory: hb-4/mod</i>	
torsed_hb-4M.sh & torsed_hb-4M.dg.sh	Writes boundary sources for TORT in rotated coordinate system
<i>Outputs:</i> torsed_hb-4M.srce & torsed_hb-4M.dg.srce	Rotated coordinates boundary sources
match_hb-4M.f & match_hb-4M.dg.f	Utility codes to write distributed source
tort_hb-4M.sh & tort_hb-4M.dg.sh	Neutron/gamma and delayed gamma TORT dpa response calculations
<i>Outputs:</i> tort_hb-4M.res & tort_hb-4M.dg.res	dpa rates
respadd_hb-4M.f	Utility program to add neutron/gamma and delayed gamma dpa response files
rip3.f	Utility code to read TORT response files and display dpa values for selected locations; used for all TORT models (HB-3, HB-4, original and modified designs)
xtorid_hb-4M.z	Writes dpa for selected plane
isoplot_hb-4M.dpa.z	Writes dpa rates at horizontal midplane

Table E.2. Software file cross index

Previous file name	Revised file name
<i>Directory: lib</i>	
axmix1.sh	axmix_hfr.sh
<i>Directory: rx</i>	
hfr84kjvp.sh11 hfr84kjvp.sh21 hfr84fsjvp.v2.sh1 hfr84fsjvp.dg.v2.sh1 flxadd_fs.f iso84fsjvp.v2.total.dpa	dort_rx_k1.sh dort_rx_k2.sh dort_rx_fs.sh dort_rx_fs.dg.sh flxadd_rx.f isoplot_rx.dpa
<i>Directory: hb-2</i>	
hfr84visjvp.v2.sh1 hfr84visjvp.dg.v2.sh1	visa.sh visa.dg.sh
<i>Directory: hb-2/unmod</i>	
dtd8429jvp.v2.carRev2.sh1 dtd8429jvp.dg.v2.carRev2.sh1 hfr84hb24.v2.sh1 hfr84hb24.dg.v2.sh1 flxadd_unnorm.f iso84hb24.total.unnorm.dpa	dtd_hb-2U.sh dtd_hb-2U.dg.sh dort_hb-2U.sh dort_hb-2U.dg.sh flxadd_hb-2U.f isoplot_hb-2U.dpa
<i>Directory: hb-2/mod</i>	
dtd8429jvp.v2.carRev2.sh1 dtd8429jvp.dg.v2.carRev2.sh1 hfr84hb29.v2.carRev2.sh1 hfr84hb29.dg.v2.carRev2.sh1 flxadd_unnorm.f iso84hb29.carRev2.total.unnorm.dpa	dtd_hb-2M.sh dtd_hb-2M.dg.sh dort_hb-2M.sh dort_hb-2M.dg.sh flxadd_hb-2M.f isoplot_hb-2M.dpa
<i>Directory: hb-3</i>	
hfr84vis.hb3.v2.sh1 hfr84vis.dg.hb3.v2.sh1 torsed.new1.hb3.v2.sh1 torsed.new1.hb3.dg.v2.sh1 matchcell.f Matchcell3_dg.f tort.new1.hb3.fs.v2.carA.sh1 tort.new1.hb3.fs.dg.v2.carA.revXS.sh1 respadd3_nonorm.f xtorid.new1.hb3.total.unnorm.carA.res.z ispl3d.new1.hb3.fs.total.unnorm.carA.dpa.z	visa_hb-3.sh visa_hb-3.dg.sh torsed_hb-3.sh torsed_hb-3.dg.sh match_hb-3.f match_hb-3.dg.f tort_hb-3.sh tort_hb-3.dg.sh respadd_hb-3.f xtorid_hb-3.res.z isoplot_hb-3.dpa.z
<i>Directory: hb-4</i>	
hfr84vis.hb4.v2.sh1 hfr84vis.dg.hb4.v2.sh1	visa_hb-4.sh visa_hb-4.dg.sh

Table E.2 (continued)

<i>Directory: hb-4/unmod</i>	
torsed.new.hb4.highz.v2.sh1	torsed_hb-4U.sh
torsed.new.hb4.dg.highz.v2.sh1	torsed_hb-4U.dg.sh
matchcell4p.f	match_hb-4U.f
matchcell4p_p.f	match_hb-4U.dg.f
tort.new.hb4.fs.highz.v2.carA.sh1	tort_hb-4U.sh
tort.new.hb4.fs.dg.highz.v2.carA.sh1	tort_hb-4U.dg.sh
respadd1_unnorm.f	respadd_hb-4U.f
xtorid.new.hb4.highz.total.unnorm.carA.z	xtorid_hb-4U.z
ispl3d.new.hb4.fs.highz.total.unnorm.carA.dpa.z	isoplot_hb-4U.dpa.z
<i>Directory: hb-4/mod</i>	
torsed.mod.hb4.highz.v2.car.sh1	torsed_hb-4M.sh
torsed.mod.hb4.dg.highz.v2.car.sh1	torsed_hb-4M.dg.sh
matchcell4m_car.f	match_hb-4M.f
matchcell4m_dg_car.f	match_hb-4M.dg.f
tort.mod.hb4.fs.highz.v2.car.rev.sh1	tort_hb-4M.sh
tort.mod.hb4.fs.dg.highz.v2.car.rev.sh1	tort_hb-4M.dg.sh
respadd4_mod_car_unnorm.f	respadd_hb-4M.f
xtorid.mod.hb4.highz.unnorm.car.rev.res.z	xtorid_hb-4M.z
ispl3d.mod.hb4.fs.highz.total.unnorm.car.rev.dpa.z	isoplot_hb-4M.dpa.z

Table E.3. Updated file-naming convention

Terminology	Description
hb-*, where * = 2,3,4	Refers to HB-2, -3, and -4 beam tubes. HB-1 is same as original HB-4.
rx	Refers to reactor.
k1, k2	Refers to k_{eff} calculation (k2 outputs results in ASCII file).
U	Refers to HB-2 or -4 original (unenlarged) design. The unenlarged HB-4 design is equivalent to HB-1.
M	Refers to HB-2 or -4 modified (enlarged) design.
unnorm	Un-normalized results.
dg	Refers to a delayed gamma source calculation. If “dg” is not included in a file name, it is assumed that the source is prompt neutrons/gammas.
fs	Fixed source calculation.
dpa	Displacements per atom in iron (dpa/s is actually calculated).
dort,tort,visa,xtorid,	Codes within the DOORS 3.2 system, quality assurance (QA)-approved for the High
torsed,isoplot	Flux Isotope Reactor (HFIR) on CPILE computer system.
dtd, axmix	Auxiliary codes not within the DOORS 3.2 system, but QA-approved for HFIR on CPILE computer system.
match	In names of short utility codes, used to match location of core regions in reactor model to similar region in beam-tube models.
flxadd	In names of short utility codes, used to add/normalize fluxes produced by prompt neutron/gamma source runs and delayed neutron source runs.
respadd	In names of short utility codes, used to add/normalize responses (dpa rates integrated over energy) produced by prompt neutron/gamma source runs and delayed neutron source runs.

INTERNAL DISTRIBUTION

- | | | | |
|--------|-------------------|-----|-------------------------------------------------------------|
| 1. | C. A. Baldwin | 22. | C. V. Parks |
| 2-6. | E. D. Blakeman | 23. | D. E. Peplow |
| 7-8. | R. D. Cheverton | 24. | R. T. Primm |
| 9. | T. L. Dickson | 25. | G. Radulescu |
| 10. | M. E. Dunn | 26. | B. T. Rearden |
| 11. | T. M. Evans | 27. | D. A. Reed |
| 12. | J. C. Gehin | 28. | I. Remec |
| 13. | D. C. Glasgow | 29. | K. A. Smith |
| 14. | R. E. Grove | 30. | M. A. Sokolov |
| 15. | G. Ilas | 31. | J. C. Wagner |
| 16. | S. K. Iskander | 32. | M. L. Williams |
| 17-18. | H. A. Kmiecik Jr. | 33. | Central Research Library,
4500N, MS-6208 |
| 19. | T. M. Miller | 34. | Return extra ORNL copies to:
H. E. Turpin, 5700, MS-6170 |
| 20. | S. W. Mosher | | |
| 21. | R. K. Nanstad | | |

